

Otto-von-Guericke-Universität Magdeburg
Medizinische Fakultät
Institut für Klinische Chemie und Pathobiochemie
Direktor: Professor Dr. med. Berend Isermann



**Cytoprotective activated protein C averts Nlrp3 inflammasome induced
ischemia reperfusion injury *via* mTORC1 inhibition**

Dissertation

zur Erlangung des Doktorgrades

Doctor rerum medicarum
(Dr. rer. medic.)

an der Medizinischen Fakultät
der Otto-von-Guericke-Universität Magdeburg

vorgelegt von Sumra Nazir
aus Pakistan
Magdeburg 2018

Bibliographical description

Sumra Nazir; M.Sc., M.Phil. Cytoprotective activated protein C averts Nlrp3 inflammasome induced ischemia reperfusion injury via mTORC1 inhibition– 2018. 100 pages, 21 figures, 2 tables.

Abstract

Cytoprotection by activated protein C (aPC) following ischemia-reperfusion injury (IRI) is associated with apoptosis inhibition. However, IRI is hallmarked by inflammation and hence conceptually cell-death forms disjunct from immunologically silent apoptosis are more likely to be relevant. As pyroptosis, cell death resulting from inflammasome activation, is typically observed in IRI we speculated that aPC ameliorates IRI by inhibiting inflammasome activation. Here we analyzed the impact of aPC on inflammasome activity in myocardial and renal IRI. aPC treatment reduced infarct size and Nlrp3 inflammasome activation in mice. Kinetic *in vivo* analyses revealed that inflammasome activation preceded myocardial injury and apoptosis. The constitutively active Nlrp3^{A350V} mutant abolished aPC's protective effect, demonstrating that Nlrp3 suppression is required for aPC-mediated protection from IRI. *In vitro* aPC inhibited inflammasome activation *via* PAR-1 and mTORC1 signaling. Inhibiting PAR-1 signaling abolished aPC's ability to restrict inflammasome activity and myocardial infarction, while specifically inhibiting aPC's anticoagulant properties did not impair aPC's effect on inflammasome activation. Targeting biased PAR-1 signaling *via* parrmodulin-2 restricted inflammasome activation and limited myocardial IRI. aPC's renal tissue protective effect was likewise dependent on Nlrp3 inflammasome suppression. These studies reveal that aPC protects from IRI by restricting mTORC1 dependent inflammasome activation and that mimicking biased aPC-PAR1 signaling using parrmodulins may be a feasible therapeutic approach to combat IRI.

Keywords: Inflammasome, caspase-1, caspase-3, ischemia reperfusion injury, myocardial infarction, mTORC.

Bibliographische Beschreibung

Sumra Nazir; M.Sc., M.Phil. Cytoprotective activated protein C averts Nlrp3 inflammasome induced ischemia reperfusion injury via mTORC1 inhibition – 2018. – 100 Bl., 21 Abb., 2 Tab.

Kurzreferat

Es war bei Beginn der Arbeiten bekannt, dass der zytoprotektive Effekt von aktiviertem Protein C (aPC) bei einer Ischämie-Reperfusionsschaden (ischemia-reperfusion injury, IRI) mit einer Apoptosehemmung assoziiert ist. Da die IRI jedoch durch eine Entzündung gekennzeichnet ist, sind konzeptionell entzündliche Zelltodformen eher von pathogenetischer Relevanz. Auch die Pyroptose, eine Zelltodform nach Inflammasom-Aktivierung, ist mit einer IRI assoziiert. Daher stellten wir die Hypothese auf, dass für den zytoprotektiven Effekt von aPC nach IRI die Hemmung des Inflammasoms relevant ist. Diese Hypothese untersuchten wir im Kontext der myokardialen und renalen IRI. Eine aPC-Behandlung vor oder nach Myokard-IRI reduzierte die Infarktgröße und Inflammasom-Aktivierung in Mäusen. Kinetische in-vivo-Analysen zeigten, dass die Inflammasomaktivierung einer Myokardverletzung und Apoptose vorausging, was eine pathogene Rolle des Inflammasoms nahelegt. Die konstitutiv aktive Nlrp3A350V-Mutante hob die schützende Wirkung von aPC auf, was einen kausalen Zusammenhang zwischen aPC und der Nlrp3-Inhibition nahe legt. aPC inhibierte die Inflammasomaktivierung in vitro via des PAR-1- und mTORC1-Signalweges. Dieser Effekt war unabhängig von den antikoagulanten Eigenschaften von aPC. Die gezielte Aktivierung des aPC-PAR-1-Signals durch den „biased“ small-compound PAR-1 Agonisten Parmodulin-2 war ausreichend, um die mTORC1- und Inflammasom-Aktivierung und die myokardiale IRI zu inhibieren. Die Relevanz der aPC-vermittelten Inflammasom-Suppression nach IRI wurde in einem Model der renalen IRI bestätigt. Diese Studien zeigen, dass aPC vor IRI schützt, indem es die mTORC1-abhängige Inflammasom-Aktivierung inhibiert, und dass die gezielte Modulation des aPC-PAR1-Signalweges durch „biased“ Agonisten (Parmodule) ein möglicher therapeutischer Ansatz der IRI ist.

Schlüsselwörter:

Inflammasom, Caspase-1, Caspase-3, Myokardinfarkt, Ischämie-Reperfusionsschädigung, mTORC.

Table of contents

List of figures	6
List of tables.....	7
List of Abbreviations.....	8
1 Introduction	13
1.1 Myocardial infarction	13
1.2 Role of cell death in the pathogenesis of myocardial IRI	13
1.2.1 Apoptosis and myocardial IRI	14
1.2.2 Inflammation and myocardial IRI.....	14
1.3 Inflammasome	16
1.3.1 Nlrp3 Inflammasome.....	18
1.3.2 Nlrp3 inflammasome and myocardial infarction.....	19
1.4 Coagulation proteases	20
1.4.1 Thrombomodulin protein C (TM-PC) system	21
1.4.2 Anticoagulant properties of aPC.....	22
1.4.3 Cytoprotective and anti-inflammatory function of the aPC.....	23
1.4.4 Protease activated receptors biased signaling	23
1.4.5 Activity-selective aPC variants	25
1.5 aPC role in myocardial IRI	27
1.6 mTOR signaling	27
2 Aim of the study	30
3 Material and methods:.....	31
3.1 Reagents:	31
3.2 Mice.....	34
3.2.1 Myocardial ischemia reperfusion injury model.....	34
3.2.2 <i>In vivo</i> intervention studies.....	35
3.2.3 Determination of Myocardial Infarct size	36
3.2.4 Renal ischemia reperfusion injury model.....	36
3.2.5 Determination of serum BUN and creatinine	37
3.3 Preparation of activated protein C.....	38
3.5 Immunoblotting	39
3.6 Bone marrow derived macrophages (BMDM)	39
3.6.1 Preparation of L929 conditioned medium (LCM)	39
3.6.2 Isolation and culture of BMDMs	40
3.7 Isolation and culture of neonatal cardiomyocytes and cardiac fibroblasts.....	40

3.8	Histology and immunohistochemistry	41
3.9	In situ caspase-1 activity assay.....	42
3.10	Hypoxia/reoxygenation (H/R) experiments.....	42
3.11	Reverse transcriptase polymerase chain reaction (RT-PCR)	43
3.12	Production of lentiviral particles.....	44
3.13	IL-1 β and IL-18 immunoassay.....	45
3.14	Statistical analysis.....	45
4	Results.....	46
4.1	aPC restricts Nlrp3 inflammasome activation following myocardial IRI.....	46
4.2	Inflammasome activation precedes apoptosis following myocardial IRI.....	46
4.3	Constitutively active Nlrp3 abolishes the protective effect of aPC in myocardial IRI	48
4.4	aPC prevents inflammasome activation in cardiac resident cells and macrophages <i>in vitro</i>	51
4.5	aPC restricts inflammasome by suppressing mTORC1 and HK1	53
4.6	aPC restricts inflammasome activation <i>via</i> PAR-1 <i>in vitro</i>	56
4.7	Cytoprotective 3K3A-aPC protects against myocardial IRI <i>via</i> PAR-1	56
4.8	PAR-1 specific parmodulin-2 ameliorates inflammasome activation in myocardial IRI	59
4.9	aPC protects against renal ischemia reperfusion injury by limiting Nlrp3 inflammasome activity	61
4.10	Constitutively active Nlrp3 abolishes the protective effect of aPC in renal IRI	61
5	Discussion	65
6	Conclusion.....	70
7	Future Outlook.....	72
8	References	74
9	Acknowledgement.....	93
10	Declaration	95
11	Curriculum Vitae and list of publications	96
11.1	Curriculum Vitae	96
11.2	List of publications	99

List of figures

Figure 1: Comparative illustration of pyroptosis and apoptosis, which both trigger cell death.	15
Figure 2: Priming and activating signals for inflammasome activation.	17
Figure 3: Nlrp3 inflammasome assembly.	18
Figure 4: The coagulation cascade.	20
Figure 5: Thrombin-TM mediated protein C activation system and signaling pathways.	22
Figure 6: Parmodulin mediated PAR1 biased agonsim.	25
Figure 7: Structural illustration of human aPC highlighting different residues involved in mediating the cytoprotective and anticoagulant functions.	26
Figure 8: The schematic illustrations of the mTORC1 pathway.	29
Figure 9: aPC pretreatment ameliorates inflammasome activation following myocardial IRI.	47
Figure 10: aPC post myocardial IRI treatment inhibits Nlrp3 inflammasome activation.	48
Figure 11: Inflammasome activation precedes apoptosis following myocardial IRI.	49
Figure 12: Constitutive active Nlrp3 abolishes the protective effect of aPC in myocardial IRI.	51
Figure 13: aPC prevents inflammasome activation in cardiac resident cells and macrophages <i>in vitro</i>	52
Figure 14: aPC restricts inflammasome by suppressing mTORC1.	54
Figure 15: aPC fails to restrict inflammasome in BMDMS expressing constitutively active mTORC1.	55
Figure 16: aPC restricts inflammasome activation via PAR1 <i>in vitro</i>	57
Figure 17: Cytoprotective 3K3A-aPC protects against myocardial IRI <i>via</i> PAR-1.	59
Figure 18: PAR-1 specific parmodulin-2 ameliorates inflammasome activation in myocardial IRI.	60
Figure 19: aPC restricts Nlrp3 inflammasome activation in renal IRI.	62
Figure 20: Constitutively active Nlrp3 abolishes the protective effect of aPC in renal IRI.	64
Figure 21: Scheme reflecting the proposed role of Nlrp3 inflammasome for cardiac dysfunction and myocardial IRI.	69

List of tables

Table 1: List of reagents used in current study.....	31
Table 2: List of primers used in current study.....	44

List of Abbreviations

aPC	Activated protein C
ApoER2	Apolipoprotein E receptor 2
AMI	Acute myocardial infarction
AMPK	5' adenosine monophosphate-activated protein kinase
Ang1	Angiopoietin1
ASC	Apoptosis speck-like protein containing a caspase recruitment domain
ATP	Adenosine triphosphate
ATCC	American type culture collection
ANOVA	Analysis of variance
Bax	Bcl-2-associated X protein
BMDM	Bone marrow derived macrophages
β -actin	Beta actin
BUN	Blood urea nitrogen
BCA	Bicinchoninic acid
Caspase	Cysteine aspartic acid proteases
cDNA	Complementary deoxyribonucleic acid
CAD	Coronary artery disease
CVD	Cardiovascular disease
cl-caspase-1	Cleaved (active) caspase-1
cl-IL-1 β	Cleaved (active) IL-1 β

CKD	Chronic kidney disease
cTNT	Cardiac troponin T
CARD	Caspase activation and recruitment domain
Cre-ERT2	Cre-recombinase under the control of the estrogen receptor T2
DAMP	Danger associated molecular pattern
DEPTOR	DEP domain containing mTOR-interacting protein
PIC	Protease inhibitor cocktail
DMEM	Modification of Basal Medium Eagle (BME)
EPCR	Endothelial cell protein C receptor
EDTA	Ethylene diamine tetra acetic acid
ERT	Estrogen receptor
EGF	Epidermal growth factor
Et-Br	Ethidium bromide
ELISA	Enzyme-linked immunosorbent assay
eIF4E	Eukaryotic initiation factor 4E
FMA	Fractional mesangial area
FACS	Fluorescence-activated cell sorting
FKBP12	FK506 binding protein
FBS	Fetal bovine serum
FCS	Fetal calf serum
FITC	Fluorescein isothiocyanate

FLICA	Fluorochrome inhibitor of caspases
GTP	Guanosine triphosphate
GAPDH	Glyceraldehyde 3-phosphate dehydrogenase
HMGB1	High mobility group box 1
HEPES	Hydroxyethyl-piperazineethane-sulfonic acid buffer
HK1	Hexokinase 1
HAPC	Human activated protein C
HBSS	Hanks' balanced salt solution
H&E	Hematoxylin and eosin
H/R	Hypoxia reoxygenation
IRI	Ischemia reperfusion injury
IL-1 β	Interleukin-1 beta
IL-18	Interleukin-18
IL-1R	Interleukin-1 receptor
i.p.	Intraperitoneal
KIM-1	Kidney injury molecule 1
LRRs	Leucine –rich repeats
LPS	Lipopolysaccharides
LAD	Left anterior descending
LCM	L929 conditioned medium
mTOR	Mammalian target of rapamycin
mTORC1	mTOR complex 1

mTORC2	mTOR complex 2
Nlrp3	NACHT, LRR and PYD domains-containing protein 3
NaF	Sodium fluoride
NOD	The nucleotide-binding oligomerization domain
NLRs	NOD-like receptors
NF- κ B	Nuclear factor kappa-light-chain-enhancer of activated B cells
PAMPs	Pathogen-associated molecular patterns respectively
PAR	Protease activator receptor
PYCARD	PYD and CARD Domain
PCI	Protein C inhibitor
PC	Protein C
P/S	Penicillin/Streptomycin
PVDF	Polyvinylidene difluoride
PBS	Phosphate buffer saline
PBST	Phosphate-buffered saline with Tween-20
p70S6K	p70 ribosomal protein S6 kinase
ROS	Reactive oxygen species
RIPA	Radioimmunoprecipitation assay buffer
RT	Room temperature
RNA	Ribonucleic acid
RT-PCR	Reverse transcriptase polymerase chain reaction

RPMI 1640	Roswell park memorial institute 1640
SEM	Standard error of the mean
s.c.	Subcutaneously
TUNEL	Terminal deoxynucleotidyl transferase dUTP nick end labeling
TLRs	Toll like receptors
TSC1	Tuberous sclerosis complex 1
TSC2	Tuberous sclerosis complex 2
TL	Tethered ligand
TM	Thrombomodulin
TM-PC	Thrombomodulin protein C
TTC	Triphenyl tetrazolium chloride

1 Introduction

1.1 Myocardial infarction

Acute myocardial infarction (AMI) remains one of the leading causes of hospitalization and cardiovascular mortality worldwide.¹ Although mortality attributable to the acute coronary event has declined substantially with improved reperfusion therapies, long-term morbidity has increased because of secondary heart failure in survivors of AMI. The major cause of MI is atherosclerosis of coronary arteries. In particular atherosclerotic plaques acquiring an unstable phenotype are prone to rupture and subsequent thrombus formation, resulting in occlusion of the coronary artery.² The prolonged occlusion of a coronary artery results in ischemic damage of the cardiac tissue. While reperfusion of the diseased blood vessel is the therapeutic mainstay and improves survival substantially, the restoration of blood flow to previously ischemic tissue can itself induce further cardiac damage, a phenomenon known as myocardial ischemia reperfusion injury (IRI).³ IRI triggers pronounced tissue-disruptive and sterile pro-inflammatory responses, which compromise the cardiac functional outcome.⁴ Current treatment strategies for AMI are based on restoring blood flow in the coronary artery (reperfusion) by dissolving the thrombus with fibrinolytic agents and/or mechanical, balloon-mediated stretching of the occluded artery and implantation of an intravascular stent. Although reperfusion strategies are successful in limiting injury to the heart, reducing infarct size and improving overall prognosis, patients with AMI have an increased short-term and long-term risk of heart failure, which is at least partially attributed to the ensuing IRI. Therefore, better understanding of the pathophysiology of myocardial IRI is a key to devise better treatment strategies for the prevention and treatment of adverse cardiac remodeling and subsequent heart failure following myocardial IRI.

1.2 Role of cell death in the pathogenesis of myocardial IRI

The heart is an organ with limited capacity for regeneration and repair. In addition, it is susceptible to numerous stresses and must respond to these insults in order to adapt to workload demands. Myocardial IRI triggers myocardial cell death within the ischemic

zone. Distinct forms of cell death, like apoptosis, pyroptosis and necrosis, have been associated with the progression of myocardial IRI induced cardiac dysfunction.⁵⁻⁸ However the relative causative contribution of different forms of death to the total cardiac cell loss and myocardial infarction following myocardial IRI remains obscure.

1.2.1 Apoptosis and myocardial IRI

Apoptosis is a form of programmed cell death that is triggered by the activation of the caspase cascade and results in the cleavage of protein substrates and fragmentation of DNA (Fig.1). Apoptosis which is an inflammatory silent form of cell death has been recognized as one of the possible cell death mechanisms during myocardial IRI.^{6,9} TUNEL-positive cardiomyocytes are frequent in the infarct area and the associated risk area. However, the typical ultrastructural morphology of apoptosis has rarely been detected in ischemic cardiomyocytes.¹⁰ Most of studies linking apoptosis with myocardial IRI employed TUNEL to detect apoptotic cell death.¹⁰⁻¹⁴ However TUNEL detects a wide range of cellular conditions, including viable cells undergoing DNA repair, apoptosis, pyroptosis, or necrosis.¹⁰ Therefore, whether TUNEL-positive cardiomyocytes in infarcted myocardium indeed reflect apoptotic cells has been brought into question.

1.2.2 Inflammation and myocardial IRI

The short occlusion of the coronary arteries (≤ 5 min) shows little if any evidence of an inflammatory reaction.^{15,16} However, coronary occlusion of longer duration results in reversible injury resulting in an inflammatory response, which is further elevated if the ischemic tissue is re-perfused.¹⁵ The inflammatory process triggers a broad spectrum of pathological insults that involves components of innate immunity, affecting both cardiomyocytes and non-cardiomyocyte cells and has profound effects on the functional deterioration of the heart.^{17,18} Myocardial IRI is regarded as a form of sterile inflammation.¹⁹ Sterile inflammation is an inflammatory response triggered by sterile stimuli including mechanical trauma, ischemia, toxins, minerals, crystals, chemicals, and antigens but not by an infectious agent such as bacteria or virus etc (Fig.1). The paradigm of inflammation associated with myocardial IRI involves the elimination of

pathogenic agents, removal of cellular debris, repair of the injured myocardium, and it contributes to cardiac regeneration. Therefore, myocardial IRI induced inflammation is considered to contribute to the healing of the cardia wound and the formation of the scar.¹⁷ In this regard, therapeutic attempts aimed at reducing inflammation following myocardial IRI has been associated with impaired healing or an increased risk of cardiac rupture or failed to show any additional benefit in addition to standard therapies.^{17,20}

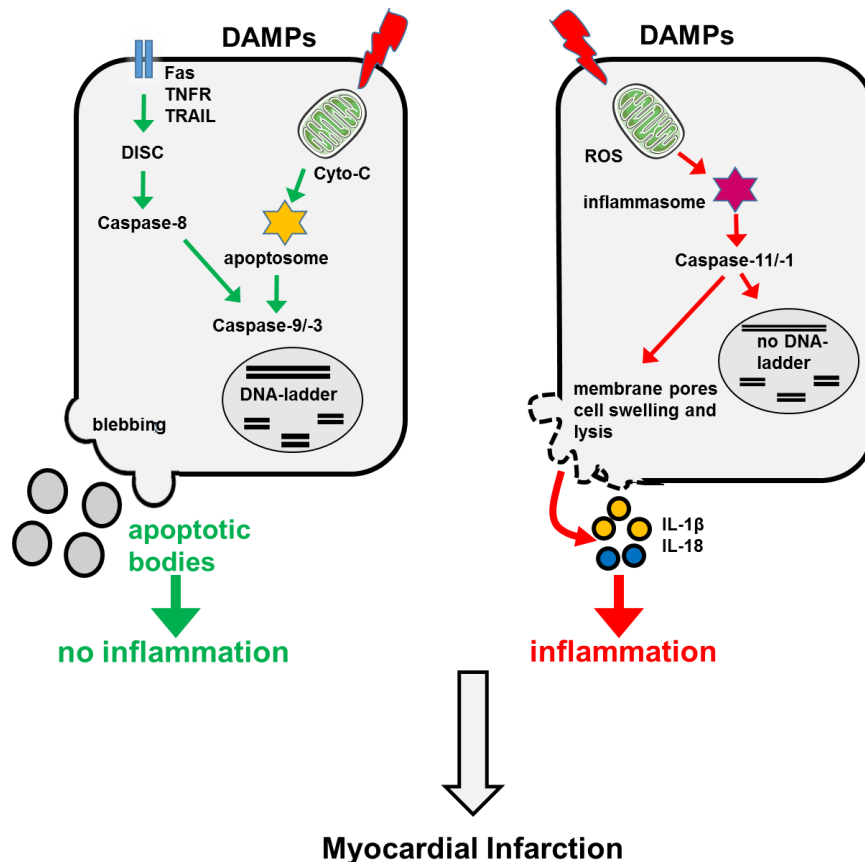


Figure 1: Comparative illustration of pyroptosis and apoptosis, which both trigger cell death.

Pyroptosis and apoptosis cell death pathways require activation of caspases, caspase-1/11 or caspase-3/8/9, respectively. However, these cell death forms differ largely, both in morphology and the associated inflammation. Pyroptosis is associated with the release of IL-1 β and IL-18 and is characterized by membrane lysis. The latter results in release of cytosolic content into the extracellular space, which act as DAMPs (such as HMGB1, IL-1 α , ATP) and further promote inflammation. On the other hand, during apoptosis, plasma membrane integrity is maintained, apoptotic bodies are formed, and cellular contents are not released. As myocardial infarction is associated with sterile inflammation, pyroptosis is a more likely pathway than apoptosis in this setting, contributing to myocardial IRI.

Therefore, there is paradigm shift and researchers have agreed that excessive inflammation following myocardial IRI impairs not only the formation of a solid scar but

also potentiate the risk of rupture.^{13,17,21,22} Thus, there is a need for a better understanding of the cellular and molecular events associated with myocardial IRI in order to develop more site-specific interventions that could mitigate inflammatory injury during early reperfusion without interfering with myocardial healing.

1.3 Inflammasome

As an integral part of the innate immune system, the inflammasome is a macromolecular protein complex which serves as a signaling platform to detect various pathogenic and sterile stressors that regulate the activation of caspase 1 and the production and secretion of pro-inflammatory cytokines such as IL-1 β and IL-18 (Fig.2).²³ Cellular stressors (e.g. mitochondrial DNA, ROS, histones) and microbial products are collectively referred to as damage-associated molecular patterns (DAMPs) or pathogen-associated molecular patterns (PAMPs), respectively (Fig.2).^{23,24}

Intracellular sensor molecules, which typically contain a NOD-like receptor (Nlr e.g. Nlrp1, Nlrp3, or Nlr4), detect appropriate stimuli and form a complex with ASC, an adaptor protein encoded by PYCARD (PYD and CARD Domain) gene. ASC contains a pyrin-domain and a caspase activation and recruitment-domain (CARD). Via its pyrin domain ASC interacts with the sensor molecule, while the CARD domain interacts with caspase-1 and initiates caspase-1 self-cleavage. Although caspase 1 has several functions unrelated to the inflammasome, its main role in the inflammasome is to cleave pro IL-1 β and IL-18 into its their active forms, and as such, caspase 1 is also known as the IL-1 β converting enzyme(Fig.2).²⁵

The typical activation of the inflammasome comprises two steps: priming step involves direct engagement of Toll-like receptors (TLRs) by pathogen-associated or damage-associated molecular patterns, resulting in the rapid activation activation of NF- κ B, which stimulates pro-IL-1 β synthesis and increased expression of Nlrp3. While during the activation step the oligomeric inflammasome complex assembles, inducing maturation of IL-1 β and IL-18.²⁶

In contrast to apoptosis (typical programmed cell death), death by pyroptosis is associated with cell swelling, increased membrane permeability, and cell rupture,

leading to the extracellular release of pro-inflammatory mediators such IL-1 β , IL- 18 and IL-1 α .²⁷⁻³⁰

The impairment of cell membrane integrity is mediated by gasdermin D (GSDMD), a substrate of caspase 1, that after its cleavage forms oligomers that fragment within the cell membrane, followed by the formation of cell membrane pores and cell dysfunction Fig.2.³¹

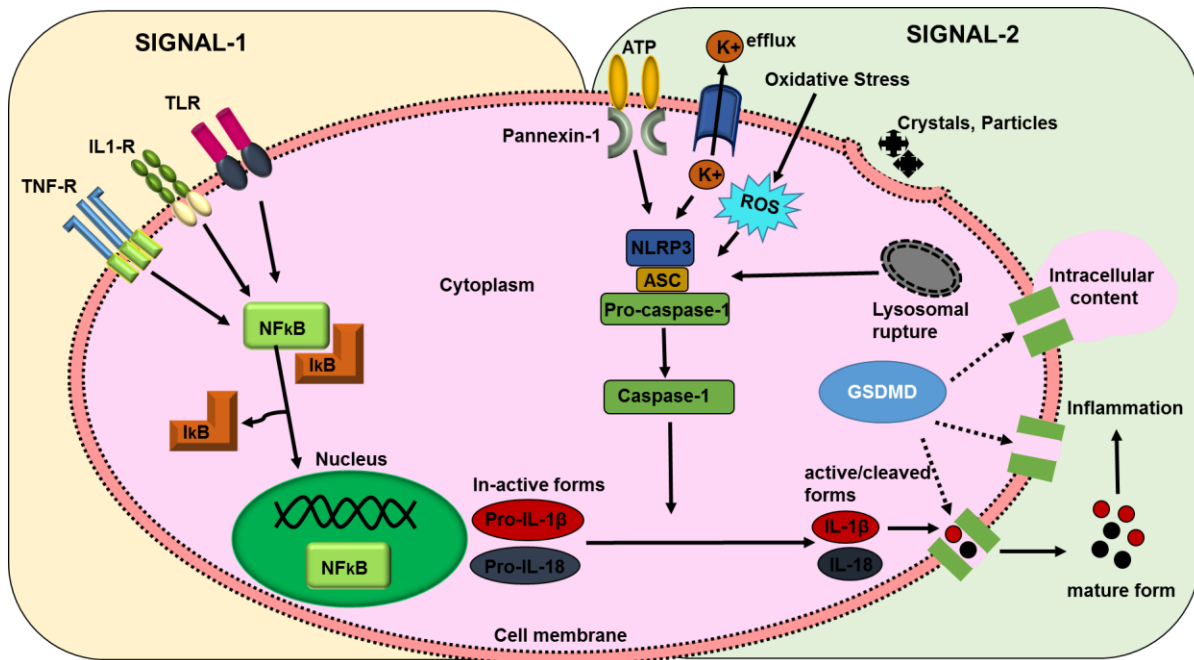


Figure 2: Priming and activating signals for inflammasome activation.

The priming signal involves binding of stimuli to TLRs, IL-1R or TNF-R, which triggers the translocation of transcription NF- κ B to the nucleus to synthesize Nlrp3, pro-IL-1 β and pro-IL-18. The second signal involves the Nlrp3 oligomerization, along with the recruitment of the adaptor molecule ASC and pro-caspase-1, resulting in caspase-1 maturation. Mature caspase-1 (as a result of auto-cleavage of pro-caspase-1) cleaves GSDMD which is able to generate membrane pores allowing extravasation of intracellular contents and release of mature IL-1 β and IL-18.

1.3.1 Nlrp3 Inflammasome

The most extensively studied inflammasome is the Nlrp3 inflammasome, which has been shown to recognize danger signals and trigger sterile inflammatory response in various disease including myocardial IRI and diabetic cardiomyopathy.^{25,32} Nlrp3 consists of three domains: a C-terminal with leucine-rich repeats (LRRs), a central nucleotide domain termed NACHT domain, and an N-terminal pyrin domain (PD) (Fig.3).

The most extensively studied inflammasome is the Nlrp3 inflammasome, which has been shown to recognize danger signals and trigger sterile inflammatory response in various disease including myocardial IRI and diabetic cardiomyopathy.^{25,32} Nlrp3 consists of three domains: a C-terminal with leucine-rich repeats (LRRs), a central nucleotide domain termed NACHT domain, and an N-terminal pyrin domain (PD) (Fig.3).

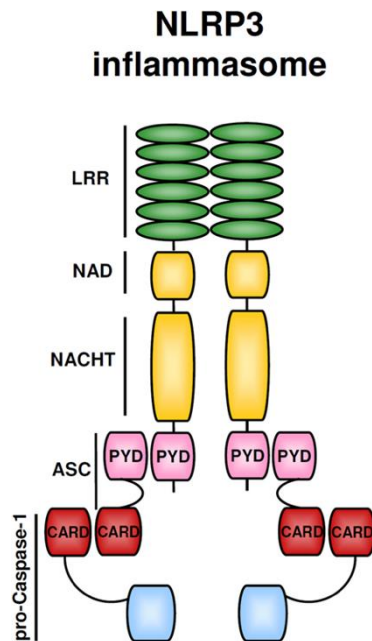


Figure 3: Nlrp3 inflammasome assembly.

Nlrp3 consists of three domains: C-terminal leucine rich repeats (LRRs), a central nucleotide domain termed NACHT domain, and an N-terminal pyrin domain (PD). Upon activation, Nlrp3 associates with the adaptor protein ASC, which comprises a caspase recruitment domain (CARD) and a pyrin domain. The Nlrp3:ASC complex oligomerizes and binds the enzyme caspase-1, thus forming active inflammasome complexes (Nlrp3, ASC, and caspase-1). (Adapted from Anders and Muruve, 2011).

1.3.2 Nlrp3 inflammasome and myocardial infarction

Nlrp3 inflammasome components ASC and caspase 1 levels have been shown to be increased in myocardial tissues obtained from patients who had died after an acute myocardial infarction.⁶ Furthermore, plasma levels of Nlrp3 and caspase 1 have been linked with increasing severity of coronary artery disease (CAD).³³ Caspase 1 activation is associated with inflammation triggered cardiac dysfunction in experimental diabetic cardiomyopathy.²⁵ Pathologically, various pro-inflammatory stimuli such as DMAPs or PAPMs that bind to Toll-like receptors (TLRs) induce the expression of Nlrp3 and the other inflammasome components in resident cells such as cardiomyocytes, fibroblasts and endothelial cells and non-resident cells such as leukocytes.^{6,28,30} Importantly, Nlrp3 inflammasome inhibition reduces infarct size, attenuates adverse cardiac remodeling, and preserves cardiac function in animal models of myocardial IRI.^{5,21,29,30}

IL-1Ra (IL-1 receptor antagonist) is an endogenous Nlrp3 inflammasome inhibitor induced during IRI.³⁴⁻³⁶ However, its induction following myocardial IRI is insufficient to provide full protection, which may reflect higher affinity of IL-1 for the receptor or excess availability of IL-1Ra.³⁷ In agreement with this IL-1Ra levels inversely correlates with extent of myocardial loss in patients with AMI.³⁶ The available clinical data in patients with AMI, together with preclinical data in animals, generate compelling arguments for further assessment of selective Nlrp3 inhibitors or other means to inhibit the Nlrp3 inflammasome.

Thus, deciphering IL-1Ra independent pathways enabling Nlrp3 inflammasome restriction is required to identify suitable therapeutic strategies to treat or prevent myocardial infarction. Targeting the coagulation system may constitute a possible approach to limit sterile inflammation in general and in particular activation of the Nlrp3 inflammasome, considering the well-established functions of coagulation proteases in inflammation. However, data supporting a mechanist link between the Nlrp3 inflammasome and coagulation are missing hitherto.

1.4 Coagulation proteases

Acute myocardial infarction is caused by thrombotic occlusion of a coronary artery after disruption of an atherosclerotic plaque. Thrombogenic factors from the plaque promote platelet activation, adhesion and aggregation, as well as activation of the coagulation cascade.^{38,39} The coagulation cascade has two initiation pathways which result in thrombin activation, which subsequently results in fibrin formation and platelet activation, forming a hemostatic plug and thus stopping bleeding. The initiation pathways are the contact activation pathway (also known as the intrinsic pathway) and the tissue factor pathway (also known as the extrinsic pathway). Both coagulation pathways activate the "final common pathway" comprising factor X and prothrombin activation. Thrombin then cleaves fibrinogen and activates platelets (Fig.4).^{38,40}

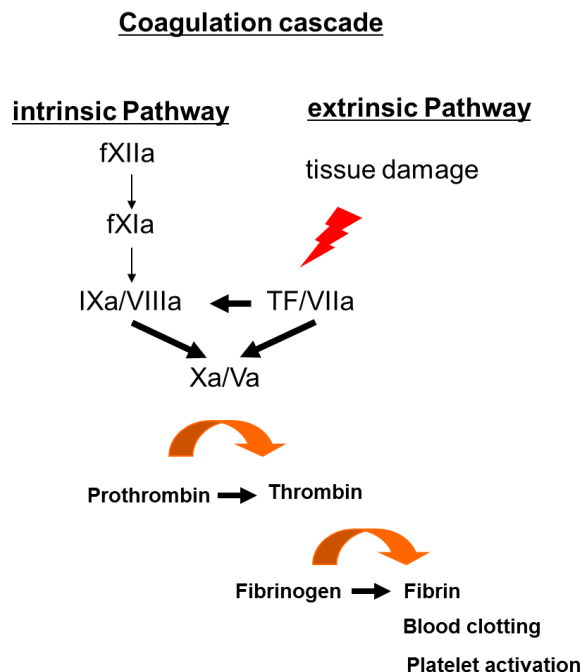


Figure 4: The coagulation cascade.

The coagulation cascade comprises two partially interacting activation pathways, the intrinsic and the extrinsic pathway. The intrinsic pathway is initiated by sequential activation of coagulation factors XII, XI and IX. FXIIa converts FXI into FXIa. Factor XIa activates FIX. FIXa interacts with its co-factor FVIIIa, yielding the tenase complex, which activates FX to FXa, thus initiating the common coagulation pathway. The extrinsic pathway is activated following damage to the blood vessel. Upon loss of vascular integrity FVII is able to interact with extravascular tissue factor (TF). Within the TF-FVII complex FVII is activated. The TF-FVIIa complex activates FX to FXa. Within the common coagulation pathways FXa and its co-factor FVa form the prothrombinase complex, which activates prothrombin to thrombin. Thrombin converts fibrinogen to fibrin and activates platelets, which together form a hemostatic plug.

Both prothrombin fragment 1+2 (F1+2), reflecting the thrombin generation, and D-dimer, reflecting fibrin formation and degradation, are elevated in acute myocardial infarction. These markers remain elevated for several months after the acute event.⁴¹ In the Acute Coronary Syndrome-Thrombolysis in Myocardial Infarction 51 (ATLAS ACS 2-TIMI 51) trial, the direct oral anticoagulant rivaroxaban reduced the risk of new ischemic events when compared with placebo in myocardial infarction patients.^{42,43} In addition treatment with anti-platelet drugs has been shown to reduce both the acute and long-term risk of new ischemic events after a myocardial infarction.^{41,44}

Thrombin has a large variety of functions, in addition to the conversion of fibrinogen to fibrin, which is important for the hemostatic plug. Importantly, it activates Factors VIII and V (feedback amplification) and – after binding to thrombomodulin – the anticoagulant protein C (for feedback inhibition), thus adding an additional level of control to the coagulation cascade.⁴⁵

1.4.1 Thrombomodulin protein C (TM-PC) system

Thrombomodulin (TM), a cell surface-expressed glycoprotein, is predominantly synthesized by vascular endothelial cells.^{45,46} TM consists of a single chain with six tandemly repeated EGF-like domains, a Serine/Threonine-rich spacer and a transmembrane domain. It binds to thrombin by the fourth and fifth EGF-like domains, forming a 1:1 complex. Upon binding to TM, thrombin acquires a new substrate specificity, becoming a potent activator of the zymogen protein C (PC). Protein C is activated on the endothelial surface by the thrombin-thrombomodulin complex to yield activated protein C (aPC), a natural anticoagulant that limits thrombin production.

The epithelial protein C receptor (EPCR) plays a role in accelerating the activation of protein C by binding protein C and moving it closer to the thrombin-thrombomodulin complex. The activation rate of PC by the thrombin-TM complex is approximately 1000-fold greater than the rate measured for a-thrombin in the absence of TM, and is further augmented ~10–20-fold if the PC is bound to EPCR. The Gla-domain of PC mediates binding to membrane-proximal regions of EPCR.⁴⁷⁻⁵⁰ In addition to the augmentation of PC-activation, EPCR is important for aPC's anti-apoptotic and anti-inflammatory

functions.^{46,51,52} aPC dissociates from EPCR and is released into plasma, where it interacts with plasma inhibitors of serine proteases, such as protein C inhibitor (PCI). aPC in the plasma is inactivated with a half-life of about 20 min.⁵³⁻⁵⁶

1.4.2 Anticoagulant properties of aPC

The anticoagulant activities of aPC are primarily based on irreversible proteolytic inactivation of factors Va and VIIIa. Cofactors involved in the inactivation of factor Va and FVIIIa include protein S, glycosphingolipids (e.g. glucosylceramide), anionic phospholipids (e.g. phosphatidylserine, cardiolipin) and high-density lipoprotein.⁵⁷ aPC inactivates factor Va by proteolysis at Arg506 and Arg306. Initial cleavage at Arg506 causes the partial inactivation of factor Va, whereas secondary cleavage at Arg306 results in the complete loss of FV procoagulant function. Proteolysis at Arg306 of FVa is accelerated ~20-fold by presence of cofactor protein S. Cleavage at Arg506 is protein S independent. Proteolysis of FVIII by aPC occurs at Arg 336 and Arg562. Cleavage of either Arg336 or Arg562 results in complete loss of FVIII procoagulant function.⁵⁸ Clinical importance is illustrated by the FVL mutation (R506Q) and further mutations of the FV-gene as risk factors for thrombosis.^{59,60}

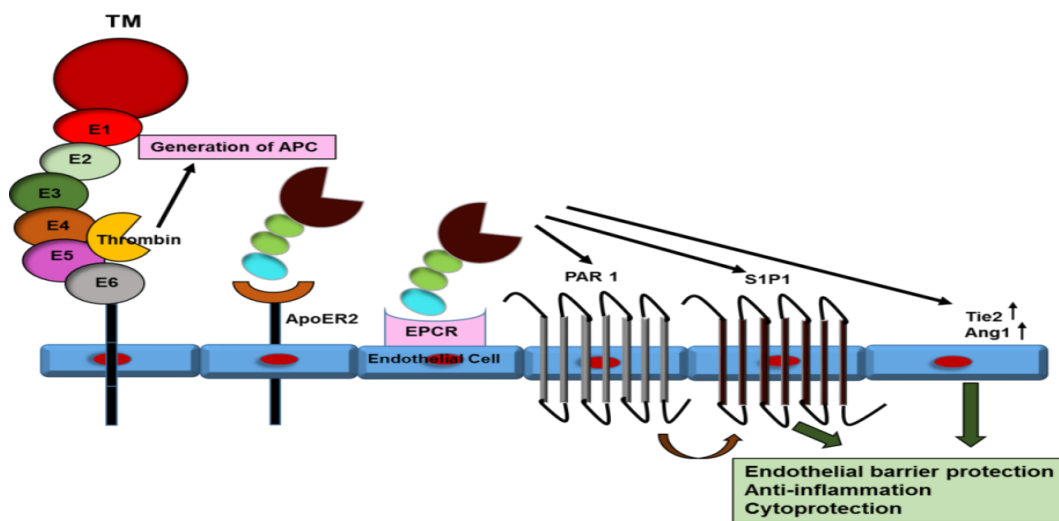


Figure 5: Thrombin-TM mediated protein C activation system and signaling pathways.

Thbd, thrombomodulin; PC, protein C; IIa, thrombin; EPCR, endothelial protein C receptor; aPC, activated protein C; PAR-1, protease activated receptor-1; ApoER2, apolipoprotein E receptor 2; S1P1, Sphingosine-1-phosphate receptor 1; Tie2, angiopoietin receptor; Ang1, angiopoietin1. See text for details.

1.4.3 Cytoprotective and anti-inflammatory function of the aPC

In addition to its anticoagulant function, aPC – frequently in association with EPCR – conveys cyto-protective signaling through cleavage of protease-activated receptors (PARs).^{61,62} The cyto-protective effects of aPC includes (1) endothelial barrier stabilization, (2) anti-apoptotic properties, (3) anti-inflammatory activity, and (4) alterations of gene expression profile (Fig. 5).⁶²⁻⁶⁵ aPC mediated anti-inflammatory effects include inhibition of NF-kappa B (NF-κB) and reduced expression of cell adhesion molecules (ICAM, VCAM), reduced leukocyte extravasation at site of injury, and inhibition of the release of inflammatory cytokines (TNF-α, IL-1β, IL-6, and IL-8).⁶⁶⁻⁶⁹

Consistent with this, the inhibition of activated protein C increases inflammatory cytokine levels, endothelial cell injury and leukocyte extravasation in response to endotoxin. These effects are reversed upon infusion of aPC.⁴⁶ However the mechanism underlying aPC's anti-inflammatory function is not clear. NF-κB mediated Nlrp3 inflammasome activation is a central molecular mechanism promoting inflammatory responses.⁷⁰ As aPC is known to prevent NF-κB activation we speculated that aPC targets Nlrp3 inflammasome activation pathway to limit inflammation. Mechanisms underlying the potential inflammasome inhibition by aPC remain unknown, but most likely are dependent on aPC-dependent signaling via protease activated receptors.

1.4.4 Protease activated receptors biased signaling

Protease activated receptors (PARs) are a family of G-protein coupled receptors (GPCRs) that are ubiquitously expressed and regulate physiological and pathological processes in various organs including heart.⁷¹ These receptors are activated by proteolytic cleavage of their extracellular N terminus, resulting in the formation of a new N terminus that serves as a tethered ligand. The tethered ligand folds back into the ligand-binding pocket of the receptor, initiating signaling. The cytoprotective function of aPC is generally mediated by the cleavage of PAR-1 in the presence of EPCR (Fig. 5).⁷² Furthermore, various other co-receptors like PAR3, sphingosine-1-phosphate (S1P) receptor 1 (S1P1), Mac-1, Tie2, and/or other receptors complement aPC

signaling *via* PAR-1 in a cell- and context-specific fashion (Fig. 5) ^{57,58,73-76} PARs are known to be activated by canonical and non-canonical cleavage.

Thrombin cleaves PARs at the canonical cleavage site (PAR1 at Arg41 and PAR3 at Lys38), unmasking the tethered ligand domain, which binds to the second extracellular loops of the cleaved receptors. ^{75,77,78} Activated PARs couple to multiple G protein-dependent and β -arrestin-dependent signaling pathways. ^{62,79} aPC cleaves the PARs at sites distinct from the canonical cleavage site, (PAR1 at Arg46 and PAR3 at Arg41) which unmask a different tethered ligand. It is thought that the binding of the specific tethered ligand activates distinct and specific signaling pathways. ^{71,76}

The phenomenon that multiple ligands bind to the same GPCR and elicit disjunct signaling events is referred to as biased signaling. ⁸⁰ Some proteases such as elastase that cleave PARs do not reveal tethered ligands, suggesting that proteolysis alone may activate the receptor. Additionally cathepsin G cleaves PARs but generates an inactive tethered ligands, thereby disarming its proteolytic activation. ⁷¹

New approaches aiming to prevent side effects of orthostatic PAR1 inhibitors, which interact at the ligand-binding site and block all signaling *via* PAR1, have led to the development of several allosteric PAR1 inhibitors. These inhibitors target PAR1 at its cytoplasmic domain and selectively block certain signaling events. For example, specific inhibition of $G\alpha_q$ signaling using pepducins and parmodulins spares the cytoprotective pathways induced by aPC (Fig. 6). ⁸¹⁻⁸³ Parmodulin-2 mediated PAR1 biased agonism preferentially blocks $G\alpha_q$ and allows $G\alpha_{12/13}$ signaling (Fig. 6). However, any *in vivo* relevance of biased PAR1 signaling is lacking.

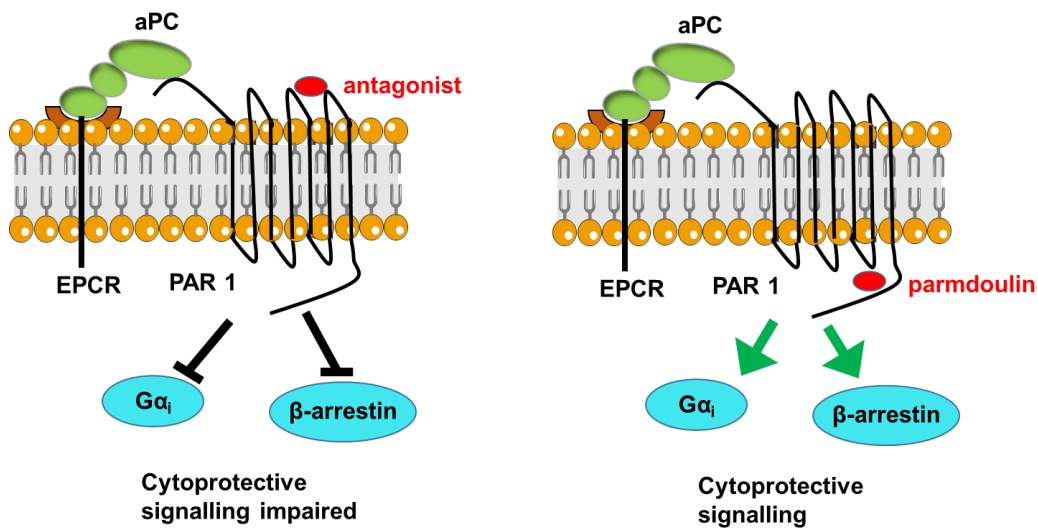


Figure 6: Parmodulin mediated PAR1 biased agonism.

PAR1 cleavage by aPC leads to cytoprotective signaling. Orthostatic PAR1 inhibitors inters at the ligand-binding site and block all signaling from PAR1 (**left**). Parmodulins bind at the cytoplasmic domain of the PAR-1 and selectively block Gα_q signaling, sparing the cytoprotective pathways induced by aPC (**right**).

1.4.5 Activity-selective aPC variants

Given aPC's strong anti-inflammatory properties human recombinant aPC received approval for sepsis treatment, but was eventually withdrawn from the market, partially due to its intrinsic anticoagulant properties and its failure to replicate previously reported efficacy.^{76,79} Protein engineering enabled the generation of aPC mutants that allow more specific studies of the mechanism of action for aPC's multiple activities, and provide safer and more effective aPC mutants with reduced bleeding risk (Fig. 7).

Protein engineering approaches for aPC were built upon the assumption that the enzymatic substrates (factors Va and VIIIa *versus* PAR1/PAR3) and aPC's cofactors (phospholipids/protein S *versus* EPCR) for its anticoagulant and cytoprotective activities require different structural domains of PC. Thus, a positively charged extended surface involving multiple polypeptide loops on aPC is essential for its interactions with its substrate factor Va (Fig. 7).^{57,62,84}

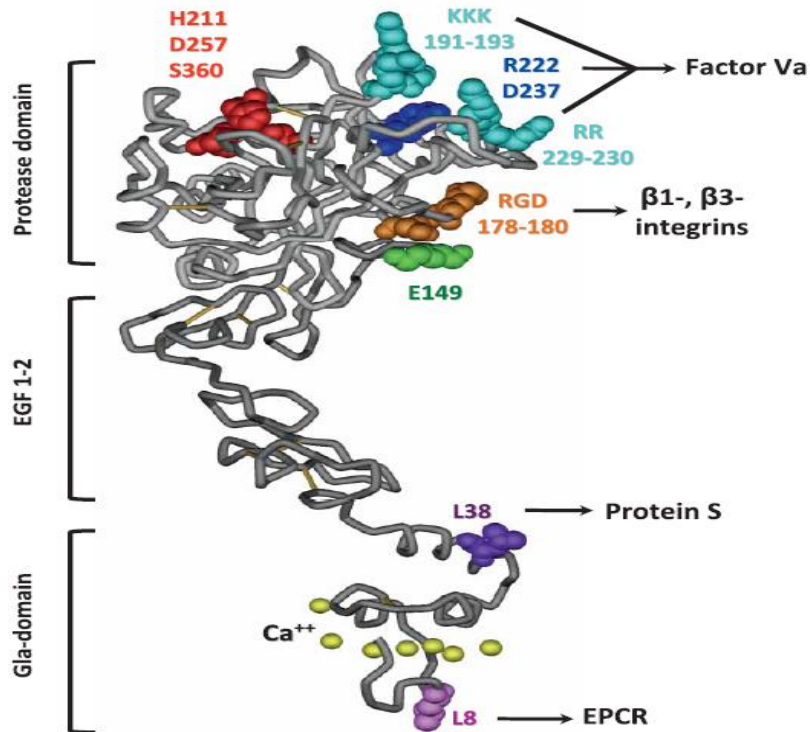


Figure 7: Structural illustration of human aPC highlighting different residues involved in mediating the cytoprotective and anticoagulant functions.

The light chain comprises the Gla-domain and EGF domains 1 and 2. The heavy chain forms the protease domain with the catalytic center triade Ser360-Asp257-His211 (red). The last residue of the light chain resolved in crystal structures is E149 (green). Alanine substitution of this residue enhances aPC's anticoagulant activity, but diminishes its capacity to signal via the EPCR-PAR1 axis. Mutations of L8 or L38 (purple) in the Gla-domain abolish the interaction with EPCR or protein S, respectively. The RGD motif in the heavy chain (orange) binds β1 and β3 integrins. Alanine substitutions of positively charged lysine and arginine residues constituting the fVa interaction site (magenta) largely eliminate anticoagulant functions, without affecting the cytoprotective functions of APC. The same effect is obtained after constraining the structure of this exosite by introducing an artificial disulfide bond between R222 and D237 (dark blue). (*Adapted from Hartmut Weiler, Hämostaseologie; Aug;31(3):185-95.2011*).

As this factor Va exosite on aPC is not required for the interaction with PAR1, mutating these specific positive residues to alanine decreased aPC's anticoagulant activity yet retained normal cytoprotective activities (Fig. 7).⁷⁶

Cytoprotective-selective aPC mutants include RR229/230AA-aPC, 3K3A-aPC (KKK191-193AAA), 5A-aPC (the combination of 3K3A-aPC with RR229/230AA-aPC), R193E-APC, and Cys67-Cys82-APC (R222C/D237C).^{76,85} Anticoagulant-selective aPC mutants display impaired EPCR binding following mutation of the Gla domain (L8W, L8V)^{57,76,86}, an exosite for PAR1 on aPC (E330A and E333A)^{76,87} or the C-terminus of the aPC light chain (E149A-APC).⁸⁸ These mutants have impaired aPC cytoprotective activities.

Cytoprotective 3K3A-aPC is currently undergoing phase-II clinical evaluation for stroke (NCT02222714).⁷⁶ It is conceivable, but remains to be shown, that cyto-protective selective aPC variants protect against ischemia reperfusion induced myocardial infarction.

1.5 aPC's role in myocardial IRI

Patients with ST-elevation myocardial infarction (STEMI) and / or cardiogenic shock have decreased circulatory levels of aPC and increased inflammation, associated with increased mortality.^{89,90} The role of inflammation, mTOR signaling and coagulation proteases in myocardial IRI is well established, but whether these systems are mechanistically linked remains unknown.^{91,92} aPC is an important endogenous inhibitor of inflammation and in regard to myocardial IRI several studies demonstrated cardioprotection by aPC, which has been linked with apoptosis inhibition.^{11,14,93-96} However, apoptosis is less likely to promote myocardial IRI than other cell death forms associated with inflammation, such as pyroptosis.^{27,29,30,37} Considering the close association of myocardial IRI – as well as other forms of IRI – with a strong sterile inflammatory response and the anti-inflammatory properties of aPC we hypothesized that aPC protects from myocardial IRI and other forms of IRI by restricting Nlrp3 inflammasome activation.

1.6 mTOR signaling

Mammalian target of rapamycin (mTOR) is serine/ threonine protein kinase and consists of two multi-protein complexes, mTOR complex 1 (mTORC1) and mTOR complex 2 (mTORC2).⁹⁷ mTORC1 stimulate protein synthesis, cell growth, autophagy, and stress responses, whereas mTORC2 appears to regulate cell survival and polarity.

Both complexes of mTOR share the same catalytic subunit, mammalian lethal with sec-13 protein 8 (mLST8, which is also known as GbL), DEP domain containing mTOR-interacting protein (DEPTOR) and the Tti1/Tel2 complex. The regulatory-associated protein of mammalian target of rapamycin (raptor) and proline-rich Akt substrate 40 kDa (PRAS40) are specific to mTORC1, whereas rapamycin-insensitive companion of

mTOR (rictor), mammalian stress-activated map kinase-interacting protein 1 (mSin1) and protein observed with rictor 1 and 2 (protor1/2) are only specific for mTORC2.

A variety of signals including insulin and growth factors activate mTORC 1 by interacting with GTP bound form of Rheb which is considered to be a vital activator of mTORC1. The negative regulator of mTORC1 is a heterodimer protein complex of tuberous sclerosis complex 1 (TSC1; also known as hamartin) and tuberous sclerosis complex 2 (TSC 2; also known as tuberin). TSC1 is a pivotal inhibitor of mTORC1 and its deficiency causes constitutive mTORC1 activation (Fig. 8). Upon activation mTORC1 activates p70 ribosomal protein S6 kinase (p70S6K) and eukaryotic initiation factor 4E (eIF4E)-binding protein (4EBP) which regulate protein translation (Fig. 8).⁹⁸

Pharmacological inhibition of mTORC1 has been shown to limit ischemic injury in an animal disease of acute^{99,100} and chronic myocardial IRI.^{101,102} This was associated with reduced infarct size and improved cardiac function.¹⁰¹ In this regard a recent study has shown that mTORC1 inhibition limits Nlrp3 inflammasome activation in bone marrow derived macrophages (BMDMs).¹⁰³ mTORC1 signaling can be restricted by activation of AMP-activated protein kinase (AMPK) .¹⁰⁴ Intriguingly, aPC-mediated protection following myocardial infarction has been linked with AMPK activation.¹⁰⁵ As the regulation of mTORC1, AMPK, and Nlrp3 activation are mutual, we hypothesize that aPC conveys myocardial protection by concurrently regulating mTOR, AMPK and Nlrp3 signalling.

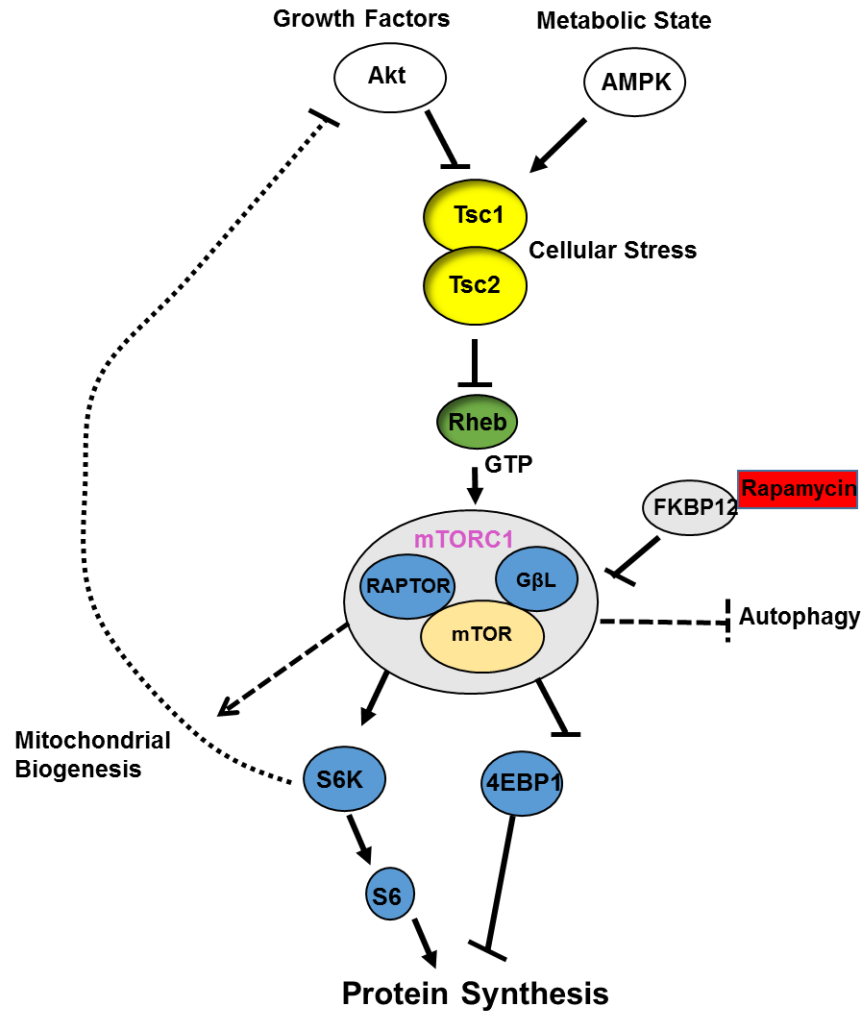


Figure 8: The schematic illustrations of the mTORC1 pathway.

mTOR complex 1 (mTORC1) is composed of mTOR, Raptor, GβL, and DEPTOR and is inhibited by rapamycin. It is a master growth regulator that senses and integrates diverse nutritional and environmental cues, including growth factors and cellular stress. It promotes cellular growth by phosphorylating substrates that potentiate anabolic processes such as mRNA translation and lipid synthesis, or limit catabolic processes such as autophagy. The small GTPase Rheb, in its GTP-bound state, is a necessary and potent stimulator of mTORC1 kinase activity, which is negatively regulated by its GAP, the tuberous sclerosis heterodimer TSC1/2. Most upstream inputs are funneled through Akt, AMPK and TSC1/2 to regulate the nucleotide-loading state of Rheb.

2 Aim of the study

Amelioration of myocardial IRI by aPC has been associated with reduced apoptosis, an immunologically silent form of cell death. However, myocardial IRI is strongly associated with inflammation and hence we speculated that inflammasome activation might be the leading pathomechanism. We first aimed at studying the kinetics of the Nlrp3 inflammasome and apoptosis activation following myocardial IRI. A function of Nlrp3 inflammasome is increasingly recognized in myocardial IRI. However, whether Nlrp3 inflammasome activation is the culprit remains obscure. Furthermore, whether inflammasome suppression is the primary mechanism underlying aPC's protective effects and the relative contributions of cyto-protective *versus* the anti-coagulant properties of aPC following myocardial IRI have not been studied. The underlying mechanism through which aPC may restrict Nlrp3 inflammasome activation, the receptors involved, and the relevant cell types remain likewise subsequently unknown. PARs are known to be elevated in myocardial IRI and demonstrate pleiotropic effects and – depending on the activator and co-receptors involved can convey cell-damaging or cell-protective effects. Thus, whether PAR1 biased agonism using parmodulins is sufficient to mimic aPC's effect to limit inflammasome activity and to convey cardioprotection in myocardial IRI has been not investigated previously. Addressing these questions is expected to provide new insights into potential innovative therapeutic approaches to myocardial IRI.

We therefore aimed to study (A) the pathogenetic role of inflammasome versus apoptosis, (B) the primary mechanism underlying aPC's cyto-protective effects in myocardial IRI, (C) the role of PAR1 biased signalling in myocardial IRI, and (C) the mechanistic relevance of mTORC1 in myocardial IRI.

Considering recent data showing that inflammasome activation contributes to IRI in other tissues, including the kidney, we inferred that suppression of inflammasome by aPC may have implications beyond myocardial IRI. To this end we aimed to study role of aPC and the Nlrp3 inflammasome in renal IRI.

3 Material and methods:

3.1 Reagents:

Table 1: List of reagents used in current study.

REAGENTS	SOURCE	CATALOGUE #
Nlrp3	Santa Cruz Biotechnology	#sc-66846
Nlrp3	Cell Signalling Technology	#15101
Caspase-1	Santa Cruz Biotechnology	#sc-56036
Caspase-1	Merck Millipore	#AB1871
IL-1 β	Boster Immunoleader	#PA1351
Caspas-3	Cell Signalling Technology	#9662S
Caspase-7	Cell Signalling Technology	#9492S
Bax	Cell Signalling Technology	#2772S
Raptor	Cell Signalling Technology	#2280
HK-1	Cell Signalling Technology	#2024
P70 S6	Cell Signalling Technology	#9202
Phospho-p70 S6	Cell Signalling Technology	#9234
TSC-1	Cell Signalling Technology	#4906
KIM-1	Abcam	#ab47635
GAPDH	Sigma-Aldrich	#G8795
Rabbit IgG	Cell Signalling Technology	#7074
Mouse IgG	Abcam	#ab6728
Caspase-11	Cell Signalling Technology	#14340
IRAK-1	Cell Signalling Technology	#4504
Rictor	Cell Signalling Technology	#2140
EPCR	R & D systems	#AF2749
ApoER2	Novus Biologicals	#NB100-2216
CD11b	Novus Biologicals	#NB110-89474SS
S1P1	Merck Millipore	#MABC94
Texas Red-conjugated anti-mouse	Vector Laboratories	#TI-1000

FITC-conjugated anti-mouse	Vector Laboratories	#FI-1000
Tamoxifen	Sigma-Aldrich	#T5648
LPS	Sigma-Aldrich	#LPS25
ATP	Sigma-Aldrich	#A2383
PAR-4 (Blocking antibody)	Santa Cruz Biotechnology	#SC-8461L
EPCR (mAb 1560; Blocking antibody)	Dr. Charles T. Esmon Laboratory of Coagulation Biology, Oklahoma Medical Research Foundation, Oklahoma City, United States.	
HAPC 1573	Dr. Charles T. Esmon Laboratory of Coagulation Biology, Oklahoma Medical Research Foundation, Oklahoma City, United States	
Parmodulin-2	Dr. Chris Dockendorff, Dept. of Chemistry, Marquette University, Milwaukee, WI, USA	
3K3A-aPC	Dr. John H. Griffin, Department of Molecular Medicine, The Scripps Research Institute, La Jolla, CA, USA	
P1pal-12S	Genescript	#RSLSSSAVANRS
Gelatin	Sigma-Aldrich	#G1393
Pancreatin	Sigma-Aldrich	#P3292
Collagenase Type II	Worthington	#LS004176
mEPCR shRNA	GE Dharmacon	#19124
mApoER2 shRNA	GE Dharmacon	#16975
CalPhos Mammalian	Takara-Clonetech	#631312

Transfection Kit		
cDNA synthesis Kit	Invitrogen	#18080051
S1P1 Antagonist	Tocris	#3602
NIF (CD11b) Antagonist	R&D systems	#5845-NF-050
FLICA™ Caspase-1 activity assay kit	ImmunoChemistry Technologies, LLC	#97
mouse IL-1beta ELISA kit	R&D Systems	#MLB00C
mouse IL-18 ELISA kit	Medical & biological laboratories co., Ltd	#7625
TTC	Sigma-Aldrich	#T8877
RPMI 1640	Sigma-Aldrich	#R0883
Trypsin-EDTA	Thermo Fisher Scientific	#2500-054
Penicillin/Streptomycin	Thermo Fisher Scientific	#15140-122
HEPES	Thermo Fisher Scientific	#15630-056
Pierce™ BCA protein assay kit	Perbio Science	#23227
Vector shield mounting medium with DAPI	Vector Laboratories	#CA94010
PVDF membrane	Merck Millipore	#IPVH00010
Immobilion™ chemiluminescent HRP substrate	Merck Millipore	#WBKLS0500
Powdered milk	CARL ROTH	#T145.2
Albumin fraction	CARL ROTH	#8076.2
Rotiphorese® Gel	CARL ROTH	#3029.1
Medium 199	Thermo Fisher Scientific	#3115002
Horse serum	Thermo Fisher Scientific	#26050088
Trizol Reagent	Life Technologies	#15596018
Phosphate Buffer Saline (PBS)	Thermo Fisher Scientific	#10-010-031
Rompun 2%	Bayer	770-081

Ketamine	Beta-pharm	798-744
Tween-20	CARL ROTH	#9127.1
2-Propanol	CARL ROTH	#CP41.1
HBSS	Thermo Fisher Scientific	#14025-050
DMEM	Sigma-Aldrich	#D6429
Paraformaldehyde	Thermo Fisher Scientific	#PI28908
Turbofect transfection kit	Thermo Fisher Scientific	#R0531
Protease Inhibitor Cocktail	Roche Diagnostics	#11 836 153 001

3.2 Mice

PAR2^{-/-}, PAR3^{-/-}, Nlrp3-A350V and RosaERT Cre mice were obtained from the Jackson Laboratory (Bar Harbor, Me). PAR1^{-/-} mice were kindly provided by Eric Camerer (Paris, France). In the current study we used littermates which have been backcrossed for at least 10 generations on a C57BL/6 or C57BL/6J background, respectively. Wild type mice (C57BL/6) were obtained from Janvier Lab (France). Only male mice were used throughout this study. All animal experiments were conducted following standards and procedures approved by the local Animal Care and Use Committee (Landesverwaltungsamt Halle, Germany).

3.2.1 Myocardial ischemia reperfusion injury model

All mice were anesthetized with sodium ketamine (100 mg/kg body weight, i.p.) and xylazine (10 mg/kg body weight, i.p.). In preliminary experiments we determined that equal dosing was required and sufficient for the different genotypes. After endotracheal intubation ventilation was performed using 0.3 L/min of oxygen and 1.5 %isoflurane. Mice were placed on a 37°C thermostatically controlled operating platform. The surgery procedure did not differ among the groups. A left parasternal incision was made between the third and fourth ribs. The epicardium was removed to expose the heart.

The left anterior descending (LAD) artery was ligated using an 8-0 silk suture. Myocardial ischemia reperfusion injury (IRI) was induced by cautiously tightening the ligature around LAD. After LAD ligation the wound was temporally closed using a tape. After 90 min of ischemia the ligation was removed to restore blood flow through the LAD artery. Recovery of blood flow was visually ensured (as indicated by a reddish color). The chest was closed with continuous 4-0 polypropylene sutures. All animals received subcutaneous analgesic (buprenorphine 0.1 mg/kg) post-surgery. Mice were placed in a temperature controlled (~35°C) environment during the recovery phase and were regularly inspected. After full recovery animals were returned to their cages with free access to food and water. No differences in the recovery time between the different genotypes were noticed. Sham surgery consisted of an identical procedure without LAD ligation. After 24 hr of reperfusion animals were sacrificed. Blood samples were obtained from the inferior vena cava and the heart was isolated for further analyses. Different mice were used for infarct size determination and for protein expression. The overall goal of this procedure is to temporarily occlude blood flow into portion of the heart to produce IRI to mimic a myocardial infarct.

3.2.2 *In vivo* intervention studies

For the myocardial IRI model (LAD ligation for 90 min followed by 24 hr of reperfusion) mice were either injected with PBS (control, equal volume, i.p.), aPC (1mg/kg, i.p.)¹⁰⁶, aPC-HAPC1573 complex (aPC was pre-incubated before injection with HAPC1573 antibody at a 1:1 molar ratio for 10 min under gentle agitation to block its anticoagulant activity)^{106,107}, an aPC variant lacking specifically anticoagulant function (3K3A-aPC, 1mg/kg, i.p.)^{96,108}, the inhibitory PAR-1 peptidic (P1pal-12S; 2.5mg/kg, subcutaneously) followed by aPC (1mg/kg, i.p.)¹⁰⁹⁻¹¹¹, or parmodulin-2 (5mg/kg, i.v.)⁸¹ 30 min prior to myocardial IRI. A subset of mice were treated with PBS (control, equal volume, i.p.) or aPC (1mg/kg, i.p.) 30 min after starting reperfusion. In renal IRI experiments (bilateral renal pedicle occlusion, 30 min followed by 24 hr of reperfusion)^{81,82} mice were either injected with PBS (control, 1mg/kg, i.p.) or aPC (1mg/kg, i.p.) 30 min prior to IRI. For generation of Nlrp3 gain of function mutant mice,

we crossed mice containing an inducible Nlrp3 gain of function mutant (Nlrp3A350V LoxP/LoxP, LoxP-Cre-recombinase dependent expression of the constitutively active Nlrp3A350V mutant) with mice ubiquitously expressing inducible Cre-recombinase under the control of the estrogen receptor T2 (RosaCre-ER^{T2}), yielding Nlrp3A350V^{LoxP/LoxP} x RosaCre-ER^{T2} mice (thereafter referred to as Nlrp3V-ER mice). Nlrp3V-ER mice were treated with tamoxifen (5 mg/kg in an ethanol: sunflower oil solution 1:9; i.p.)³⁰ daily for 5 days to induce expression of the mutant gene. 24 h after the last tamoxifen injection mice were subjected to myocardial IRI or sham surgery.

3.2.3 Determination of Myocardial Infarct size

After 24 hours of reperfusion, animals were sacrificed and hearts were removed for further analyses. Fresh hearts were cut into 5 slices beginning from the tip of the heart upto the level where the ligature was set. Heart slices were dropped into tubes containing 1% TTC solution and were kept on a heating plate at 37 °C for 5 minutes. The slices were then fixed in 10% formalin solution and incubated for 10 minutes at room temperature (RT). Photos of heart slices were taken using digital camera (Nikon D750 KIT2) and infarct area was determined using Image J software.

3.2.4 Renal ischemia reperfusion injury model

Renal ischemia reperfusion injury was induced as described.¹⁰⁷ All mice were anesthetized with sodium ketamine (100 mg/kg body weight, i.p.) and xylazine (10 mg/kg body weight, i.p.). In preliminary experiments we determined that equal dosing was required and sufficient for the different genotypes. Mice were routinely observed during the post-operative recovery phase and no differences in the recovery time between the different genotypes were noticed. Body temperature was maintained by placing the mice on a 37°C thermostatically controlled operating platform. Post-surgery mice were kept in a heated environment during the recovery phase.

The surgery procedure did not differ among the groups. Only age-matched mice were used. Body fluid was maintained in all mice by subcutaneous administration of 300 µL 0.9% normal saline pre-operatively. After anaesthetizing the mice, midline abdominal incision was made and both kidneys were exposed. The main renal arteries and veins

were identified using a stereotactic microscope (Olympus, Germany), and great care was taken to identify all vascular branches. All renal arteries and veins were then bilaterally occluded for 30 min with non-traumatic microaneurysm clamps (F.S.T Instruments, Germany). To help maintain thermoregulation during surgery, the intestine was relocated and the abdomen was temporarily closed with few stitches. After 30 min of renal ischemia the abdomen was reopened and the clamps were removed. The kidneys were inspected for at least 1 minute to ensure restoration of blood flow (as indicated by a pink color) and 0.5 ml of pre-warmed (37°C) normal saline was instilled into the abdominal cavity. The abdomen was closed with continuous 4-0 polypropylene sutures. All animals received subcutaneous analgesic (buprenorphine 0.1 mg/kg) at the end of surgery. Mice were placed in a temperature controlled (~35°C) environment during the recovery phase and regularly inspected. After full recovery animals were returned to their cages with free access to food and water. Sham surgery consisted of an identical procedure without application of the micro aneurysm clamps. Animals were sacrificed 24h after renal ischemia reperfusion injury or sham surgery to obtain blood and tissue samples.

3.2.5 Determination of serum BUN and creatinine

Serum BUN and creatinine were measured as described.^{107,112} Mice were anesthetized 24h after reperfusion with sodium ketamine (100 mg/kg body weight, i.p.) and xylazine (10 mg/kg body weight, i.p.) and sacrificed. Blood samples were obtained from the abdominal vena cava and collected into tubes pre-filled with sodium citrate (final concentration 0.38%). Plasma was obtained by centrifugation at 2000 x g for 10 min. Renal dysfunction was evaluated by measuring serum levels of blood urea nitrogen (BUN) and creatinine according to the manufacturer's instructions. Serum BUN was measured using a kinetic test kit with urease (Roche Diagnostics, Cobas c501 module) and creatinine was determined by an enzymatic based kit (Roche Diagnostics, Cobas c501 module) at the Institute of Clinical Chemistry and Pathobiochemistry, medical faculty, Otto-von-Guericke University, Magdeburg, Germany.

3.3 Preparation of activated protein C

Activated protein C was generated as previously described with slight modifications.¹⁰⁷ Prothrombin complex (Prothromplex NF600), containing all vitamin K dependent coagulation factors, was reconstituted with sterile water and supplemented with CaCl_2 at a final concentration of 20 mM. The column for purification of protein C was equilibrated at RT with 1 liter of washing buffer (0.1 M NaCl, 20 mM Tris, pH 7.5, 5 mM benzamidine HCl, 2 mM Ca^{2+} , 0.02% sodium azide). The reconstituted prothrombin complex was gravity eluted on a column filled with Affigel-10 resin covalently linked to a calcium-dependent monoclonal antibody to PC (HPC4). The column was washed first with two column volumes of washing buffer and then two column volumes with a wash buffer rich in salt (0.5 M NaCl, 20 mM Tris, pH 7.5, mM benzamidine HCl, 2 mM Ca^{2+} , 0.02% sodium azide). Then the benzamidine was washed off the column with a buffer of 0.1 M NaCl, 20 mM Tris, pH 7.5, 2 mM Ca^{2+} , 0.02% sodium azide. To elute PC the column was gravity eluted with elution buffer (0.1 M NaCl, 20 mM Tris, pH 7.5, 5 mM EDTA, 0.02% sodium azide, pH 7.5) and 3 ml fractions were collected. The peak fractions were identified by measuring absorbance at 280 nm. The peak fractions were pooled. The recovered PC was activated with human plasma thrombin (5% w/w, 3 hr at 37°C). To isolate activated protein C (aPC) ion exchange chromatography with FPLC (ÄKTAFPLC®, GE Healthcare Life Sciences) was used. First, thrombin was removed with a cation exchange column MonoS (GE Healthcare Life Sciences). Then a MonoQ anion exchange column (GE Healthcare Life Sciences) was equilibrated with 10% of a 20 mM Tris, pH 7.5, 1 M NaCl buffer. After applying the solution that contains aPC a 10-100% gradient of a 20 mM Tris, pH 7.5, 1 M NaCl buffer was run through the column to elute aPC at a flow of 1-2 ml/min under continuous monitoring of OD and conductivity. APC eluted at ~36 mS/cm by conductivity or at 40% of the buffer. Fractions of 0.5 ml were collected during the peak and pooled. Proteolytic activity of purified aPC was ascertained with the chromogenic substrate SPECTROZYME® PCa.

3.5 Immunoblotting

Proteins were isolated and immunoblotting was performed as described.^{106,107,110,112-114} Cell lysates were prepared in RIPA buffer (50 mM Tris at pH 7.4, 1% Nonidet P-40, 0.25% sodium deoxycholate, 150 mM NaCl, 1 mM EDTA, 1 mM Na₃VO₄, and 1 mM NaF supplemented with protease inhibitor cocktail). Lysates were centrifuged (10,000 × g for 10 min at 4 °C) and insoluble debris was discarded. The protein concentration in supernatants was quantified using BCA reagent. Equal amounts of protein were electrophoretically separated on 7.5%, 10% (vol/vol) or 12.5% (vol/vol) SDS polyacrylamide gels, transferred to PVDF membranes, and probed with the desired primary antibodies overnight at 4 °C. Membranes were then washed with TBST and incubated with anti-mouse (1:2,000), anti-rat IgG (1:2,000) or anti-rabbit IgG (1:2,000) horseradish peroxidase-conjugated antibodies, as indicated. Blots were developed with the enhanced chemiluminescence system. To compare and quantify levels of proteins, the density of each band was measured by using ImageJ software. Equal loading was confirmed by immuno-blotting with GAPDH antibody.

3.6 Bone marrow derived macrophages (BMDM)

3.6.1 Preparation of L929 conditioned medium (LCM)

A vial of L929 fibroblasts was thawed at 37°C and gently decanted into 15 ml falcon and 10ml DMEM-10 medium was added. Following centrifugation at 200 x g for 5 minutes at room temperature (RT), pellet was resuspended in 5 ml DMEM-10 medium. With gentle pipetting cells were grown into a T25 tissue culture flask in a humidified incubator with 5 % CO₂ at 37°C. When cells were grown to 80-90 % confluency, they were lifted with 5 ml 1x trypsin/PBS and centrifuged. Pellet was again resuspended in 15 ml DMEM-10 medium and transferred to T75 tissue culture flask. Again after 80-90 % confluency same procedure was repeated and after centrifugation cells were transferred to T175 tissue culture flask. When cells reached to 80-90% confluency, they were split into 1:5 to new T175 cell culture flasks. When there were enough cells to make 20-25 flasks, cells were split into 1:5 into new T175 flasks containing 50 ml rather than 30 ml DMEM-10 medium and left for 10 days. Afterwards, supernatant was harvested and centrifuged

at 1200 x g, filtered through 0.45 µm filters and frozen at -20°C. L929 conditioned medium was filtered through 0.22 µm filter when added to RPMI-1640 medium.

3.6.2 Isolation and culture of BMDMs

Bone marrow derived macrophages (BMDM) were isolated and cultured as described elsewhere.¹¹⁵⁻¹¹⁷ Mice were sacrificed and femurs were flushed with medium (RPMI 1640 with 2% FBS, 10 units/ml heparin, penicillin, and streptomycin) using a 25 G needle. To remove osseous particles the solution was passed through sterile 40 µm nylon Cell Strainer (Falcon) and collected in a 50 ml tube. Cells were centrifuged at 900 x g, for 10 min, at 4°C. Supernatant was discarded and the cell pellet was washed twice with 50 ml of serum-free RPMI (RPMI 1640 with 20 mM HEPES, penicillin, and streptomycin). Following centrifugation at 900 x g, for 5 min, at 4°C cells were further washed with 1 x PBS and resuspended in culture medium RPMI-1640 supplemented with 30 % L929 cell-conditioned medium and 20 % FBS. This procedure was repeated twice to remove dead cells. After the final washing step pelleted cells were resuspended in above culture medium. Cells were cultured for 7 to 10 days until ~80 % confluence. The purity of cells was confirmed by CD11b staining and FACS analyses and was consistently found to be higher than 90 %. These cells were used as BMDM for experiments.

3.7 Isolation and culture of neonatal cardiomyocytes and cardiac fibroblasts

Primary neonatal cardiomyocytes and cardiac fibroblasts were isolated as described elsewhere.¹¹⁸ New born mice (age: 1 day) were decapitated and hearts were removed and placed in ice-cold 1 x ADS solution (6.8 g NaCl, 4.76 g HEPES, 0.12 g NaH₂PO₂, 1.0 g glucose, 0.4 g KCl, 0.1 g MgSO₄, pH was adjusted to 7.4 using 1 M NaOH) in a petri dish. After removing the atria heart ventricles were transferred to a tube containing 1 ml fresh 1 x ADS solution. Using sharp scissors heart ventricles were cut into small pieces, which were allowed to settle down. Then ADS solution was removed and 1.5 ml of freshly prepared enzyme solution was added (180 ml 1 x ADS with ~16800 U collagenase II (60 mg) and 160 mg pancreatin). Tubes containing tissues pieces were

placed on a shaker at 800 rpm at 37°C. After 6 min tissue were taken from shaker and homogenate were pipetted up and down, digested tissues samples were allowed to settle down, and enzyme solution was discarded. Fresh 1.5 ml enzyme solution was added again and the same procedure was repeated, except that the incubation time was increased from 6 to 10 min. After each digestion step the supernatant were collected and eventually pooled in “dark” medium containing 25 ml horse serum, 12.5 ml FCS and 212.5 ml of “light” medium (375 ml DMEM 4500 mg/l glucose, 125 ml Medium 199, 5 ml HEPES, 5 ml of Penicillin/Streptomycin). Tubes containing cell suspension were centrifuged at 1200 x g for 6 min at room temperature (RT). Following centrifugation supernatant was discarded and the pellet was re-suspended in 1 ml FBS and placed on ice. This final cell preparation was initially seeded into non-coated cultured dishes for 30 min and cardiac fibroblasts were allowed to adhere. These fibroblasts were used as neonatal cardiac fibroblasts for experiments. For cardiomyocytes, non-adherent cells were collected and centrifuged at 1200 x g for 10 min at RT. After resuspension of the pellet in 37°C “dark” medium cells were seeded onto plates pre-coated with gelatin (0.2% gelatin in PBS) and maintained at 37°C, in 5% CO₂. The purity of cells, which was routinely determined using the cardiomyocytes marker cTNT, was higher than 90% as measured by FACS analysis. These cells were used as cardiomyocytes for further experiments.

3.8 Histology and immunohistochemistry

Sacrificed mice were perfused with ice-cold PBS and then with 4% buffered paraformaldehyde. Tissues were further fixed in 4 % buffered paraformaldehyde for 2 days at 4°C, embedded in paraffin and processed for sectioning. Kidney injury was evaluated using hematoxylin and eosin stained histological sections. Images of the outer third of the kidney sections were randomly chosen and captured using an Olympus Bx43 Microscope (Olympus, Hamburg, Germany). All tubule within an image were individually scored on a scale of 0-4 based on the cellular damage as indicated by morphological signs of cell-swelling and tubular dilatation. The following scores were assigned: 0 – no cellular or tubular damage visible; 1 – damage visible, but less than 25% of the tubuli affected; 2 – 25 % to 50 % tubular damage; 3 – 50 % to 75 % tubular damage; and 4 –

more than 75 % damage. At least 5 random images per mouse and at least 6 mice per group were included in each group. All histological analyses were done by two independent blinded investigators. Images were obtained using an Olympus Bx43 Microscope (Olympus, Hamburg, Germany) at 20 x or 40 x magnification.

3.9 In situ caspase-1 activity assay

Caspase-1 activity was determined on frozen heart sections using the FLICA™ (Fluorochrome Inhibitor of Caspases) casp-1 assay (Immunochemistry Technologies lcc.).¹¹³ Frozen tissue sections (5 µM thick) were prepared and allowed to air-dry. Then slides were fixed with acetone for 1 min, rehydrated by washing (twice for 5 min) in PBST and slides were blocked for 20 min with blocking solution containing 20% aqua-block in media with 0.2 % Tween. Blocking solution was decanted and then 50 µL of 3 x FLICA™ working solution (freshly prepared by diluting 150 x stock solution into 1:50 in PBS) was applied per section and incubated at RT for 2 hr, protected from light. Tissues were washed with PBST (twice for 5 min). Tissues were mounted with vectashield mounting medium containing DAPI and fluorescent images were captured with an Olympus Bx43-Microscope (Olympus, Hamburg, Germany). Images analyses were done by using Image J software.

3.10 Hypoxia/reoxygenation (H/R) experiments

For hypoxia-reoxygenation (HR) injury neonatal cardiomyocytes cells were moved from routine culture conditions (“dark medium”, 37°C, in 5 % CO₂, 21 % O₂) into hypoxic atmosphere (1 % O₂, 94 % N₂, and 5 % CO₂) and serum- and glucose-depleted medium (HBSS) for 6 hr. For reoxygenation cells were returned to normal “dark” medium and 5 % CO₂, 21 % O₂.⁴ Control cells were serum-starved and maintained in HBSS for 6 hr, but they were continuously exposed to 21 % O₂. Cells were harvested after 12 hr of reoxygenation for protein isolation.

3.11 Reverse transcriptase polymerase chain reaction (RT-PCR)

To isolate RNA from cells, 3 ml TRIzol was added to 10 cm² dish. Cells lysed in TRIzol were incubated for 5 min at RT before adding 0.2 ml of chloroform per 1 ml of TRIzol. Following vigorous shaking, the mixture was centrifuged at 12,000 x g for 15 min at 4°C to separate different phases. The aqueous phase containing the RNA was transferred to a fresh tube and RNA was precipitated by adding 0.5 ml of 2-propanol per 1 ml of TRIzol reagent.

Following incubation at RT for 10 min samples were centrifuged at 12,000 x g for 10 min at 4°C. Supernatant was removed and RNA was washed by adding 1 ml 75 % ethanol per 1 ml of TRIzol. Samples were vortexed and centrifuged at 7,500 x g for 5 min at 4°C. The RNA pellet was air-dried for 5 min, redissolved in 20 µl DEPC-water at 55°C for 10 min. RNA concentration was measured in a photometer and a 1.8 % agarose gel was run to verify the purity and integrity of RNA.

cDNA was synthesized using 1 µg total RNA following treatment with DNase (5 U/5 µg RNA) followed by reverse transcription using RevertAid™ H Minus First Strand cDNA Synthesis kit (Fermentas, Heidelberg, Germany). Primers were custom synthesized by Thermo Fisher Scientific and PCR was performed using the Taq polymerase. PCR conditions were optimized as follows: (95°C for 3 min, then 35 cycles of 94°C, for 30 sec; 60°C for 20 sec; 72 °c for 20 sec; final extension at 72°C for 10 min) to detect the logarithmic increase of the PCR product, which was separated on a 1.8 % agarose gel and visualized by ethidium bromide (Et-Br) staining.

Expression was normalized to β-actin. Reactions lacking reverse transcriptase served as negative controls. Primers used in the current study are shown in table 2.

Table 2: List of primers used in current study.

Target	Primer Sequence
mPAR1	5'CCAGCCAGAATCAGAGAGGA3'
	5'TCGGAGATGAAGGGAGGAG3'
mPAR2	5'CCAGGAAGAAGGCAAACATC3'
	5'TGTCCCCCACCATAACCTC3'
mPAR3	5'CATCCTGCTGTTTGTGGTTG3'
	5'TACCCAGTTGTTGCCATTGA3'
mPAR4	5'GCAGACCTTCCGATTAGCTG3'
	5'CACTGCCGAGAACAGTACCA3'
mEPCR	5'CTACAACCGGACTCGGTATGAA3'
	5'CCAGGACCAGTGATGTGTAAG A3'
m β -actin	5'CTAGACTTCGAGCAGGAGATGG3'
	5'GCTAGGAGCCAGAGCAGTAATC3'

3.12 Production of lentiviral particles

VSV-G pseudo typed lentiviral particles were generated as described previously.^{112,119,120} Briefly, HEK 293T cells were transfected with pLKO1-PAR4 and pLKO1-EPCR plasmids together with the packaging plasmid (pCMV-dR8.91) and VSV-G-expressing plasmid (pVSV-G) using the standard calcium phosphate method. Lentiviral particles were harvested 2 and 3 days after transfection and concentrated by ultracentrifugation (50,000 x g, 2h, 2 times). After resuspension in HBSS buffer the viral particle concentration was determined by measuring p24 gag antigen by ELISA according to manufacturer's instruction (Biocat, Heidelberg Germany). Viral particles were stored at -80°C.

Knock down of PAR4 and EPCR in BMDMs was performed by lentiviral transduction with PLKO1-PAR4 and PLKO1-EPCR viral particles (GE Dharmacon). To specify the optimal titer for transduction, cells were infected with serial dilutions of viral particles and the number of surviving cells in the presence of 1 μ g/ml puromycin was determined.

Efficiency of knock down was assayed by RT-PCR and western blot. Cells transduced with non-specific shRNA served as controls.

3.13 IL-1 β and IL-18 immunoassay

Mouse blood samples were obtained from the inferior vena cava of anticoagulated mice (sodium citrate). Serum was obtained by centrifugation of blood samples for 10 min at 2000 x g at RT. Serum samples was stored at -80°C until analyses. We measured the concentrations of mouse IL-1 β by ELISA (R & D system) and mouse IL-18 by ELISA (Medical & biological laboratories co., Ltd), according to manufacturer's instructions.¹¹²⁻¹¹⁴

3.14 Statistical analysis

The data are summarized as the mean \pm SEM (standard error of the mean). Statistical analyses were performed with Student's t-test, ANOVA and post-hoc comparison with the method of Tukey or Bonferroni as appropriate. Statistics XL (www.statistixl.com) and Prism 5 (www.graphpad.com) software were used for statistical analyses. Statistical significance was accepted at values of $P < 0.05$.

4 Results

4.1 aPC restricts Nlrp3 inflammasome activation following myocardial IRI

To determine whether aPC restricts inflammasome activation in myocardial ischemia-reperfusion injury (IRI) we treated mice with aPC (1 mg/kg i.p.) or PBS (control). After 30 min we induced myocardial ischemia for 90 min and analyzed mice after 24^ohr of reperfusion (Fig. 9a). Congruent with previous reports aPC markedly reduced infarct size (Fig. 9b,c).^{11,14,93-95,121}

Reduction of infarct size by aPC was associated with reduced Nlrp3 inflammasome activation within the heart. Cardiac expression of Nlrp3 and cleavage of caspase-1 (cl-Casp1) and IL-1 β (cl-IL-1 β) were increased following myocardial IRI, but reduced following aPC pre-treatment (Fig. 9d,e). Concurrently, in situ caspase-1 activity after myocardial IRI was reduced by aPC (Fig. 9f,g). These changes were reflected by plasma cytokine levels. Thus, increased plasma IL-1 β and IL-18 levels after myocardial IRI were attenuated by aPC (Fig. 9h,i).

Additionally, treatment with aPC 30^omin after myocardial IRI also reduced myocardial infarct size and markers of inflammasome activation within the heart and plasma as efficient as aPC pre-treatment (Fig. 10). Thus, aPC efficiently restricts inflammasome activation following myocardial IRI.

4.2 Inflammasome activation precedes apoptosis following myocardial IRI

Amelioration of myocardial IRI by aPC has been associated with reduced apoptosis. Myocardial IRI is strongly associated with inflammation¹²². Hence, we speculated that inflammasome activation might be the leading pathomechanism. To gain insights into the temporal pattern of inflammasome and apoptosis activation following myocardial IRI we conducted kinetic studies. Hearts isolated at various time points after reperfusion (1 hr to 24 hr) were compared with hearts of sham-operated mice. An infarcted area was detected as early as 3 hr after reperfusion (Fig. 11a,b). Inflammasome activation within the heart preceded the detectable infarcted area (1 hr time point, cl-Casp1 and cl-IL-1 β , Fig. 11c,d), while markers of apoptosis activation increased at later time points (12 hr time point; cl-Casp3, cl-Casp7, BAX, Fig. 11c,d). These data establish that

myocardial inflammasome activation occurs early in IRI and precedes the detection of an infarcted area and – importantly – apoptosis activation.

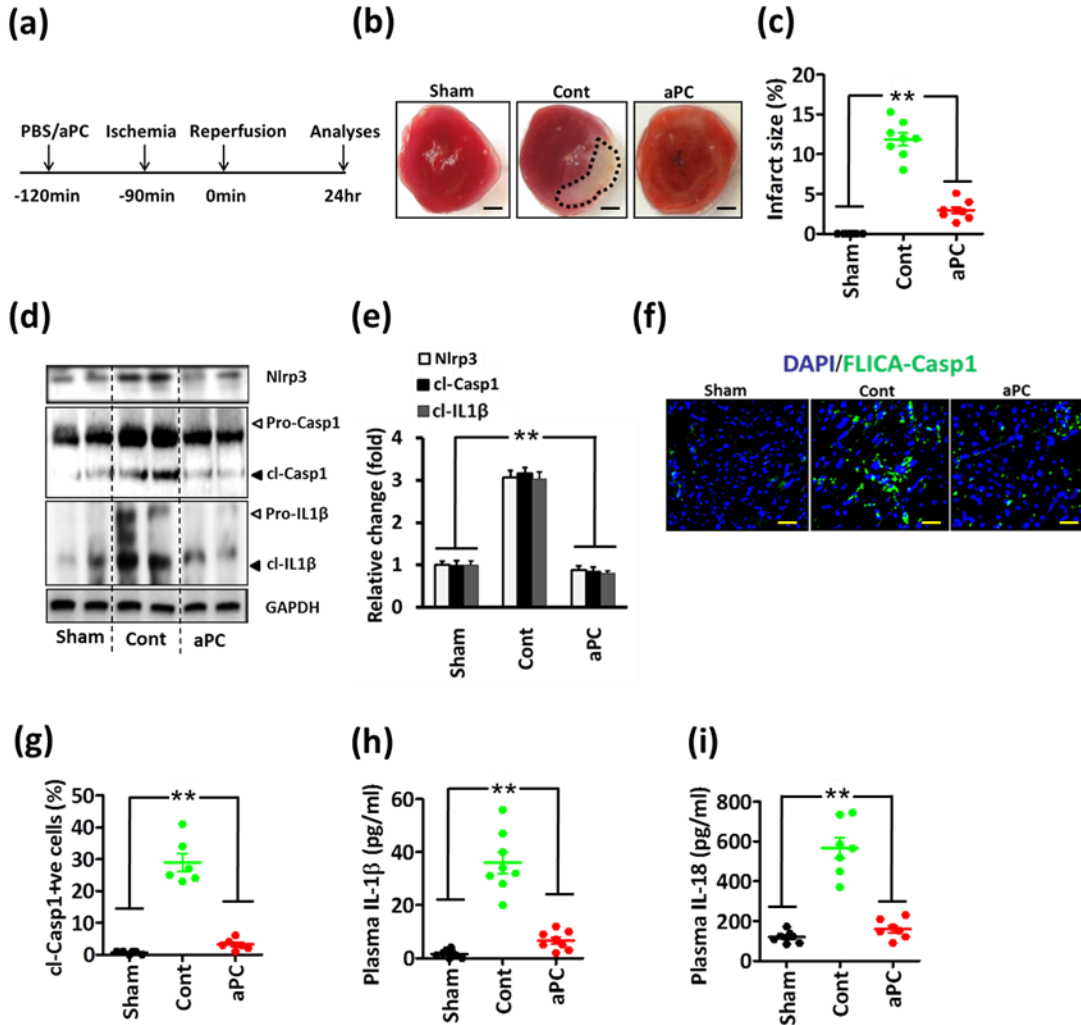


Figure 9: aPC pretreatment ameliorates inflammasome activation following myocardial IRI.

a: Experimental design.

b,c: aPC treatment reduces infarct size. Representative heart sections showing infarcted area detected by TTC staining (**b**, black dotted encircled area, size bar: 20 μ m) and dot-plot summarizing data (**c**).

d-i: aPC pretreatment significantly reduced cardiac Nlrp3 expression and cleavage of caspase-1 (cl-Casp1) and IL-1 β (cl-IL-1 β). Representative immunoblots (**d**, GAPDH: loading control) and bar graph summarizing data (**e**). Arrowheads indicate inactive (white arrowheads) and active (black arrowheads) form of caspase-1 or IL-1 β (**d**). The active form was quantified (**e**). aPC treatment reduces caspase-1 activity within infarcted area. Representative images of frozen sections incubated with FLICA-Casp1 probes (**f**, size bar: 20 μ m) and dot-plot summarizing data (**g**). aPC reduces plasma IL-1 β (**h**) and IL-18 levels (**i**) following myocardial IRI, dot-plots summarizing data. Sham operated mice (Sham) or mice with myocardial IRI without (Cont, PBS) or with aPC pretreatment (aPC). Data shown represent mean \pm SEM of at least 6 mice per group; ** P <0.01 (**c,e,g,i**: ANOVA, **b**: Mann-Whitney U test).

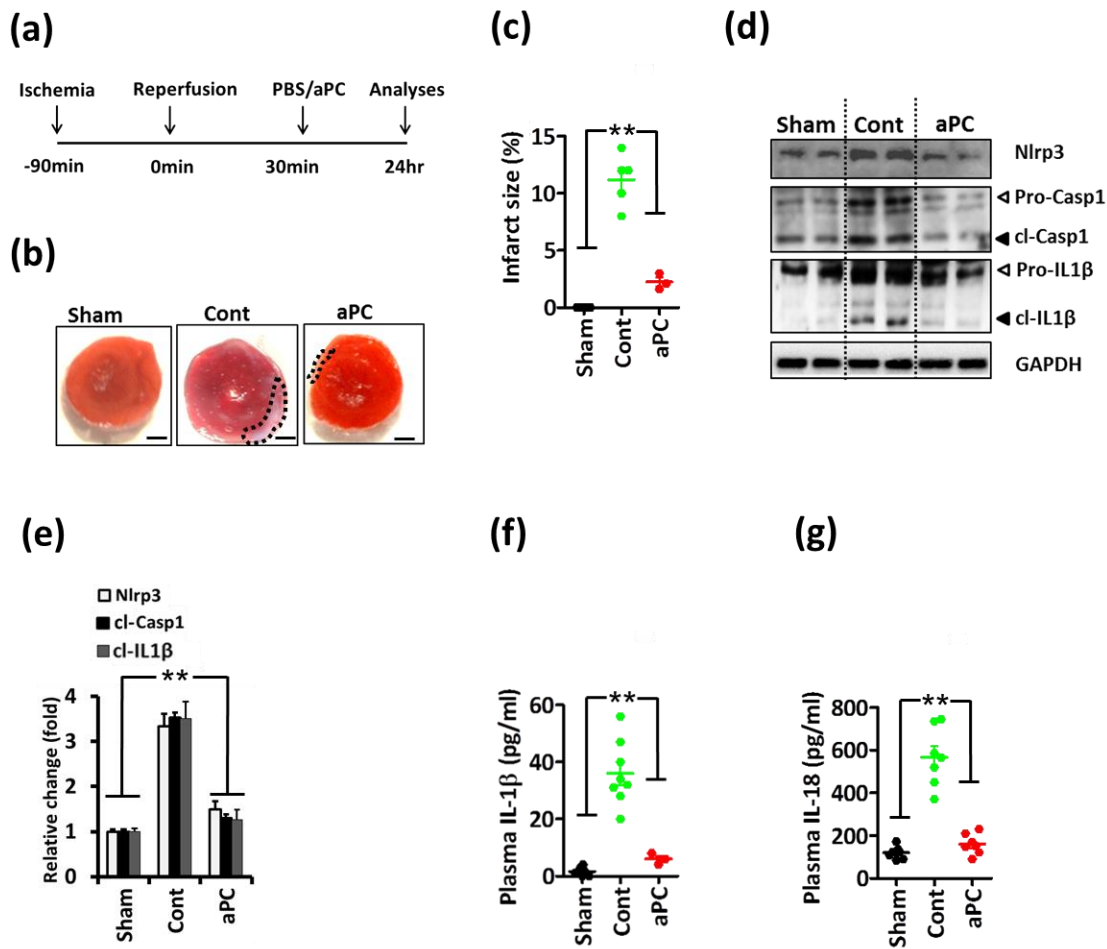


Figure 10: aPC post myocardial IRI treatment inhibits Nlrp3 inflammasome activation.

a: Experimental design.

b,c: aPC treatment 30 minutes after reperfusion reduces infarct size. Representative heart sections showing infarcted area detected by TTC staining (**b**, black dotted encircled area, size bar: 20 μ m) and dot-blot summarizing data (**c**).

d-g: aPC treatment 30 minutes after reperfusion significantly reduced cardiac Nlrp3 expression and cleaved caspase-1 (cl Casp1) and cleaved IL-1 β (cl IL-1 β). Representative immunoblots (**d**) and bar graph summarizing data (**e**); GAPDH: loading control. Arrowheads indicate inactive (white arrowheads) and active (black arrow heads) form of caspase-1 or IL-1 β (**d**). The active form was quantified (**e**).

Reduced plasma IL-1 β (**f**) and IL-18 levels (**g**), dot blots summarizing data.

Sham operated mice (Sham) or mice with myocardial IRI without (Cont, PBS) or with aPC posttreatment (aPC). Data shown represent mean \pm SEM of at least 6 mice per group; ** $P < 0.01$ (**c,e,f,g**: ANOVA).

4.3 Constitutively active Nlrp3 abolishes the protective effect of aPC in myocardial IRI

The kinetics of inflammasome and apoptosis activation following myocardial IRI suggest that inflammasome activation is the culprit and hence that inflammasome suppression is the primary mechanism underlying aPC's cytoprotective effect following myocardial IRI.

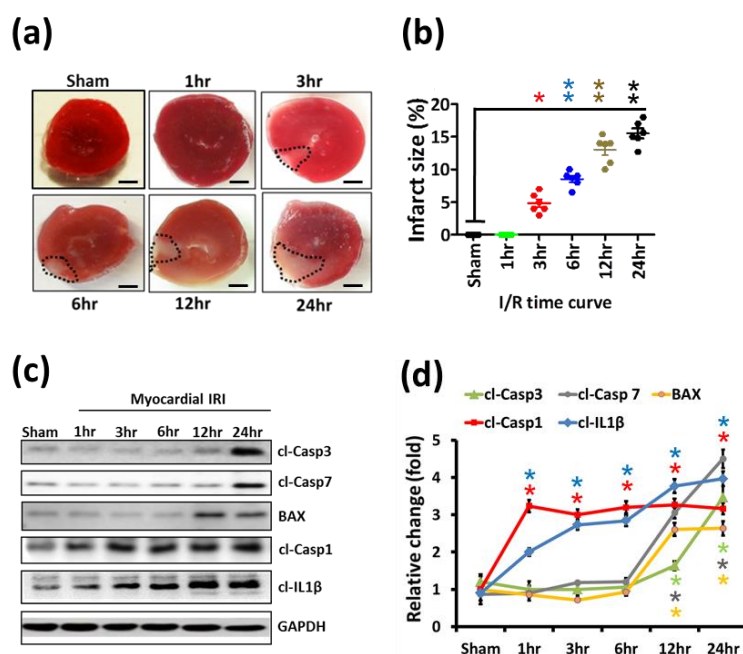


Figure 11: Inflammasome activation precedes apoptosis following myocardial IRI.

a-d: Kinetic analyses of infarct size and markers of inflammasome and apoptosis activation in hearts isolated at various time points after IRI (1 hr to 24 hr) compared to sham-operated mice were analyzed. **(a)** Representative images of TTC staining (infarct area: black dotted encircled area, size bar: 20 μm), **(b)** dot-plot summarizing data of infarct size (**b**, individual data points and mean±SEM), and **(c)** representative immunoblots of inflammasome (cleaved caspase-1, cl-Casp1; cleaved IL-1β, cl-IL1β) or apoptosis activation (cleaved caspase-3, cl-Casp3; cleaved caspase-7, cl-Casp7; BAX expression) markers; GAPDH; loading control (**d**, line graph summarizing immunoblot data. Data shown represent mean±SEM of at least 6 mice per group; *P<0.05, **P<0.01 (ANOVA).

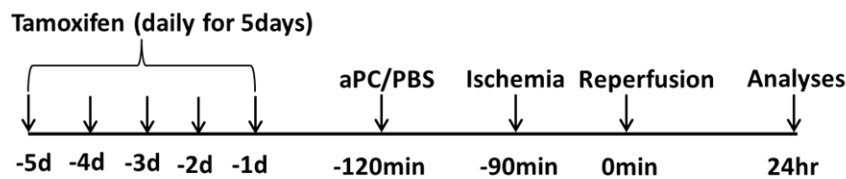
To ascertain whether inflammasome restriction is required for aPC's protective effect in myocardial IRI we crossed mice containing an inducible Nlrp3 gain of function mutant (Nlrp3A350V^{LoxP/LoxP}, LoxP-Cre-recombinase dependent expression of the constitutively active Nlrp3A350V mutant) with mice ubiquitously expressing inducible Cre-recombinase under the control of the estrogen receptor T2 (Rosa Cre-ER^{T2}), yielding Nlrp3A350V^{LoxP/LoxP} x Rosa Cre-ER^{T2} mice (thereafter referred to as Nlrp3V-ER mice).

Expression of the Nlrp3A350V mutant does not cause heart injury by itself and requires a second stimulus for inflammasome activation.³⁰ Mice were treated for 5 days with tamoxifen (5 mg/kg, i.p.) or PBS (control), which increased Nlrp3 expression in tamoxifen treated mice (Fig. 12a,b). Mice were injected with aPC or PBS (control) 24 hr after the last tamoxifen injection. After another 30 min myocardial ischemia was induced for 90 min and analyses were conducted 24 hr after reperfusion (Fig. 12a). In tamoxifen

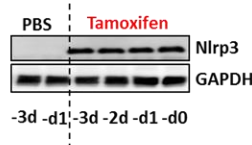
treated but sham operated mice no myocardial infarction was detected (Fig. 12c,d) and indices of inflammasome activation, remained normal (Fig. 12e-h), corroborating that expression of Nlrp3A350V mutant is not sufficient to cause myocardial inflammasome activation. Following myocardial IRI an infarcted area was readily detectable in Nlrp3V-ER mice (Fig. 12c,d).

Importantly, aPC treatment failed to reduce the infarct size in Nlrp3V-ER mice (Fig. 12c,d). Concurrently, aPC failed to reduce protein levels of Nlrp3 and cleavage of caspase-1 (cl-Casp1) and IL-1 β (cl-IL-1 β , Fig. 12e,f) and plasma IL-1 β and IL-18 levels (Fig. 12g,h) in Nlrp3V-ER mice following myocardial IRI. These data establish that in mice with a genetically superimposed bias for inflammasome activation aPC's protective effect in myocardial IRI is lost.

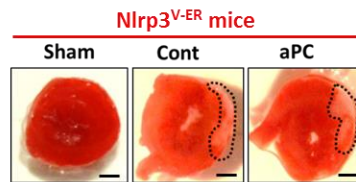
(a)



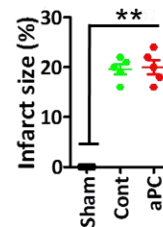
(b)



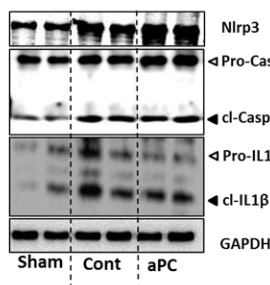
(c)



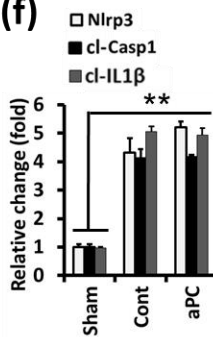
(d)



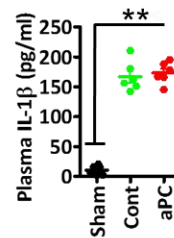
(e)



(f)



(g)



(h)

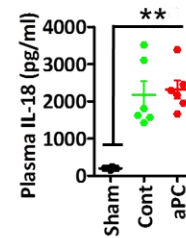


Figure 12: Constitutive active Nlrp3 abolishes the protective effect of aPC in myocardial IRI.

a: Experimental design.

b: Constitutively active Nlrp3^{A350V} abolishes the protective effect of aPC in myocardial IRI. Induction of Nlrp3^{A350V} expression following tamoxifen injection into Nlrp3^{V-ER} mice compared to PBS treated mice; representative immunoblots; GAPDH: loading control (**b**).

c,d: aPC treatment fails to protect against myocardial IRI in Nlrp3^{V-ER} mice. Representative heart sections showing infarcted area detected by TTC staining (**c**, black dotted encircled area; size bar: 20 μ m) and dot-plot summarizing data (**d**).

e-h: aPC fails to reduce Nlrp3 expression, cleavage of caspase-1 (cl-Casp1) and IL-1 β (cl-IL-1 β), and plasma IL-1 β and IL-18 levels in Nlrp3^{V-ER} mice following myocardial IRI. Representative immunoblots (**e**) and bar graphs (**f**) summarizing results; GAPDH: loading control; arrowheads indicate inactive (white arrowheads) and active (black arrowheads) form of caspase-1 or IL-1 β (**e**). The active form was quantified (**f**). Dot-plots of plasma IL-1 β and IL-18 levels (**g,h**).

Sham operated mice (Sham) or mice with myocardial IRI without (Cont, PBS) or with aPC pretreatment (aPC). Data shown represent mean \pm SEM of at least 6 mice per group; ** P <0.01 (**d,f-h**: ANOVA).

4.4 aPC prevents inflammasome activation in cardiac resident cells and macrophages *in vitro*

A role of the inflammasome in innate immune cells like macrophages is firmly established, but recent data demonstrated functional inflammasome in tissue resident cells, including cardiomyocytes.^{6,7,28-30,123} To identify in which cell types aPC prevents inflammasome activation in myocardial IRI we isolated primary bone marrow derived macrophages (BMDMs), primary neonatal cardiomyocytes, and primary neonatal cardiac fibroblasts. Cells were primed with LPS (500 ng/ml) and after 3 hr cells were either exposed to aPC (20 nM) or PBS (control). After 1 hr cells were exposed to adenosine-triphosphate (ATP) or PBS (control) for 3 hr to activate the Nlrp3 inflammasome.^{103,124} The LPS/ATP mediated induction of Nlrp3 expression and cleavage of caspase-1 (cl-Casp1) and IL-1 β (cl-IL-1 β) were prevented by aPC in all three cell-types (Fig. 13a-f). Thus, aPC dampens inflammasome activation not only in innate immune cells, but also in resident cardiac cells. While ATP is considered to induce inflammasome activation during myocardial IRI¹²⁴ we ascertained the efficacy of aPC in the context of hypoxia reoxygenation (H/R) injury in cardiomyocytes. Exposure of primary neonatal cardiomyocytes to hypoxia (6 hr) followed by reoxygenation (12 hr) without prior LPS stimulation was sufficient for inflammasome activation, increased Nlrp3 expression and cleavage of caspase-1 (cl-Casp1) and IL-1 β (cl-IL-1 β , Fig. 13g,h). H/R-induced inflammasome activation in primary cardiomyocytes was efficiently prevented by aPC (Fig. 13g,h). Taken together, aPC prevents inflammasome activation

both in innate immune cells (macrophages) and resident cardiac cells (cardiomyocytes, cardiac fibroblasts).

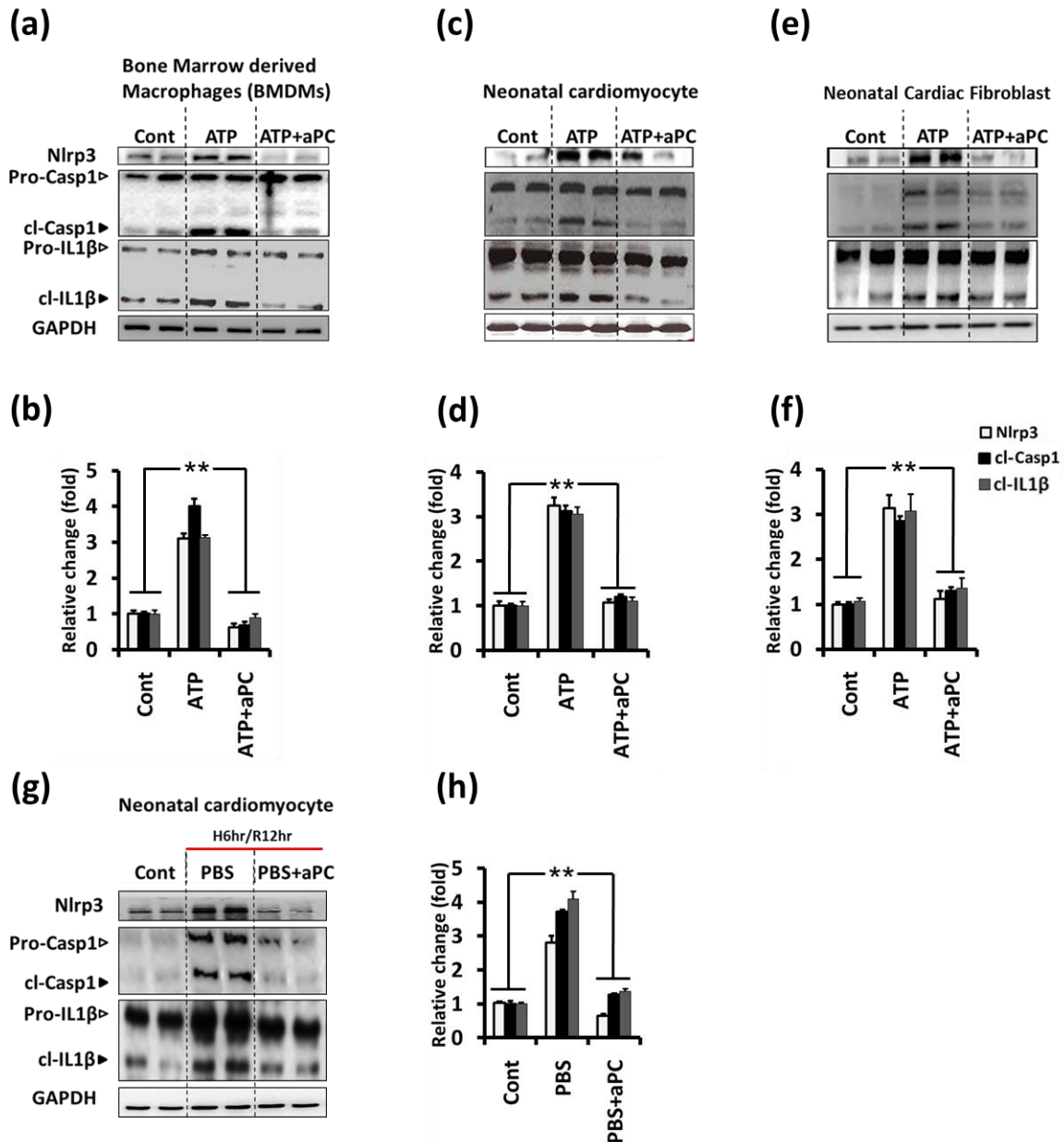


Figure 13: aPC prevents inflammasome activation in cardiac resident cells and macrophages *in vitro*.

a-f: In mouse bone marrow derived macrophages (BMDMs) (**a,b**), mouse neonatal cardiomyocytes (**c,d**), and mouse neonatal cardiac fibroblasts (**e,f**) inflammasome activation was induced by priming with lipopolysaccharide (LPS; 500 ng/ml, 3 hr) followed by adenosine triphosphate (ATP, 10 μ M, 3 hr; control: PBS). Concomitant treatment with aPC (20 nM; added once 30 min before ATP stimulation) markedly reduced the LPS/ATP mediated induction of Nlrp3 and cleavage of caspase-1 and IL-1 β ; representative immunoblots (**a,c,e**) and corresponding bar graphs summarizing results (**b,d,f**). Arrowheads indicate inactive (white arrowheads) and active (black arrowheads) form of caspase-1 or IL-1 β (**a,c,e**). The active form was quantified (**b,d,f**).

g,h: Nlrp3 expression and cleavage of caspase-1 (cl-Casp-1) and IL-1 β (cl-IL-1 β) is increased in mouse neonatal cardiomyocytes subjected to 6 hr of hypoxia (H: 1% O₂) and serum and glucose deprivation (HBSS medium), followed by 12 hr of reoxygenation (R: 21% O₂) in complete medium. H/R induces inflammasome activation, which is prevented by aPC (20 nM; added once at the time of reoxygenation); representative immunoblots of whole cell lysates (**g**) and bar graph summarizing results (**h**); GAPDH: loading control. Arrowheads indicate inactive (white arrowheads) and active (black arrowheads) form of caspase-1 or IL-1 β , respectively (**g**). The active form was quantified (**h**). Data shown represent mean \pm SEM. Data obtained from at least three independent experiments each with at least two technical replicates (**a-h**); GAPDH: loading control (**a,c,e,g**); ** P <0.01 (**b,d,f,h**: ANOVA).

4.5 aPC restricts inflammasome by suppressing mTORC1 and HK1

We next investigated the underlying mechanism by which aPC restricts Nlrp3 inflammasome activation. Cardioprotection by aPC following IRI has been linked with 5' adenosine monophosphate-activated protein kinase (AMPK) activation.^{105,121} Furthermore, mammalian target of rapamycin complex 1 (mTORC1), which is negatively regulated by AMPK, has recently been shown to activate Nlrp3 inflammasome in macrophages via hexokinase 1 (HK1).¹⁰³ Hence, we hypothesized that aPC restricts inflammasome activation by restricting mTORC1 signaling in the setting of myocardial IRI.

To this end we determined expression of Raptor (regulatory-associated protein of mTOR) and HK1 as well as total and phosphorylated ribosomal p70-S6 kinase (p70S6K) in BMDMs, neonatal cardiac fibroblasts and neonatal cardiomyocytes. Expression of Raptor and HK1 as well as phosphorylation of p70S6K was enhanced in LPS primed ATP-stimulated BMDMs (Fig. 14a,d) and neonatal cardiac fibroblasts (Fig. 14b,e).¹⁰³ Likewise, Raptor, and HK1 expression and p70S6K phosphorylation in neonatal cardiomyocytes subjected to H/R (Fig. 14c,f).

Treatment with aPC normalized expression of Raptor, HK1 and p70S6K phosphorylation levels in LPS-primed and ATP-stimulated cells or in H/R injured primary cardiomyocytes (Fig. 14a-f). To corroborate the *in vivo* relevance of these findings we analyzed heart tissue of mice with myocardial IRI. Treatment with aPC markedly reduced expression of Raptor and HK1 as well as phosphorylation of p70S6K in comparison to PBS treated mice (control, Fig. 14g,h). These data suggest that aPC restricts inflammasome activation by limiting mTORC1 activation.

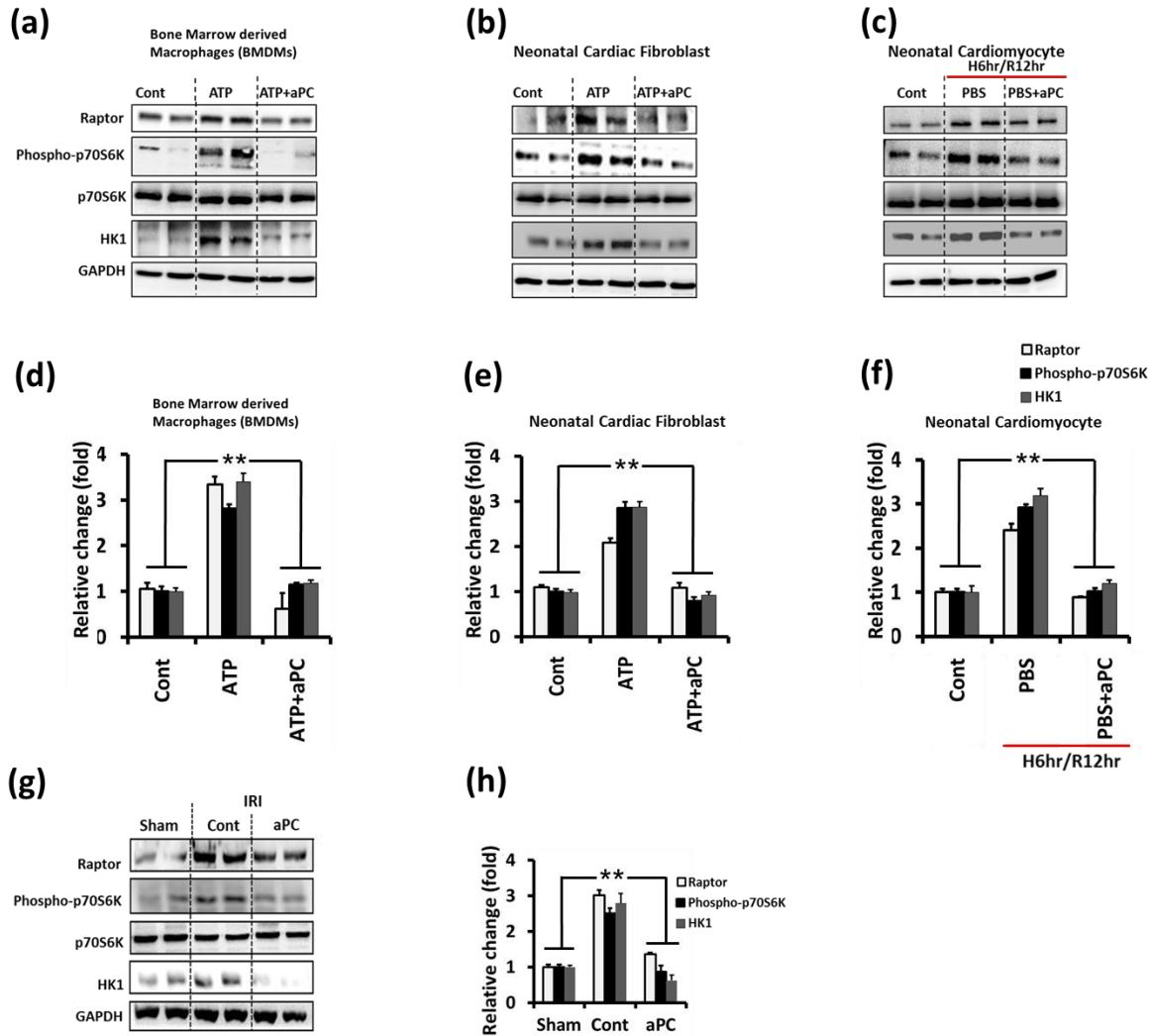


Figure 14: aPC restricts inflammasome by suppressing mTORC1.

a-f: Expression of Raptor, HK1 and phosphorylation of ribosomal p70-S6 kinase (pS6K70) were analyzed in LPS primed and ATP-challenged BMDMs (**a,d**) and mouse neonatal cardiac fibroblasts (**b,e**) or mouse neonatal cardiomyocytes subjected to H/R (**c,f**). aPC inhibits expression of Raptor, HK1 and p70S6K phosphorylation levels in LPS-primed and ATP-stimulated cells (**a,b**) or in H/R injured primary cardiomyocytes (**c**). Representative immunoblots (GAPDH as loading control, a-c) and corresponding bar graphs (d-f). **g,h:** Treatment of mice with aPC inhibits mTORC1 signaling. Representative immunoblots showing cardiac Raptor and HK1 expression as well as total and phosphorylated pS6K70. Representative immunoblots (**g**) and bar graph summarizing results (**h**).

Data shown represent mean±SEM. Data obtained from at least three independent experiments each with at least two technical replicates (**a-h**); GAPDH: loading control (a-c,g,h); ** $P < 0.01$ (**d-f,h**: ANOVA).

To determine the mechanistic relevance of aPC-dependent mTORC1 regulation for inflammasome restriction we used cells lacking tuberous sclerosis 1 (TSC1). TSC1 is a pivotal inhibitor of mTORC1 and its deficiency causes constitutive mTORC1 activation.¹²⁵ BMDMs were isolated from mice with inducible TSC1 deficiency and TSC1 expression was inhibited by transient expression with Cre recombinase *ex vivo* (Fig.

15a; control cells expressed transiently GFP).¹²⁵ In TSC1 deficient BMDMs aPC failed to inhibit expression of Raptor, HK1, and phosphorylation of p70S6K (Fig. 15b,c) and – importantly – aPC-mediated Nlrp3 inflammasome restriction was abolished (Fig. 15d,e). These results demonstrate that constitutive activation of mTORC1 signaling abolishes aPC’s inhibitory effect on inflammasome activation, establishing that aPC limits inflammasome activation by restricting mTORC1 activation.

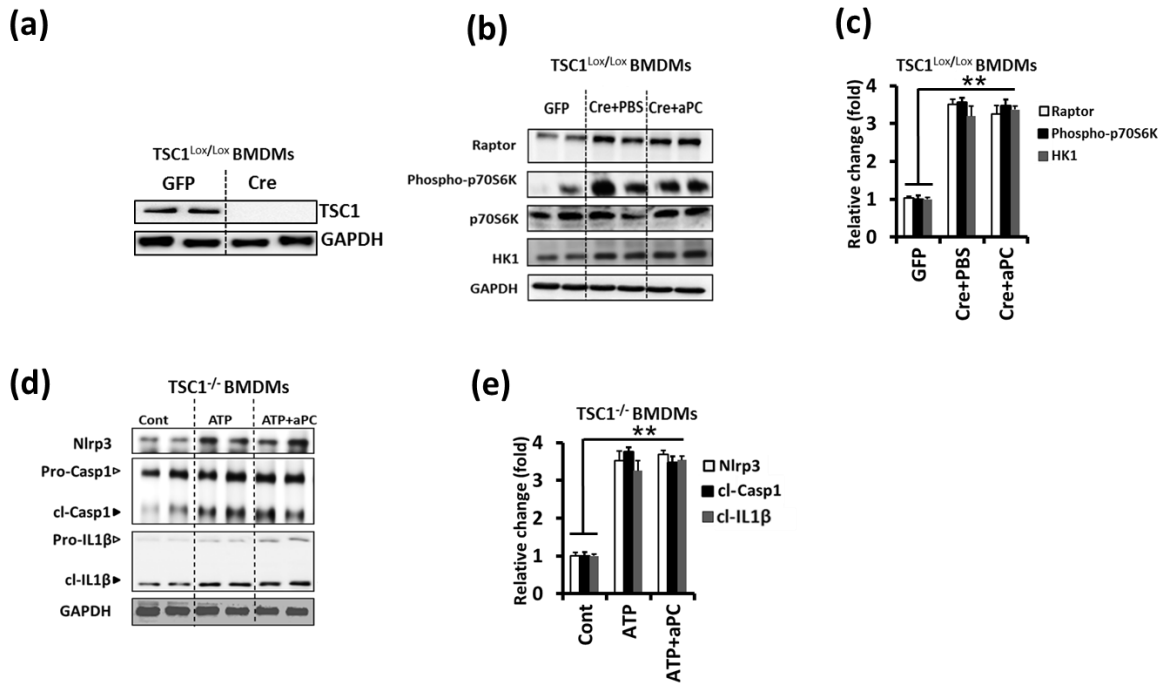


Figure 15: aPC fails to restrict inflammasome in BMDMs expressing constitutively active mTORC1.

a-e: BMDMs from TSC1^{LoxP/LoxP} mice were transiently transfected with GFP or Cre expressing plasmids, resulting in loss of TSC1 expression after 48 hr. Representative immunoblots of TSC1; GAPDH: loading control (**a**). In TSC1 deficient BMDMs cells aPC treatment fails to reduce Raptor, HK1 expression and phosphorylation of p70S6K (TSC1^{LoxP/LoxP}+Cre+aPC) when compared to PBS treated cells (TSC1^{LoxP/LoxP}+Cre+PBS) Representative immunoblots (**b**) and bar graph summarizing results (**c**). Likewise, aPC fails to reduce Nlrp3 expression and cleavage of caspase-1 (cl Casp-1) and IL-1β (cl IL-1β) in TSC1-deficient BMDMs. Representative immunoblots (**d**) and bar graph summarizing results (**e**). Arrowheads indicate inactive (white arrowheads) and active (black arrowheads) form of caspase-1 or IL-1β (**d**). The active form was quantified (**e**). Data shown represent mean±SEM. Data obtained from at least three independent experiments each with at least two technical replicates (**a-j**); GAPDH: loading control (**a,b,d**); ***P*<0.01 (**c,e**: ANOVA).

4.6 aPC restricts inflammasome activation via PAR-1 *in vitro*

To gain further mechanistic insights and to identify potential therapeutic targets we ascertained the receptors involved. First, we analyzed expression of protease-activated receptors (PARs) and endothelial PC receptor (EPCR) in the different cell types employed in our study. Expression of PAR1, PAR2, PAR3, PAR4, and EPCR was readily detectable in these cells (data not shown).

To determine the functional relevance of these receptors we isolated BMDMs, neonatal cardiomyocytes, and cardiac fibroblasts from PAR1^{-/-}, PAR2^{-/-}, or PAR3^{-/-} mice and PAR4 or EPCR function was blocked in wild-type cells using inhibitory antibodies.^{107,110} PAR1 deficiency efficiently abolished Nlrp3 inflammasome suppression by aPC, whereas PAR2, PAR3 deficiency and PAR4 or EPCR blockage had no effect in all cell types studied (Fig.16). These *in vitro* results suggest that aPC restricts the inflammasome activation *via* PAR1 in various cell types relevant for myocardial IRI.

4.7 Cytoprotective 3K3A-aPC protects against myocardial IRI via PAR-1

To corroborate the *in vivo* relevance of the *in vitro* receptor studies we employed the myocardial IRI model. Prior to myocardial IRI mice were either exposed to PBS (control), aPC alone, aPC-HAPC1573 complex (the antibody HAPC1573 blocks specifically the anticoagulant function of aPC), an aPC variant lacking specifically anticoagulant function (3K3A-aPC), or mice were first treated with an inhibitory PAR-1 pepducin (P1pal-12S) followed by aPC treatment.

Treatment with 3K3A-aPC or preincubation of aPC with the HAPC1573 antibody did not abolish aPC's protective effect, as reflected by reduced infarct size (Fig. 17a-c), reduced myocardial Nlrp3 expression and reduced cleavage of caspase-1 (cl-Casp1) and IL-1 β (cl-IL-1 β , Fig. 17d,e), reduced myocardial caspase-1 activity (FLICA-Casp1 assay, Fig. 17f,g), and reduced plasma IL-1 β and IL-18 levels (Fig. 17h,i).

However, following inhibition of PAR1 all these protective effects of aPC were lost (Fig. 17b-i), verifying a pivotal function of PAR1 for the cardiac-protective effect of aPC in regard to myocardial IRI and inflammasome suppression.

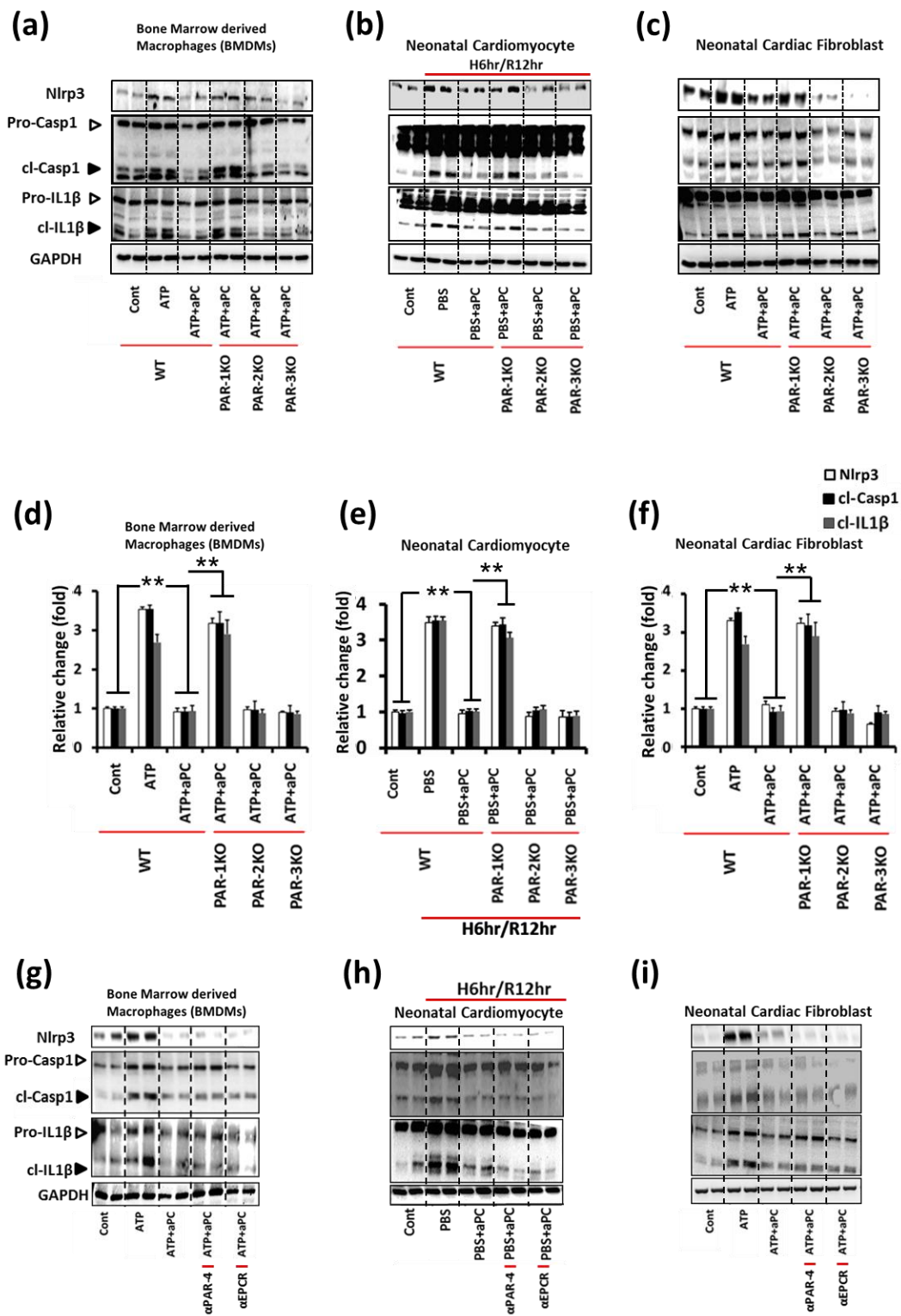


Figure 16: aPC restricts inflammasome activation via PAR1 *in vitro*.

a-c: The effect of aPC on inflammasome activation was analysed following receptor inhibition. BMDMs (a), neonatal cardiomyocytes (b), or neonatal cardiac fibroblasts (c) were isolated from wt, PAR1^{-/-}, PAR2^{-/-}

^{-/-} or PAR3^{-/-} mice. aPC fails to suppress LPS/ATP (a,c) or hypoxia-reoxygenation (b) induced Nlrp3 expression and cleavage of caspase-1 (cl-Casp-1) and IL-1 β (cl-IL-1 β) in the absence of PAR1 in all cell types, while loss of other receptors had no effect; representative immunoblots, GAPDH: loading control (a-c) and corresponding bar graphs (d-e).

g-i: The effect of aPC on inflammasome activation was analysed following loss or inhibition of PARs or EPCR. BMDMs (**g**), neonatal cardiomyocytes (**h**), or neonatal fibroblast (**i**) were isolated from wt, PAR4 and EPCR function was blocked using inhibitory antibodies (α ; **g-i**). In all three cell types blocking of PAR4 and EPCR receptors had no effect Representative immunoblots of inflammasome activation in BMDMs (**g**), neonatal cardiomyocytes (**h**), and neonatal cardiac fibroblast (**i**) following PAR4 and EPCR inhibition using inhibitory antibodies (α). Arrowheads indicate inactive (white arrowheads) and active (black arrow heads) form of caspase-1 or IL-1 β (e-g). The active form was quantified (d-f); GAPDH: loading control. Data shown represent mean \pm SEM. Data obtained from at least three independent experiments each with at least two technical replicates (d-f). **P<0.01 (d-f: ANOVA).

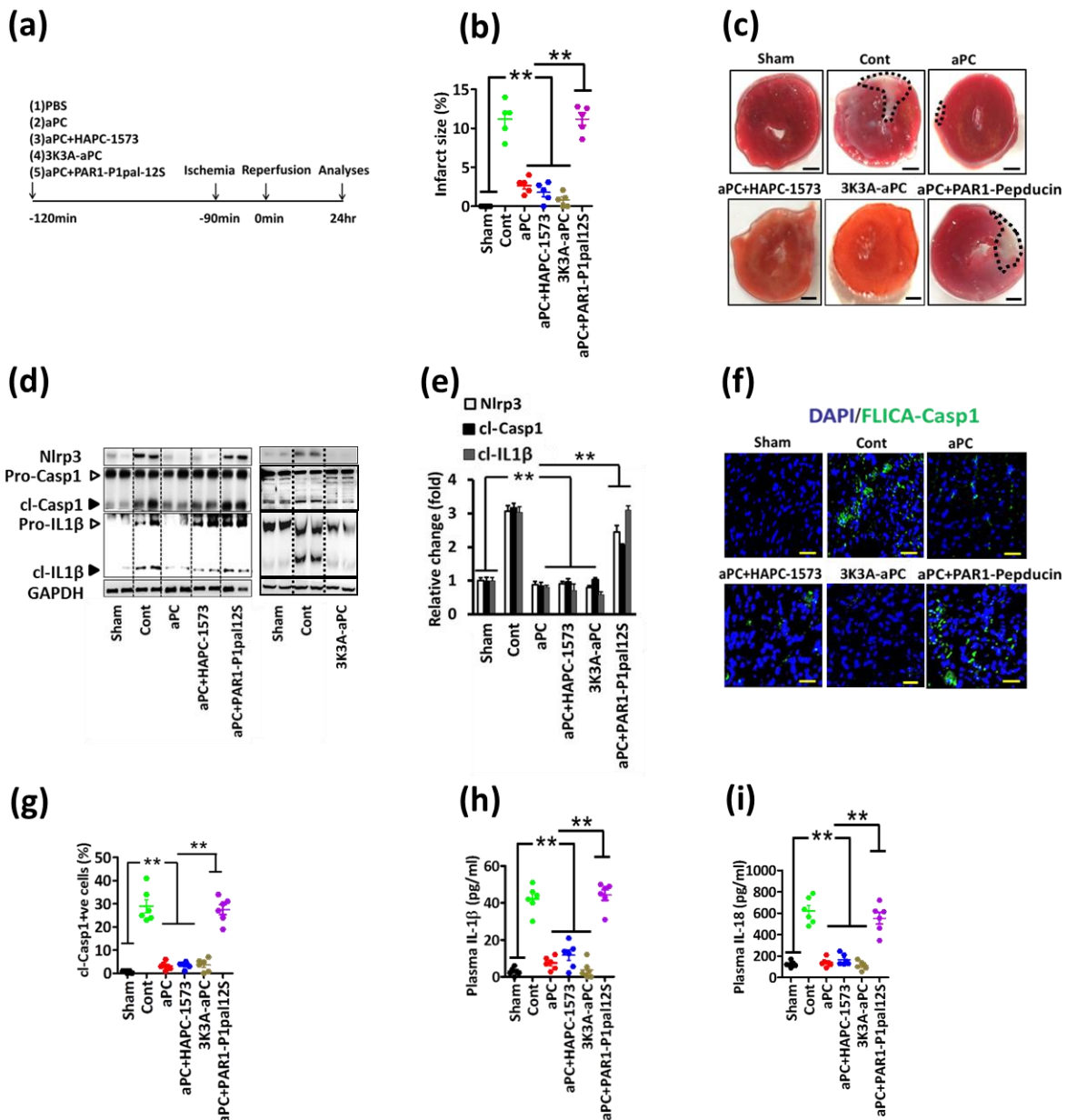


Figure 17: Cytoprotective 3K3A-aPC protects against myocardial IRI *via* PAR-1.

a: Experimental design.

b,c: Treatment of mice with aPC–HAPC1573 complex or 3K3A-aPC reduces the infarct size as efficient as aPC, while blocking PAR1 signaling (pepducin P1pal-12S) abolishes aPC’s inhibitory effect. Representative heart sections showing infarcted area detected by TTC staining (**b**, black dotted encircled area, size bar: 20 μ m) and dot-plots summarizing data (**c**).

d-i: Treatment of mice with aPC–HAPC1573 complex or 3K3A-aPC reduces markers of inflammasome activation as efficient as aPC, while blocking PAR1 signaling (pepducin P1pal-12S) abolishes aPC inhibitory effect. Representative immunoblots of cardiac Nlrp3 expression and cleaved caspase-1 (cl-casp1) and cleaved IL-1 β (cl-IL-1 β , **d**); loading control: GAPD. Bar graphs (**e**) summarizing results. Arrowheads indicate inactive (white arrowheads) and active (black arrowheads) form of caspase-1 or IL-1 β (**d**) and dot plots. Representative images of active caspase-1 within the infarcted tissue (**f**, frozen sections incubated with FLICA-Casp1 probes, size bar: 20 μ m) and dot-plots summarizing results (**g**). Dot-plots summarizing plasma IL-1 β (**h**) and IL-18 (**i**) levels. Sham operated (Sham) or mice with myocardial IRI without (PBS, Cont), with aPC (aPC), with aPC–HAPC1573 complex (aPC+HAPC1573), with an aPC variant lacking specifically anticoagulant function (3K3A-aPC) or with aPC and PAR1 pepducin P1pal-12S (aPC+P1pal-12S) pretreatment.

Data shown represent mean \pm SEM. Data obtained from at least 6 mice per group (**b-i**); ** P <0.01 (**b,e,g-i**: ANOVA).

4.8 PAR-1 specific parmodulin-2 ameliorates inflammasome activation in myocardial IRI

Considering that aPC requires predominately PAR1 for inflammasome restriction following myocardial IRI we speculated that targeting PAR1 is sufficient to mimic aPC’s effect. However, PAR-1 has pleiotropic effects and – depending on the activator and co-receptors involved – can convey via biased signaling cell-damaging or cell-protective effects.^{75,78,126} Recently, structural biochemistry procreated compounds, parmodulins, blocking only specific aspects of biased PAR-signaling.^{81,82} We used parmodulin-2, which blocks cyto-disruptive, but not cytoprotective PAR-1 signaling^{81,82} and evaluated its anti-inflammatory and cytoprotective effect in myocardial IRI.

Treatment of mice with parmodulin-2 (5 mg/kg, Fig. 18a) prior to myocardial IRI was as sufficient as aPC, reducing the infarct size (Fig. 18b,c), cardiac expression of inflammasome regulators (Nlrp3, cl-Casp1, cl-IL1 β , Fig. 18d,e), and plasma IL-1 β levels (Fig. 18f). Furthermore, parmodulin-2 efficiently reduced expression of Raptor and HK1 and phosphorylation of p70S6K (Fig. 18g,h). Thus, mimicking biased aPC-signaling *via* PAR1 using parmodulins is sufficient to limit inflammasome activity and to convey cardioprotection in myocardial IRI.

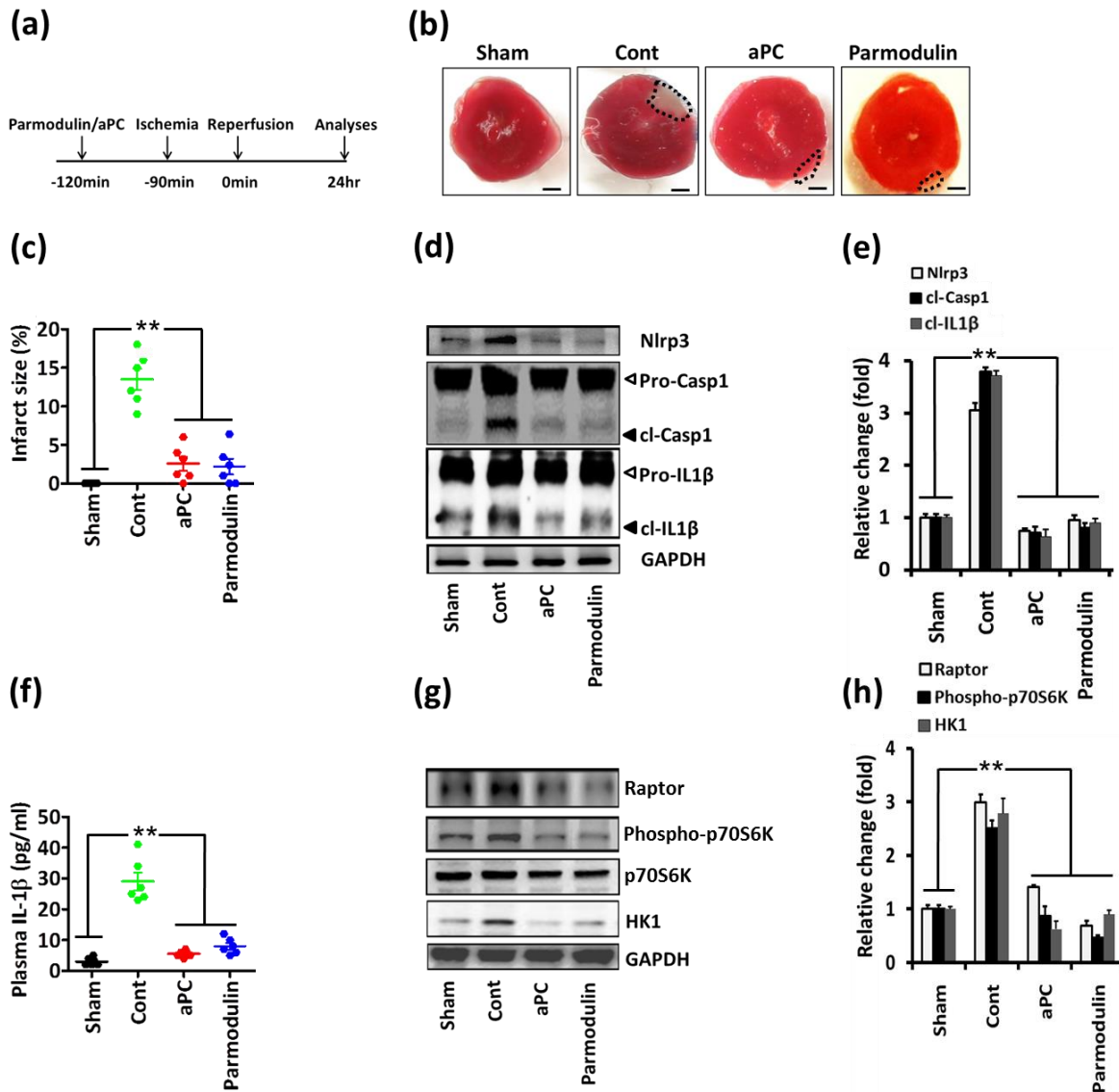


Figure 18: PAR-1 specific parmodulin-2 ameliorates inflammasome activation in myocardial IRI.

a: Experimental design.

b,c: The biased PAR1 antagonists parmodulin-2 (5 mg/kg) reduces the infarcted area to the same extent as aPC. Representative heart sections showing infarcted area detected by TTC staining (**b**, infarcted area: black dotted encircled area, size bar: 20 μm) and dot-plot summarizing data (**c**).

d-h: Treatment of mice with parmodulin-2 reduces markers of inflammasome activation and mTORC1 signaling as efficient as aPC. Representative immunoblots showing cardiac Nlrp3 expression and cleaved caspase-1 (cl-Casp1) and cleaved IL-1β (cl-IL1β, **d**); and bar graph summarizing results (**e**) loading control: GAPDH. Arrowheads indicate inactive (white arrowheads) and active (black arrowheads) form of caspase-1 or IL-1β (**d**). The active form was quantified (**e**). Dot-plots summarizing plasma IL-1β (**f**) and representative immunoblots showing Raptor, HK1 and total and phosphorylated p70S6K (**g**) and bar graph summarizing results (**h**); loading control: GAPDH.

Sham operated mice (Sham) or mice with myocardial IRI without (Cont, PBS) or with aPC (aPC) or parmodulin-2 (Parmodulin) pretreatment. Data shown represent mean±SEM of at least 6 mice per group (**b-h**); ***P*<0.01 (**c,e,f,h**: ANOVA).

4.9 aPC protects against renal ischemia reperfusion injury by limiting Nlrp3 inflammasome activity

Considering recent data showing that inflammasome activation contributes to IRI in other tissues, including the kidney^{127,128}, we hypothesized that inflammasome suppression by aPC may have implications beyond myocardial IRI. To this end we conducted renal IRI following an established protocol.¹⁰⁷ Mice were pretreated with aPC (1 mg/kg bodyweight, i.p.) or PBS 30 min prior to renal IRI (bilateral renal pedicle occlusion, 30 min). After 24 hr we determined indices of renal failure and inflammasome activation (Fig. 19a). As expected, BUN, creatinine, tubular injury, and expression of KIM-1 (kidney-injury-molecule 1) were induced in control mice as compared to sham-operated mice (Fig. 19b-f). Likewise, renal expression of Nlrp3 and cleavage of caspase-1 (cl-Casp1) and IL-1 β (cl-IL-1 β) as well as the presence of cl-Casp1 within renal medullary tubular cells were markedly reduced by aPC treatment (Fig. 19g-j). In parallel, aPC treatment decreased plasma cytokines (IL-1 β , IL-18, Fig. 19k,l). Importantly, Nlrp3 expression, which conveys renal injury at least in part independent of the canonical inflammasome (caspase-1, IL-1 β , IL-18), was not different in aPC treated and sham-operated mice, suggesting that aPC treatment efficiently blocks canonical and non-canonical effects of Nlrp3.

4.10 Constitutively active Nlrp3 abolishes the protective effect of aPC in renal IRI

Congruent with results from myocardial IRI (Fig. 9) aPC failed to protect against renal IRI in Nlrp3V-ER mice. BUN, creatinine, tubular injury, and expression of KIM-1 remained elevated in aPC treated Nlrp3V-ER mice following renal IRI. (Fig. 20a-f) Concurrently, aPC failed to reduce protein levels of Nlrp3 and cleavage of caspase-1 (cl-Casp1) and IL-1 β (cl-IL-1 β , Fig. 20g,h) and plasma IL-1 β and IL-18 levels (Fig. 20i,j) in Nlrp3V-ER mice following myocardial IRI. These data establish that in mice with a genetically superimposed bias for inflammasome activation aPC's protective effect in renal IRI is lost.

Thus, as in the heart, renal inflammasome restriction by aPC depends on Nlrp3 suppression.

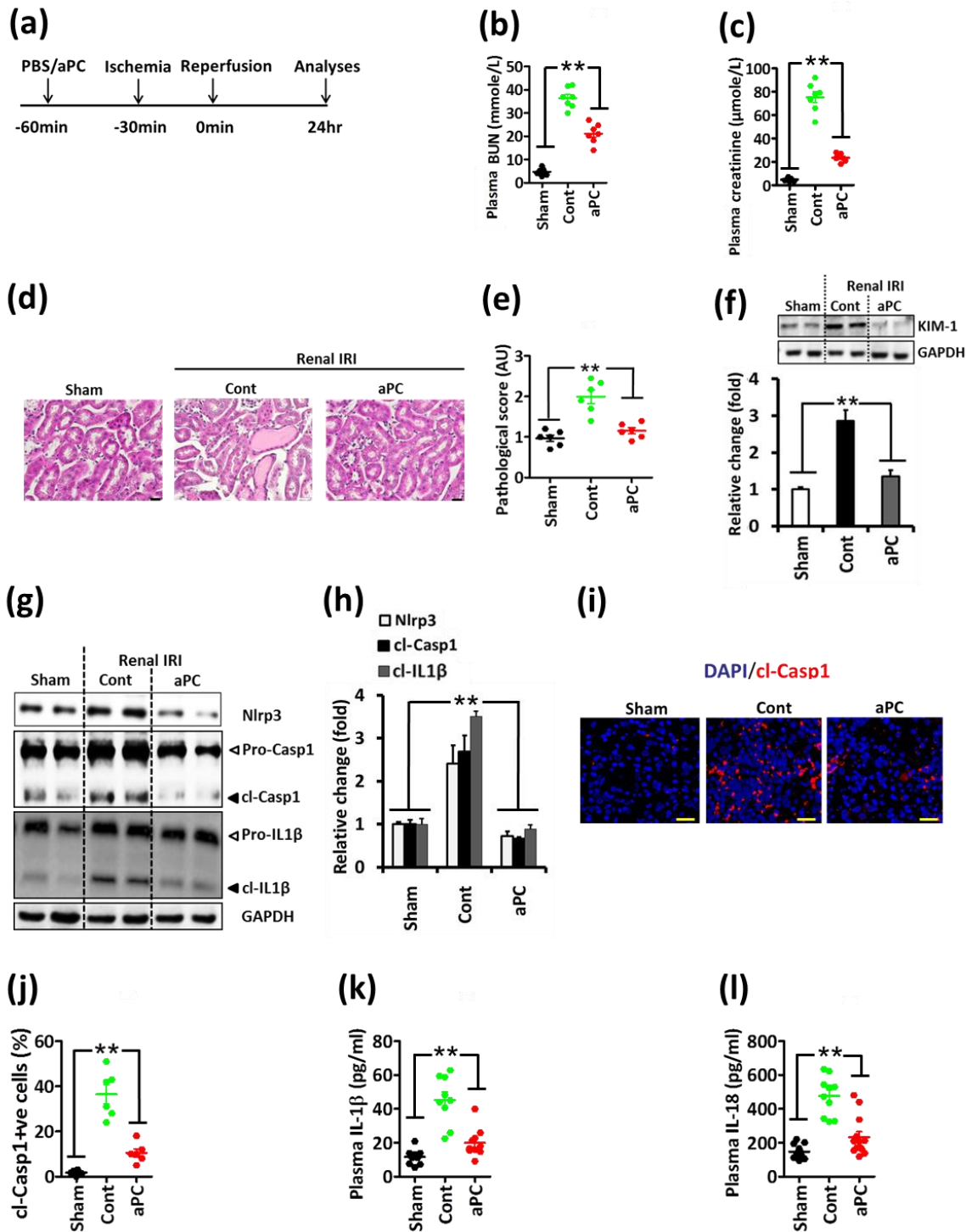


Figure 19: aPC restricts Nlrp3 inflammasome activation in renal IRI.

a: Experimental design.

b-f: aPC treatment reduces plasma BUN (b) creatinine (c) levels and tubular injury (d,e) in mice with bilateral renal pedicle occlusion (30 min) and reperfusion for 24 hr. Exemplary images of H&E-stained kidney section from wild-type sham operated mice and IRI mice without (Cont) or with aPC treatment (d) and dot-blot summarizing results of pathologic scores (e). aPC treatment inhibits expression of the tubular injury marker KIM1 in renal IRI. Representative immunoblots (GAPDH: loading control) and bar graph summarizing results (f).

g-l: aPC reduces renal IRI induced inflammasome activation. Representative immunoblots of renal Nlrp3 expression and cleaved caspase-1 (cl-Casp1) and cleaved IL-1 β (cl-IL-1 β) (**g**) and bar graph summarizing results (**h**), loading control: GAPDH. Arrowheads indicate inactive (white arrowheads) and active (black arrowheads) form of caspase-1 or IL-1 β (**h**) The active form was quantified (**i**). Representative images of active caspase-1 within renal medullary tubular cells (**i**, frozen sections, antibody specific for cleaved caspase-1, cl-Casp-1; size bar: 20 μ m) and dot-plot summarizing data (**j**). Dot-plots summarizing plasma IL-1 β (**k**) and IL-18 levels (**l**). Sham operated mice (Sham) or mice with renal IRI with PBS (Cont) or aPC treatment. Data shown represent mean \pm SEM of at least 6 mice per group; **P<0.01 (**b,c,e-h,j-l**: ANOVA).

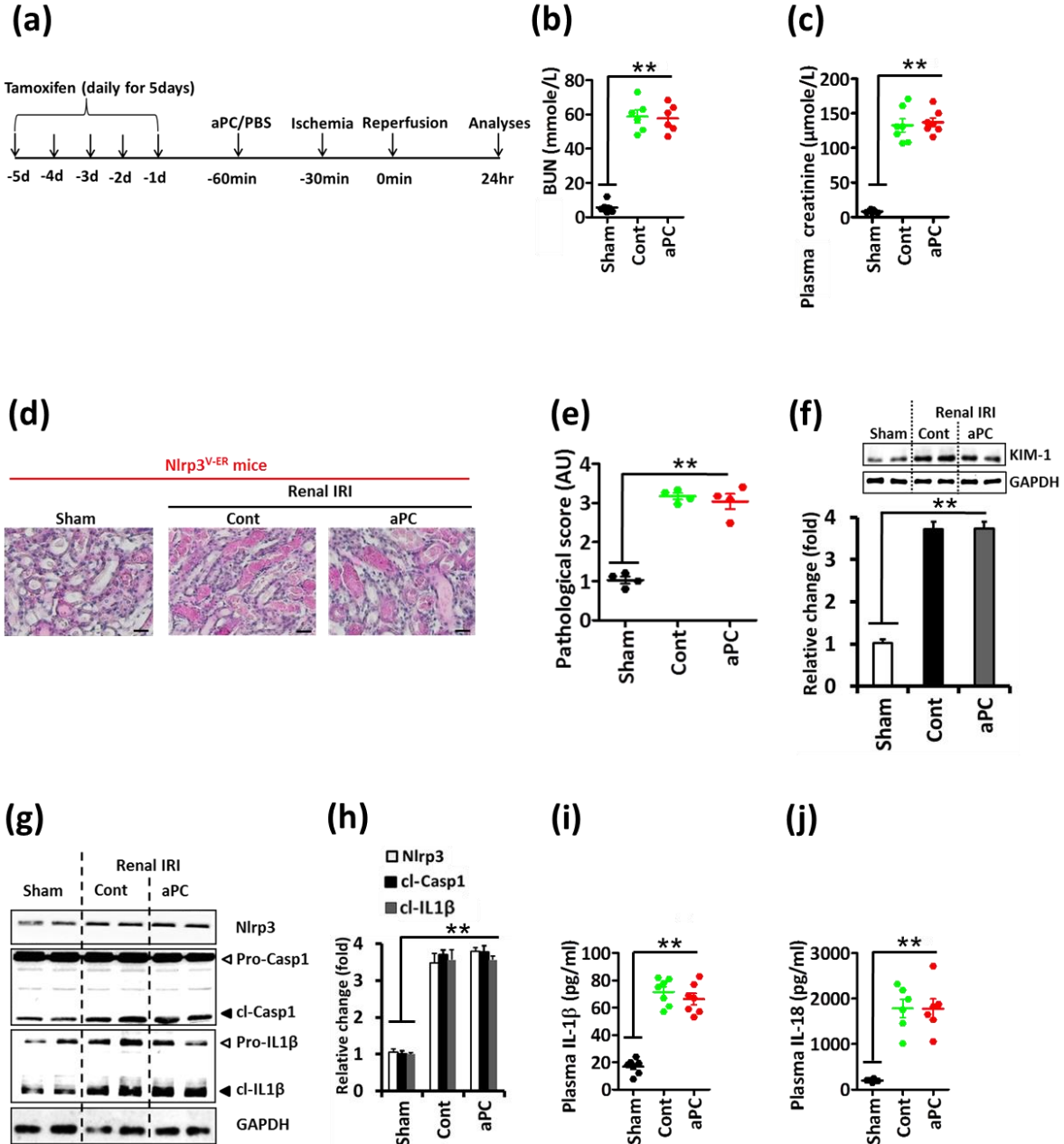


Figure 20: Constitutively active Nlrp3 abolishes the protective effect of aPC in renal IRI.

(a): Experimental design.

b-f): aPC treatment fails to protect against renal IRI in Nlrp3^{V-ER} mice. Plasma BUN (**b**) and creatinine (**c**) levels (dot-plots, b, c); Exemplary images of H&E-stained kidney section from Nlrp3^{V-ER} mice (**d**) and dot-blot summarizing results of pathologic scores (**e**). aPC treatment failed to reduce expression of the tubular injury marker KIM1 in Nlrp3^{V-ER} mice in renal IRI. Representative immunoblots (GAPDH: loading control) and bar graph summarizing results (**f**).

g-j): aPC fails to reduce Nlrp3 expression, cleavage of caspase-1 (cl-Casp1) and IL-1 β (cl-IL-1 β), and plasma IL-1 β and IL-18 levels in Nlrp3^{V-ER} mice following renal IRI. representative immunoblots of renal Nlrp3 expression, cleaved caspase- 1 (cl-Casp1) and cleaved IL-1 β (cl-IL-1 β) (**g**) and bar graph summarizing results (**h**). Arrowheads indicate inactive (white arrowheads) and active (black arrowheads) form of caspase-1 or IL-1 β (g), only the active form was quantified (**h**); loading control: GAPDH; plasma IL-1 β and IL-18 levels (dot-plot, **i,j**)

Sham operated mice (Sham) or mice with renal IRI without (Cont, PBS) or with aPC pretreatment (aPC) treatment. Data shown represent mean \pm SEM of at least 6 different mice per group (**b-j**); ** $P < 0.01$ (**b,c,e,f,h-j**: ANOVA).

5 Discussion

Here we establish that aPC is an endogenous negative regulator of inflammasome activation following IRI, uncovering a new anti-inflammatory mechanism of aPC. We use two independent models, myocardial and renal IRI, to demonstrate that aPC restricts Nlrp3 expression and activation of caspase-1 and IL-1 β . aPC treatment after onset of IRI efficiently restricts Nlrp3 inflammasome activation and is sufficient for cytoprotection, which is congruent with an improved outcome following inflammasome inhibition after myocardial IRI.⁵ In addition, we demonstrate that inflammasome restriction by aPC is independent of its anticoagulant properties but depends on signaling via PAR-1. Importantly, a biased agonist of PAR-1 (parmodulin-2) mimics inflammasome suppression and cytoprotection following myocardial IRI. Thus, we propose that biased agonists mimicking aPC signaling may be a new therapeutic approach in IRI.

Inflammasome activation following IRI occurs in various organs other than the heart and the kidney, including the brain and the liver.¹²⁹ In these organs aPC likewise conveys cytoprotection following IRI¹²⁶, suggesting that limiting inflammasome activation by aPC may be relevant not only in the heart and kidney (as shown here), but also in other organs. Of note, the 3K3A aPC variant has pronounced neuro-protective effects in animal models of cerebral IRI and is undergoing clinical trials in stroke patients (NCT02222714).¹³⁰ As Nlrp3 inflammasome inhibition ameliorates experimental cerebral IRI it is conceivable, but remains to be shown, that aPC restricts Nlrp3 inflammasome activation in cerebral IRI.

Nlrp3 overexpression itself is not sufficient to cause myocardial dysfunction³⁰ (and current study), corroborating that both the priming and activation step are required for inflammasome activation following IRI.^{2,30} Importantly, by restricting Nlrp3 expression and caspase-1 and IL-1 β activation aPC appears to target both inflammasome activation steps. As the priming step of inflammasome activation is largely mediated by NF- κ B and as aPC inhibits NF- κ B activity the proposed function of aPC in restricting inflammasome priming is plausible.^{131,132} Considering the results obtained here using aPC and parmodulin-2 or recent studies using small compound Nlrp3 inhibitors¹³³

targeting both steps of Nlrp3 inflammasome appears to be therapeutically feasible. Based on these observations we propose that simultaneously restricting the priming (induction of Nlrp3 expression) and activation (formation of the inflammasome complex) step may be superior to inhibition of IL-1 receptor signaling or of caspases.¹³⁴⁻¹³⁶

Both canonical (IL-1 β , IL-18) as well as non-canonical (Nlrp3 or caspase-1) inflammasome dependent effects cause tissue damage after IRI.^{6,28,123,137} Thus, in myocardial fibroblasts Nlrp3 induces mitochondrial ROS and Smad-signalling directly through its NACHT domain.¹³⁷ Likewise, in renal IRI Nlrp3 conveys tissue damage independent of ASC and cytokine production.¹³⁸ Whether aPC regulates the canonical Nlrp3 activation pathway, the non-canonical Nlrp3 activation *via* caspase-11, or both needs to be further evaluated in future studies.

The current results suggest that inflammasome activation and associated cell death (pyroptosis) are mechanistically more relevant than apoptosis in IRI. A role of apoptosis – an immunologically silent cell death form – in myocardial IRI has been repeatedly proposed, but these studies typically used TUNEL assay, which is not specific for apoptosis and additionally detects pyroptosis and other cell-death forms.^{14,21,94,136} Our *in vivo* kinetic studies demonstrate that inflammasome activation precedes apoptosis (Fig. 11). Additionally, Nlrp3 deficiency is protective in myocardial IRI.¹²³ Inflammasome activation and pyroptosis in tissue resident cell following IRI may generate a pro-inflammatory micromilieu leading to the recruitment of professional immune-cells. This may trigger a vicious cycle promoting tissue damage.^{2,139,140} Targeting the Nlrp3 inflammasome or caspase-1 may inhibit very early tissue-disruptive events and may be thus superior to other approaches limiting inflammation associated with IRI. Yet the current study does not exclude the occurrence or relevance of apoptosis in IRI. Indeed, the induction of apoptosis at later stages following IRI may reflect a protective mechanism, eliminating damaged cells without simultaneously inducing an inflammatory response.

What may be the mechanisms underlying aPC mediated inflammasome inhibition? Here we show that inflammasome inhibition by aPC depends on mTORC1 inhibition. mTORC1 activation and induction of HK1 expression and glycolysis constitutes a mechanism of Nlrp3, but not of Nlrp1 and Nlrp4 activation in macrophages.¹⁴¹ Likewise, we observed inhibition of mTORC1 and HK1 in LPS and ATP challenged macrophages and cardiac fibroblasts by aPC. In addition, aPC inhibited mTORC1 and HK1 in HR challenged cardiomyocytes as well as in the heart following myocardial IRI. Inhibition of mTORC1 by aPC is congruent with AMPK activation (an inhibitor of mTORC1 signaling) by aPC following myocardial infarction.^{105,121} mTORC1 activation in IRI has frequently been observed^{142,143}, corroborating a mechanistic relevance of mTORC1 inhibition by aPC.

We acknowledge that the role of mTOR signaling in myocardial IRI is complex and depends on its temporal activation pattern, the cell-type, the extent of mTOR activity, and the involvement of mTORC1 versus mTORC2.^{125,144,145} The ability of TSC1 deficiency to abolish aPC-mediated mTORC1 inhibition indicates that aPC regulates the mTORC1 complex.^{144,146} However, considering the multifaceted interactions of TSC1/TSC2, mTORC1, and mTORC2 the precise mechanism needs to be evaluated in future studies.

We and other demonstrated that aPC restricts mitochondrial ROS^{106,147}, a known inducer of Nlrp3 inflammasome activation.¹²⁹ Intriguingly, mTORC1 regulates mitochondrial quality and ROS¹⁴⁸, suggesting that inhibition of mTORC1 and mitochondrial ROS by aPC may be mechanistically linked. As the regulation of mitochondrial ROS and mTORC1 is mutual¹⁴⁹, further studies are required to decipher the exact mechanism through which aPC regulates mTORC1 and mitochondrial ROS. While providing new insights into the cytoprotective effects of aPC, the current study also raises questions. Thus, while parmodulin-2 demonstrated efficacy in the current study it remains currently unknown whether mimicking biased signaling via PAR1 is sufficient to copy the versatile cytoprotective effects of aPC. Considering that parmodulin-2 targets Gαq-signaling we suspect that aPC-PAR1-Gαq-signaling conveys

aPC-mediated inflammasome suppression.⁸¹ Furthermore, various receptors complement aPC signaling *via* PAR-1 in a cell and context specific fashion.^{58,110,150} The co-receptors required for aPC-PAR1-mediated inflammasome suppression remain to be uncovered. Deciphering the specific co-receptors and signaling pathways involved may allow further optimization of a molecular targeted therapy to inhibit inflammasome activation after IRI.

Additionally, the long-term outcome following interventions with aPC in the setting of myocardial IRI remains to be evaluated. Several groups have shown that inflammasome inhibition improves cardiac remodeling and function at later time-points.^{21,136,151} As aPC ameliorates angiotensin II triggered myocardial remodeling⁹⁵ an improved outcome following aPC mediated inflammasome restriction seems conceivable, but remains to be shown.

We demonstrate inflammasome suppression by aPC in various cell types relevant in myocardial IRI. Whether inflammasome suppression in a particular cell type is more important than in others in the context of IRI remains to be shown. Intriguingly, the proposed initiation of a vicious cycle by inflammasome activation in resident tissue cells, which then promotes the recruitment and activation of inflammatory cells, implies that it may be sufficient to inhibit inflammasome activation specifically in ischemic organs. This may allow tissue protection without compromising the function of innate immune cells, which may constitute an advantage in organ transplantation or in patients in an intensive care unit setting.

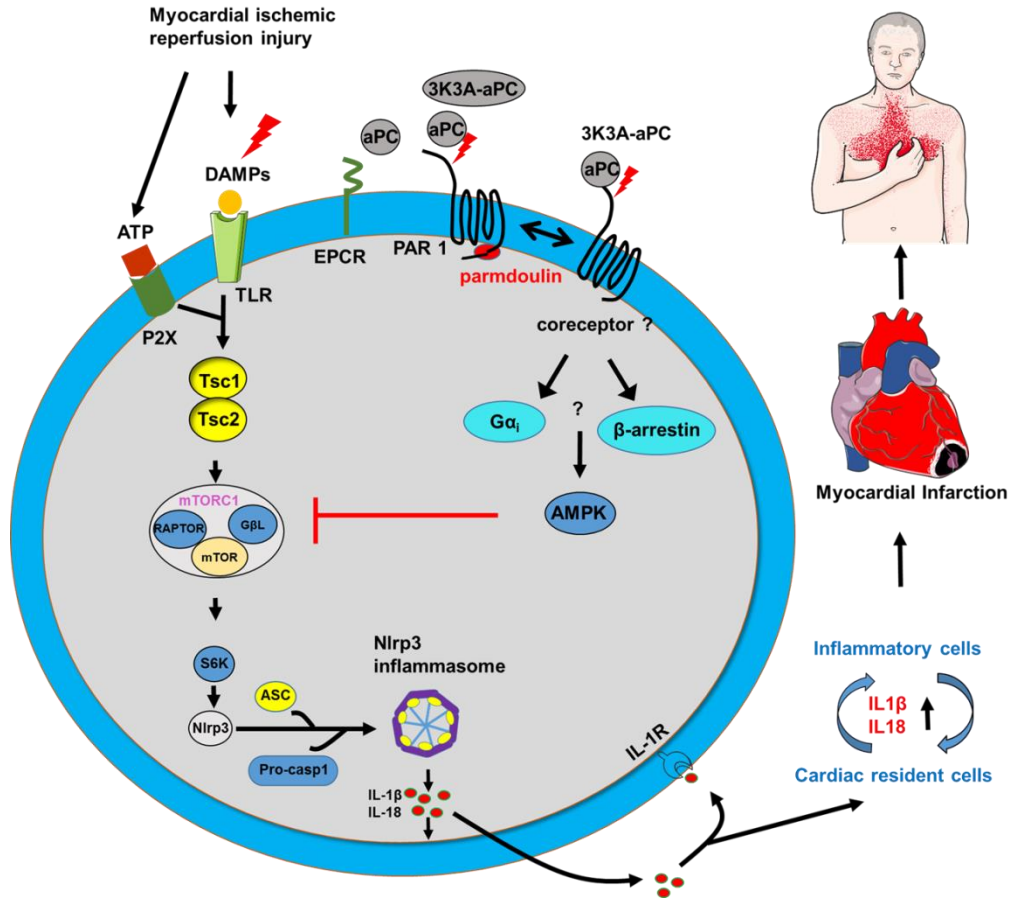


Figure 21: Scheme reflecting the proposed role of Nlrp3 inflammasome for cardiac dysfunction and myocardial IRI.

Myocardial ischemia reperfusion (IRI) injury triggers DAMPs release, which results in TSC1-mTORC1 mediated Nlrp3 inflammasome activation in cardiac resident cells, promoting cell death and hence myocardial infarction. Inflammasome activation in cardiac resident cells triggers further inflammatory cytokines release and inflammatory cells recruitment. Thus, the initial and localized inflammasome activation may trigger a vicious cycle resulting in a robust inflammatory response and cardiac dysfunction. aPC treatment inhibits Nlrp3 inflammasome activation *via* a mechanism involving inhibition of PAR1 and mTORC1 signaling, potentially through AMPK activation. Inhibition of PAR1 signaling abolished the protective effect of aPC in myocardial IRI, whereas blocking the anticoagulant function of aPC had no effect. In addition, targeting PAR1 signaling using parmodulin-2 mimicked the protective effects of aPC in IRI.

6 Conclusion

This study evaluates novel aspects of aPC mediated Nlrp3 inflammasome restriction following myocardial and renal IRI. Previous studies have shown that aPC has anti-inflammatory and anti-apoptotic effects and can protect against IRI in various organs, but the mechanism was unclear. We use two independent models, myocardial and renal IRI, to demonstrate that aPC restricts Nlrp3 expression and activation of caspase-1 and IL-1 β . We show Nlrp3 inflammasome activation precedes the induction of apoptosis and the detection of an infarction, suggesting a pathogenic role of inflammasome activation in IRI.

Treatment with aPC was protective even when administered 30 minutes after the onset of reperfusion. These protective effects were abolished in mice that expressed constitutively active Nlrp3, confirming that inhibition of inflammasome activation is required for aPC-mediated protection in the setting of IRI. Further studies showed that aPC treatment limits Nlrp3 inflammasome activation *via* a mechanism involving PAR1 mediated mTORC1 signaling inhibition. Inhibition of PAR1 signaling abolished the protective effect of aPC in myocardial IRI, whereas blocking the anticoagulant function of aPC had no effect. In addition, targeting PAR1 signaling using parmodulin-2 mimicked the protective effects of aPC in IRI.

The identification of the Nlrp3 inflammasome as a key target of aPC-PAR-1 signaling suggests several potential therapeutic strategies, including aPC analogs, parmodulins, and Nlrp3 inhibitors for the prevention of myocardial reperfusion injury. Finally, these findings imply a potential to target biased PAR-1 signaling in other inflammatory conditions such as stroke and in the setting of organ transplantation. Perfusion of a donor organ with aPC or an aPC-based therapeutic agent (parmodulin, pepducin) before transplantation may inhibit inflammasome activation and thus may improve organ function.

Zusammenfassung

Diese Studie untersucht neue Aspekte der aPC-vermittelten Nlrp3-Inflammasom-Inhibition nach myokardialer und renaler IRI. Frühere Studien haben gezeigt, dass aPC entzündungshemmende und antiapoptotische Wirkungen hat und gegen IRI in verschiedenen Organen schützen kann, aber der Mechanismus war unklar. Wir verwendeten zwei unabhängige Modelle, myokardiale und renale IRI, um zu zeigen, dass aPC die Nlrp3-Expression und die Aktivierung von Caspase-1 und IL-1 β inhibiert. Wir zeigen, dass die Nlrp3-Inflammasom-Aktivierung der Induktion von Apoptose und dem Nachweis eines Infarkts vorausgeht, was auf eine pathogene Rolle des Inflammasoms hindeutet.

aPC war schützend, selbst wenn es 30 Minuten nach Beginn der Reperfusion verabreicht wurde. Dieser schützende Effekt war bei Mäusen, die konstitutiv aktives Nlrp3 exprimierten, aufgehoben. Letzteres bestätigt, dass die Hemmung der Inflammasom-Aktivierung für den aPC-vermittelten Schutz bei IRI notwendig ist. Weitere mechanistische Untersuchungen zeigten, dass aPC via PAR1 die mTORC1 Signaltransduktion und somit dann auch das Nlrp3-Inflammasom inhibiert. Die Hemmung der aPC-PAR1-Signaltransduktion, nicht aber Inhibition der antikoagulatorischen Eigenschaften von aPC, hob die schützende Wirkung von aPC auf. Darüber hinaus ahmte die Modulation der PAR1-Signalisierung unter Verwendung von Parmodulin-2 die schützenden Wirkungen von aPC in IRI nach.

Die Identifizierung des Nlrp3-Inflammasoms als molekulare Zielstruktur der aPC-PAR-1-vermittelten Signaltransduktion legt mehrere innovative therapeutische Strategien nahe. So erscheint es möglich, dass aPC-Analoga, Parmoduline oder Nlrp3-Inhibitoren zur Prävention von myokardialen oder renalen Reperfusionsschäden entwickelt werden. Schließlich könnten die aPC-PAR-1-vermittelten Effekte auch bei anderen post-ischämischen entzündlichen Zuständen, z.B. nach Schlaganfall oder Organtransplantation, einen Nutzen darstellen. Die Perfusion eines Spenderorgans mit aPC oder einem aPC-basierten Therapeutikum (Parmodulin, Pepducin) vor der Transplantation könnte die Aktivierung des Inflammasoms hemmen und somit die Organfunktion verbessern.

7 Future Outlook

While providing new insights into the cytoprotective effects of aPC, the current study also raises questions.

- 1) We demonstrate that inflammasome activation and associated cell death (pyroptosis) was mechanistically more relevant than apoptosis in myocardial IRI. However, whether the induction of apoptosis at later stages following IRI may prevent excessive inflammation, thus providing protection in IRI, remains unknown. Additionally, the long-term outcome following interventions with aPC in the setting of myocardial IRI remains to be evaluated.
- 2) We demonstrate inflammasome suppression by aPC in various cell types relevant in myocardial IRI. The relative contribution of cardiac resident cells and immune cells to inflammasome activation in myocardial IRI remains unclear. Intriguingly, the proposed initiation of a vicious cycle by inflammasome activation in resident tissue cells, which then promotes the recruitment and activation of inflammatory cells, implies that targeting the inflammasome in cardiac resident cells may prevent myocardial tissue loss from pyroptosis and prevent excess recruitment of inflammatory cells to infarcted tissue without impeding inflammasome activation in the periphery.
- 3) Whether aPC regulates the canonical Nlrp3 activation pathway, the non-canonical Nlrp3 activation *via* caspase-11, or both needs to be further evaluated in future studies.
- 4) The mechanisms controlling inflammasome activation, e.g. the co-receptors required for aPC-PAR1-mediated inflammasome suppression, remain to be uncovered. Deciphering the specific co-receptors and signaling pathways involved may allow further optimization of a molecular targeted therapy to inhibit inflammasome activation after IRI. While parmodulin-2 demonstrated efficacy in the current study it remains unknown whether mimicking biased signaling *via* PAR1 by parmodulin-2 is sufficient to convey the versatile effects of aPC.
- 5) We and other demonstrated that aPC restricts mitochondrial ROS, a known inducer of Nlrp3 inflammasome activation. Intriguingly, mTORC1 regulates ROS,

suggesting that inhibition of mTORC1 and mitochondrial ROS by aPC may be mechanistically linked. Further studies are required to decipher the exact mechanism through which aPC regulates mTORC1 and mitochondrial ROS.

- 6) It is not known whether the inflammasome activation associated with myocardial IRI contributes to accelerated atherosclerosis following myocardial IRI.

The delineation of these questions is expected to provide novel insights into the relevance of inflammasome activation following myocardial IRI and its contribution to myocardial damage and dysfunction as well as to accelerated atherosclerosis.

8 References

- 1 Anderson, J. L. & Morrow, D. A. Acute Myocardial Infarction. *N Engl J Med* **376**, 2053-2064, doi:10.1056/NEJMra1606915 (2017).
- 2 Takahashi, M. NLRP3 inflammasome as a novel player in myocardial infarction. *Int Heart J* **55**, 101-105 (2014).
- 3 Rohrbach, S., Troidl, C., Hamm, C. & Schulz, R. Ischemia and reperfusion related myocardial inflammation: A network of cells and mediators targeting the cardiomyocyte. *IUBMB Life* **67**, 110-119, doi:10.1002/iub.1352 (2015).
- 4 Marchant, D. J., Boyd, J. H., Lin, D. C., Granville, D. J., Garmaroudi, F. S. & McManus, B. M. Inflammation in myocardial diseases. *Circulation research* **110**, 126-144, doi:10.1161/CIRCRESAHA.111.243170 (2012).
- 5 Abbate, A., Salloum, F. N., Vecile, E., Das, A., Hoke, N. N., Straino, S., Biondi-Zoccai, G. G., Houser, J. E., Qureshi, I. Z., Ownby, E. D., Gustini, E., Biasucci, L. M., Severino, A., Capogrossi, M. C., Vetrovec, G. W., Crea, F., Baldi, A., Kukreja, R. C. & Dobrina, A. Anakinra, a recombinant human interleukin-1 receptor antagonist, inhibits apoptosis in experimental acute myocardial infarction. *Circulation* **117**, 2670-2683, doi:10.1161/CIRCULATIONAHA.107.740233 (2008).
- 6 Kawaguchi, M., Takahashi, M., Hata, T., Kashima, Y., Usui, F., Morimoto, H., Izawa, A., Takahashi, Y., Masumoto, J., Koyama, J., Hongo, M., Noda, T., Nakayama, J., Sagara, J., Taniguchi, S. & Ikeda, U. Inflammasome activation of cardiac fibroblasts is essential for myocardial ischemia/reperfusion injury. *Circulation* **123**, 594-604, doi:10.1161/CIRCULATIONAHA.110.982777 (2011).
- 7 Toldo, S. & Abbate, A. The NLRP3 inflammasome in acute myocardial infarction. *Nat Rev Cardiol* **15**, 203-214, doi:10.1038/nrcardio.2017.161 (2018).
- 8 Whelan, R. S., Kaplinskiy, V. & Kitsis, R. N. Cell death in the pathogenesis of heart disease: mechanisms and significance. *Annu Rev Physiol* **72**, 19-44, doi:10.1146/annurev.physiol.010908.163111 (2010).
- 9 Eefting, F., Rensing, B., Wigman, J., Pannekoek, W. J., Liu, W. M., Cramer, M. J., Lips, D. J. & Doevendans, P. A. Role of apoptosis in reperfusion injury. *Cardiovasc Res* **61**, 414-426, doi:10.1016/j.cardiores.2003.12.023 (2004).

- 10 Yaoita, H., Ogawa, K., Maehara, K. & Maruyama, Y. Apoptosis in relevant clinical situations: contribution of apoptosis in myocardial infarction. *Cardiovasc Res* **45**, 630-641 (2000).
- 11 Ding, J. W., Tong, X. H., Yang, J., Liu, Z. Q., Zhang, Y., Yang, J., Li, S. & Li, L. Activated protein C protects myocardium via activation of anti-apoptotic pathways of survival in ischemia-reperfused rat heart. *J Korean Med Sci* **25**, 1609-1615, doi:10.3346/jkms.2010.25.11.1609 (2010).
- 12 Fliss, H. & Gattinger, D. Apoptosis in ischemic and reperfused rat myocardium. *Circulation research* **79**, 949-956 (1996).
- 13 Gottlieb, R. A., Gruol, D. L., Zhu, J. Y. & Engler, R. L. Preconditioning rabbit cardiomyocytes: role of pH, vacuolar proton ATPase, and apoptosis. *J Clin Invest* **97**, 2391-2398, doi:10.1172/JCI118683 (1996).
- 14 Loubele, S. T., Spek, C. A., Leenders, P., van Oerle, R., Aberson, H. L., Hamulyak, K., Ferrell, G., Esmon, C. T., Spronk, H. M. & ten Cate, H. Activated protein C protects against myocardial ischemia/ reperfusion injury via inhibition of apoptosis and inflammation. *Arteriosclerosis, thrombosis, and vascular biology* **29**, 1087-1092, doi:10.1161/ATVBAHA.109.188656 (2009).
- 15 Heusch, G. The Coronary Circulation as a Target of Cardioprotection. *Circulation research* **118**, 1643-1658, doi:10.1161/CIRCRESAHA.116.308640 (2016).
- 16 Heusch, G., Kleinbongard, P., Skyschally, A., Levkau, B., Schulz, R. & Erbel, R. The coronary circulation in cardioprotection: more than just one confounder. *Cardiovasc Res* **94**, 237-245, doi:10.1093/cvr/cvr271 (2012).
- 17 Seropian, I. M., Toldo, S., Van Tassell, B. W. & Abbate, A. Anti-inflammatory strategies for ventricular remodeling following ST-segment elevation acute myocardial infarction. *J Am Coll Cardiol* **63**, 1593-1603, doi:10.1016/j.jacc.2014.01.014 (2014).
- 18 Westman, P. C., Lipinski, M. J., Luger, D., Waksman, R., Bonow, R. O., Wu, E. & Epstein, S. E. Inflammation as a Driver of Adverse Left Ventricular Remodeling After Acute Myocardial Infarction. *J Am Coll Cardiol* **67**, 2050-2060, doi:10.1016/j.jacc.2016.01.073 (2016).

- 19 Shen, H., Kreisel, D. & Goldstein, D. R. Processes of sterile inflammation. *Journal of immunology* **191**, 2857-2863, doi:10.4049/jimmunol.1301539 (2013).
- 20 Kloner, R. A., Fishbein, M. C., Lew, H., Maroko, P. R. & Braunwald, E. Mummification of the infarcted myocardium by high dose corticosteroids. *Circulation* **57**, 56-63 (1978).
- 21 Abbate, A., Salloum, F. N., Van Tassell, B. W., Vecile, E., Toldo, S., Seropian, I., Mezzaroma, E. & Dobrina, A. Alterations in the interleukin-1/interleukin-1 receptor antagonist balance modulate cardiac remodeling following myocardial infarction in the mouse. *PLoS One* **6**, e27923, doi:10.1371/journal.pone.0027923 (2011).
- 22 Savvatis, K., Pappritz, K., Becher, P. M., Lindner, D., Zietsch, C., Volk, H. D., Westermann, D., Schultheiss, H. P. & Tschope, C. Interleukin-23 deficiency leads to impaired wound healing and adverse prognosis after myocardial infarction. *Circ Heart Fail* **7**, 161-171, doi:10.1161/CIRCHEARTFAILURE.113.000604 (2014).
- 23 Martinon, F., Burns, K. & Tschopp, J. The inflammasome: a molecular platform triggering activation of inflammatory caspases and processing of proIL-beta. *Mol Cell* **10**, 417-426 (2002).
- 24 Schroder, K. & Tschopp, J. The inflammasomes. *Cell* **140**, 821-832, doi:10.1016/j.cell.2010.01.040 (2010).
- 25 Westermann, D., Van Linthout, S., Dhayat, S., Dhayat, N., Escher, F., Buecker-Gartner, C., Spillmann, F., Noutsias, M., Riad, A., Schultheiss, H. P. & Tschope, C. Cardioprotective and anti-inflammatory effects of interleukin converting enzyme inhibition in experimental diabetic cardiomyopathy. *Diabetes* **56**, 1834-1841, doi:10.2337/db06-1662 (2007).
- 26 Guo, H., Callaway, J. B. & Ting, J. P. Inflammasomes: mechanism of action, role in disease, and therapeutics. *Nat Med* **21**, 677-687, doi:10.1038/nm.3893 (2015).
- 27 Dinarello, C. A. Interleukin-1 in the pathogenesis and treatment of inflammatory diseases. *Blood* **117**, 3720-3732, doi:10.1182/blood-2010-07-273417 (2011).
- 28 Mezzaroma, E., Toldo, S., Farkas, D., Seropian, I. M., Van Tassell, B. W., Salloum, F. N., Kannan, H. R., Menna, A. C., Voelkel, N. F. & Abbate, A. The

- inflammasome promotes adverse cardiac remodeling following acute myocardial infarction in the mouse. *Proc Natl Acad Sci U S A* **108**, 19725-19730, doi:10.1073/pnas.1108586108 (2011).
- 29 Toldo, S., Mezzaroma, E., Mauro, A. G., Salloum, F., Van Tassell, B. W. & Abbate, A. The inflammasome in myocardial injury and cardiac remodeling. *Antioxid Redox Signal* **22**, 1146-1161, doi:10.1089/ars.2014.5989 (2015).
- 30 Toldo, S., Mezzaroma, E., McGeough, M. D., Pena, C. A., Marchetti, C., Sonnino, C., Van Tassell, B. W., Salloum, F. N., Voelkel, N. F., Hoffman, H. M. & Abbate, A. Independent roles of the priming and the triggering of the NLRP3 inflammasome in the heart. *Cardiovasc Res* **105**, 203-212, doi:10.1093/cvr/cvu259 (2015).
- 31 Liu, X., Zhang, Z., Ruan, J., Pan, Y., Magupalli, V. G., Wu, H. & Lieberman, J. Inflammasome-activated gasdermin D causes pyroptosis by forming membrane pores. *Nature* **535**, 153-158, doi:10.1038/nature18629 (2016).
- 32 Chen, G. Y. & Nunez, G. Sterile inflammation: sensing and reacting to damage. *Nat Rev Immunol* **10**, 826-837, doi:10.1038/nri2873 (2010).
- 33 Wang, L., Qu, P., Zhao, J. & Chang, Y. NLRP3 and downstream cytokine expression elevated in the monocytes of patients with coronary artery disease. *Arch Med Sci* **10**, 791-800, doi:10.5114/aoms.2014.44871 (2014).
- 34 Airaghi, L., Lettino, M., Manfredi, M. G., Lipton, J. M. & Catania, A. Endogenous cytokine antagonists during myocardial ischemia and thrombolytic therapy. *Am Heart J* **130**, 204-211 (1995).
- 35 Patti, G., D'Ambrosio, A., Mega, S., Giorgi, G., Zardi, E. M., Zardi, D. M., Dicuonzo, G., Dobrina, A. & Di Sciascio, G. Early interleukin-1 receptor antagonist elevation in patients with acute myocardial infarction. *J Am Coll Cardiol* **43**, 35-38 (2004).
- 36 Patti, G., Mega, S., Pasceri, V., Nusca, A., Giorgi, G., Zardi, E. M., D'Ambrosio, A., Dobrina, A. & Di Sciascio, G. Interleukin-1 receptor antagonist levels correlate with extent of myocardial loss in patients with acute myocardial infarction. *Clin Cardiol* **28**, 193-196 (2005).
- 37 Dinarello, C. A. Interleukin-1. *Cytokine Growth Factor Rev* **8**, 253-265 (1997).

- 38 Achneck, H. E., Sileshi, B., Parikh, A., Milano, C. A., Welsby, I. J. & Lawson, J. H. Pathophysiology of bleeding and clotting in the cardiac surgery patient: from vascular endothelium to circulatory assist device surface. *Circulation* **122**, 2068-2077, doi:10.1161/CIRCULATIONAHA.110.936773 (2010).
- 39 Rauch, U., Osende, J. I., Fuster, V., Badimon, J. J., Fayad, Z. & Chesebro, J. H. Thrombus formation on atherosclerotic plaques: pathogenesis and clinical consequences. *Ann Intern Med* **134**, 224-238 (2001).
- 40 Palta, S., Saroa, R. & Palta, A. Overview of the coagulation system. *Indian J Anaesth* **58**, 515-523, doi:10.4103/0019-5049.144643 (2014).
- 41 Christersson, C., Oldgren, J., Bylock, A., Siegbahn, A. & Wallentin, L. Early decrease in coagulation activity after myocardial infarction is associated with lower risk of new ischaemic events: observations from the ESTEEM Trial. *Eur Heart J* **28**, 692-698, doi:10.1093/eurheartj/ehl564 (2007).
- 42 Atar, D., Bode, C., Stuerzenbecher, A. & Verheugt, F. W. Anticoagulants for secondary prevention after acute myocardial infarction: lessons from the past decade. *Fundam Clin Pharmacol* **28**, 353-363, doi:10.1111/fcp.12063 (2014).
- 43 Cavender, M. A., Gibson, C. M., Braunwald, E., Wiviott, S. D., Murphy, S. A., Toda Kato, E., Plotnikov, A. N., Amuchastegui, M., Oude Ophuis, T., van Hesse, M. & Mega, J. L. The effect of rivaroxaban on myocardial infarction in the ATLAS ACS 2 - TIMI 51 trial. *Eur Heart J Acute Cardiovasc Care* **4**, 468-474, doi:10.1177/2048872614554109 (2015).
- 44 Testa, L., Van Gaal, W., Biondi-Zoccai, G., Abbate, A., Trotta, G. & Agostoni, P. Re: early decrease in coagulation activity after myocardial infarction is associated with lower risk of new ischaemic events: observations from the ESTEEM trial. *Eur Heart J* **28**, 1782-1783; author reply 1783, doi:10.1093/eurheartj/ehm139 (2007).
- 45 Van de Wouwer, M., Collen, D. & Conway, E. M. Thrombomodulin-protein C-EPCR system: integrated to regulate coagulation and inflammation. *Arteriosclerosis, thrombosis, and vascular biology* **24**, 1374-1383, doi:10.1161/01.ATV.0000134298.25489.92 (2004).

- 46 Esmon, C. T. Coagulation and inflammation. *J Endotoxin Res* **9**, 192-198, doi:10.1179/096805103125001603 (2003).
- 47 Freyssinet, J. M., Beretz, A., Klein-Soyer, C., Gauchy, J., Schuhler, S. & Cazenave, J. P. Interference of blood-coagulation vitamin K-dependent proteins in the activation of human protein C. Involvement of the 4-carboxyglutamic acid domain in two distinct interactions with the thrombin-thrombomodulin complex and with phospholipids. *Biochem J* **256**, 501-507 (1988).
- 48 Nishioka, J., Ido, M., Hayashi, T. & Suzuki, K. The Gla26 residue of protein C is required for the binding of protein C to thrombomodulin and endothelial cell protein C receptor, but not to protein S and factor Va. *Thromb Haemost* **75**, 275-282 (1996).
- 49 Preston, R. J., Ajzner, E., Razzari, C., Karageorgi, S., Dua, S., Dahlback, B. & Lane, D. A. Multifunctional specificity of the protein C/activated protein C Gla domain. *J Biol Chem* **281**, 28850-28857, doi:10.1074/jbc.M604966200 (2006).
- 50 Regan, L. M., Mollica, J. S., Rezaie, A. R. & Esmon, C. T. The interaction between the endothelial cell protein C receptor and protein C is dictated by the gamma-carboxyglutamic acid domain of protein C. *J Biol Chem* **272**, 26279-26284 (1997).
- 51 Esmon, C. T. The endothelial cell protein C receptor. *Thromb Haemost* **83**, 639-643 (2000).
- 52 Esmon, C. T. The protein C pathway. *Chest* **124**, 26S-32S (2003).
- 53 Espana, F., Gruber, A., Heeb, M. J., Hanson, S. R., Harker, L. A. & Griffin, J. H. In vivo and in vitro complexes of activated protein C with two inhibitors in baboons. *Blood* **77**, 1754-1760 (1991).
- 54 Heeb, M. J. & Griffin, J. H. Physiologic inhibition of human activated protein C by alpha 1-antitrypsin. *J Biol Chem* **263**, 11613-11616 (1988).
- 55 Heeb, M. J., Gruber, A. & Griffin, J. H. Identification of divalent metal ion-dependent inhibition of activated protein C by alpha 2-macroglobulin and alpha 2-antiplasmin in blood and comparisons to inhibition of factor Xa, thrombin, and plasmin. *J Biol Chem* **266**, 17606-17612 (1991).

- 56 Pratt, C. W. & Church, F. C. General features of the heparin-binding serpins antithrombin, heparin cofactor II and protein C inhibitor. *Blood Coagul Fibrinolysis* **4**, 479-490 (1993).
- 57 Mosnier, L. O., Zlokovic, B. V. & Griffin, J. H. The cytoprotective protein C pathway. *Blood* **109**, 3161-3172, doi:10.1182/blood-2006-09-003004 (2007).
- 58 Weiler, H. Multiple receptor-mediated functions of activated protein C. *Hamostaseologie* **31**, 185-195, doi:10.5482/ha-1166 (2011).
- 59 Dahlback, B. Resistance to activated protein C caused by the factor VR506Q mutation is a common risk factor for venous thrombosis. *Thromb Haemost* **78**, 483-488 (1997).
- 60 Dahlbck, B. Resistance to activated protein C caused by the R506Q mutation in the gene for factor V is a common risk factor for venous thrombosis. *J Intern Med Suppl* **740**, 1-8 (1997).
- 61 Bouwens, E. A., Stavenuiter, F. & Mosnier, L. O. Mechanisms of anticoagulant and cytoprotective actions of the protein C pathway. *Journal of thrombosis and haemostasis : JTH* **11 Suppl 1**, 242-253, doi:10.1111/jth.12247 (2013).
- 62 Rezaie, A. R. Regulation of the protein C anticoagulant and antiinflammatory pathways. *Curr Med Chem* **17**, 2059-2069 (2010).
- 63 Feistritzer, C. & Riewald, M. Endothelial barrier protection by activated protein C through PAR1-dependent sphingosine 1-phosphate receptor-1 crossactivation. *Blood* **105**, 3178-3184, doi:10.1182/blood-2004-10-3985 (2005).
- 64 Finigan, J. H., Dudek, S. M., Singleton, P. A., Chiang, E. T., Jacobson, J. R., Camp, S. M., Ye, S. Q. & Garcia, J. G. Activated protein C mediates novel lung endothelial barrier enhancement: role of sphingosine 1-phosphate receptor transactivation. *J Biol Chem* **280**, 17286-17293, doi:10.1074/jbc.M412427200 (2005).
- 65 Mosnier, L. O. & Griffin, J. H. Inhibition of staurosporine-induced apoptosis of endothelial cells by activated protein C requires protease-activated receptor-1 and endothelial cell protein C receptor. *Biochem J* **373**, 65-70, doi:10.1042/BJ20030341 (2003).

- 66 Baltch, A. L., Bopp, L. H., Ritz, W. J., Michelsen, P. B., Yan, S. B., Um, S. & Smith, R. P. Effect of recombinant human activated protein C on the bactericidal activity of human monocytes and modulation of pro-inflammatory cytokines in the presence of antimicrobial agents. *J Antimicrob Chemother* **59**, 1177-1181, doi:10.1093/jac/dkm080 (2007).
- 67 Galley, H. F., El Sakka, N. E., Webster, N. R., Lowes, D. A. & Cuthbertson, B. H. Activated protein C inhibits chemotaxis and interleukin-6 release by human neutrophils without affecting other neutrophil functions. *Br J Anaesth* **100**, 815-819, doi:10.1093/bja/aen079 (2008).
- 68 Ku, D. H., Arkel, Y. S., Paidas, M. P. & Lockwood, C. J. Circulating levels of inflammatory cytokines (IL-1 beta and TNF-alpha), resistance to activated protein C, thrombin and fibrin generation in uncomplicated pregnancies. *Thromb Haemost* **90**, 1074-1079, doi:10.1160/TH03-02-0119 (2003).
- 69 Ohkuma, K., Matsuda, K., Kariya, R., Goto, H., Kamei, S., Hamamoto, T. & Okada, S. Anti-inflammatory effects of activated protein C on human dendritic cells. *Microbiol Immunol* **59**, 381-388, doi:10.1111/1348-0421.12262 (2015).
- 70 Elliott, E. I. & Sutterwala, F. S. Initiation and perpetuation of NLRP3 inflammasome activation and assembly. *Immunol Rev* **265**, 35-52, doi:10.1111/imr.12286 (2015).
- 71 Zhao, P., Metcalf, M. & Bunnett, N. W. Biased signaling of protease-activated receptors. *Front Endocrinol (Lausanne)* **5**, 67, doi:10.3389/fendo.2014.00067 (2014).
- 72 Coughlin, S. R. Protease-activated receptors in hemostasis, thrombosis and vascular biology. *Journal of thrombosis and haemostasis : JTH* **3**, 1800-1814, doi:10.1111/j.1538-7836.2005.01377.x (2005).
- 73 Cao, C., Gao, Y., Li, Y., Antalis, T. M., Castellino, F. J. & Zhang, L. The efficacy of activated protein C in murine endotoxemia is dependent on integrin CD11b. *J Clin Invest* **120**, 1971-1980, doi:10.1172/JCI40380 (2010).
- 74 Healy, L. D., Rigg, R. A., Griffin, J. H. & McCarty, O. J. T. Regulation of immune cell signaling by activated protein C. *J Leukoc Biol*, doi:10.1002/JLB.3MIR0817-338R (2018).

- 75 Mosnier, L. O., Sinha, R. K., Burnier, L., Bouwens, E. A. & Griffin, J. H. Biased agonism of protease-activated receptor 1 by activated protein C caused by noncanonical cleavage at Arg46. *Blood* **120**, 5237-5246, doi:10.1182/blood-2012-08-452169 (2012).
- 76 Mosnier, L. O., Zlokovic, B. V. & Griffin, J. H. Cytoprotective-selective activated protein C therapy for ischaemic stroke. *Thromb Haemost* **112**, 883-892, doi:10.1160/TH14-05-0448 (2014).
- 77 Griffin, J. H., Zlokovic, B. V. & Mosnier, L. O. Activated protein C: biased for translation. *Blood*, doi:10.1182/blood-2015-02-355974 (2015).
- 78 Sinha, R. K., Wang, Y., Zhao, Z., Xu, X., Burnier, L., Gupta, N., Fernandez, J. A., Martin, G., Kupriyanov, S., Mosnier, L. O., Zlokovic, B. V. & Griffin, J. H. PAR1 biased signaling is required for activated protein C in vivo benefits in sepsis and stroke. *Blood* **131**, 1163-1171, doi:10.1182/blood-2017-10-810895 (2018).
- 79 Griffin, J. H., Zlokovic, B. V. & Mosnier, L. O. Activated protein C: biased for translation. *Blood* **125**, 2898-2907, doi:10.1182/blood-2015-02-355974 (2015).
- 80 Bologna, Z., Teoh, J. P., Bayoumi, A. S., Tang, Y. & Kim, I. M. Biased G Protein-Coupled Receptor Signaling: New Player in Modulating Physiology and Pathology. *Biomol Ther (Seoul)* **25**, 12-25, doi:10.4062/biomolther.2016.165 (2017).
- 81 Aisiku, O., Peters, C. G., De Ceunynck, K., Ghosh, C. C., Dilks, J. R., Fustolo-Gunnink, S. F., Huang, M., Dockendorff, C., Parikh, S. M. & Flaumenhaft, R. Parmodulins inhibit thrombus formation without inducing endothelial injury caused by vorapaxar. *Blood* **125**, 1976-1985, doi:10.1182/blood-2014-09-599910 (2015).
- 82 De Ceunynck, K., Peters, C. G., Jain, A., Higgins, S. J., Aisiku, O., Fitch-Tewfik, J. L., Chaudhry, S. A., Dockendorff, C., Parikh, S. M., Ingber, D. E. & Flaumenhaft, R. PAR1 agonists stimulate APC-like endothelial cytoprotection and confer resistance to thromboinflammatory injury. *Proc Natl Acad Sci U S A* **115**, E982-E991, doi:10.1073/pnas.1718600115 (2018).
- 83 Zhang, P., Gruber, A., Kasuda, S., Kimmelstiel, C., O'Callaghan, K., Cox, D. H., Bohm, A., Baleja, J. D., Covic, L. & Kuliopulos, A. Suppression of arterial

- thrombosis without affecting hemostatic parameters with a cell-penetrating PAR1 pepducin. *Circulation* **126**, 83-91, doi:10.1161/CIRCULATIONAHA.112.091918 (2012).
- 84 Wildhagen, K. C., Lutgens, E., Loubele, S. T., ten Cate, H. & Nicolaes, G. A. The structure-function relationship of activated protein C. Lessons from natural and engineered mutations. *Thromb Haemost* **106**, 1034-1045, doi:10.1160/TH11-08-0522 (2011).
- 85 Bae, J. S., Yang, L., Manithody, C. & Rezaie, A. R. Engineering a disulfide bond to stabilize the calcium-binding loop of activated protein C eliminates its anticoagulant but not its protective signaling properties. *J Biol Chem* **282**, 9251-9259, doi:10.1074/jbc.M610547200 (2007).
- 86 Harmon, S., Preston, R. J., Ni Ainle, F., Johnson, J. A., Cunningham, M. S., Smith, O. P., White, B. & O'Donnell, J. S. Dissociation of activated protein C functions by elimination of protein S cofactor enhancement. *J Biol Chem* **283**, 30531-30539, doi:10.1074/jbc.M802338200 (2008).
- 87 Yang, X. V., Banerjee, Y., Fernandez, J. A., Deguchi, H., Xu, X., Mosnier, L. O., Urbanus, R. T., de Groot, P. G., White-Adams, T. C., McCarty, O. J. & Griffin, J. H. Activated protein C ligation of ApoER2 (LRP8) causes Dab1-dependent signaling in U937 cells. *Proc Natl Acad Sci U S A* **106**, 274-279, doi:10.1073/pnas.0807594106 (2009).
- 88 Mosnier, L. O., Zampolli, A., Kerschen, E. J., Schuepbach, R. A., Banerjee, Y., Fernandez, J. A., Yang, X. V., Riewald, M., Weiler, H., Ruggeri, Z. M. & Griffin, J. H. Hyperantithrombotic, noncytoprotective Glu149Ala-activated protein C mutant. *Blood* **113**, 5970-5978, doi:10.1182/blood-2008-10-183327 (2009).
- 89 Chiba, N., Nagao, K., Mukoyama, T., Tominaga, Y. & Tanjoh, K. Decreased activated protein C levels as a clinical predictor in patients with ST-elevation myocardial infarction. *Am Heart J* **156**, 931-938, doi:10.1016/j.ahj.2008.06.015 (2008).
- 90 Fellner, B., Rohla, M., Jarai, R., Smetana, P., Freynhofer, M. K., Egger, F., Zorn, G., Weiss, T. W., Huber, K. & Geppert, A. Activated protein C levels and outcome in patients with cardiogenic shock complicating acute myocardial

- infarction. *Eur Heart J Acute Cardiovasc Care* **6**, 348-358, doi:10.1177/2048872616637036 (2017).
- 91 Borissoff, J. I., Spronk, H. M. & ten Cate, H. The hemostatic system as a modulator of atherosclerosis. *N Engl J Med* **364**, 1746-1760, doi:10.1056/NEJMra1011670 (2011).
- 92 Volkers, M., Konstandin, M. H., Doroudgar, S., Toko, H., Quijada, P., Din, S., Joyo, A., Ornelas, L., Samse, K., Thuerauf, D. J., Gude, N., Glembotski, C. C. & Sussman, M. A. Mechanistic target of rapamycin complex 2 protects the heart from ischemic damage. *Circulation* **128**, 2132-2144, doi:10.1161/CIRCULATIONAHA.113.003638 (2013).
- 93 Maehata, Y., Miyagawa, S. & Sawa, Y. Activated protein C has a protective effect against myocardial I/R injury by improvement of endothelial function and activation of AKT1. *PLoS One* **7**, e38738, doi:10.1371/journal.pone.0038738 (2012).
- 94 Pirat, B., Muderrisoglu, H., Unal, M. T., Ozdemir, H., Yildirim, A., Yucel, M. & Turkoglu, S. Recombinant human-activated protein C inhibits cardiomyocyte apoptosis in a rat model of myocardial ischemia-reperfusion. *Coron Artery Dis* **18**, 61-66, doi:10.1097/MCA.0b013e328010a44a (2007).
- 95 Sopel, M. J., Rosin, N. L., Falkenham, A. G., Bezuhyly, M., Esmon, C. T., Lee, T. D., Liwski, R. S. & Legare, J. F. Treatment with activated protein C (aPC) is protective during the development of myocardial fibrosis: an angiotensin II infusion model in mice. *PLoS One* **7**, e45663, doi:10.1371/journal.pone.0045663 (2012).
- 96 Wang, Y., Zhao, Z., Chow, N., Rajput, P. S., Griffin, J. H., Lyden, P. D. & Zlokovic, B. V. Activated protein C analog protects from ischemic stroke and extends the therapeutic window of tissue-type plasminogen activator in aged female mice and hypertensive rats. *Stroke* **44**, 3529-3536, doi:10.1161/STROKEAHA.113.003350 (2013).
- 97 Laplante, M. & Sabatini, D. M. mTOR signaling in growth control and disease. *Cell* **149**, 274-293, doi:10.1016/j.cell.2012.03.017 (2012).

- 98 Proud, C. G. Role of mTOR signalling in the control of translation initiation and elongation by nutrients. *Curr Top Microbiol Immunol* **279**, 215-244 (2004).
- 99 Sciarretta, S., Zhai, P., Shao, D., Maejima, Y., Robbins, J., Volpe, M., Condorelli, G. & Sadoshima, J. Rheb is a critical regulator of autophagy during myocardial ischemia: pathophysiological implications in obesity and metabolic syndrome. *Circulation* **125**, 1134-1146, doi:10.1161/CIRCULATIONAHA.111.078212 (2012).
- 100 Zhai, P., Sciarretta, S., Galeotti, J., Volpe, M. & Sadoshima, J. Differential roles of GSK-3beta during myocardial ischemia and ischemia/reperfusion. *Circulation research* **109**, 502-511, doi:10.1161/CIRCRESAHA.111.249532 (2011).
- 101 Buss, S. J., Muenz, S., Riffel, J. H., Malekar, P., Hagenmueller, M., Weiss, C. S., Bea, F., Bekeredjian, R., Schinke-Braun, M., Izumo, S., Katus, H. A. & Hardt, S. E. Beneficial effects of Mammalian target of rapamycin inhibition on left ventricular remodeling after myocardial infarction. *J Am Coll Cardiol* **54**, 2435-2446, doi:10.1016/j.jacc.2009.08.031 (2009).
- 102 Wu, X., Cao, Y., Nie, J., Liu, H., Lu, S., Hu, X., Zhu, J., Zhao, X., Chen, J., Chen, X., Yang, Z. & Li, X. Genetic and pharmacological inhibition of Rheb1-mTORC1 signaling exerts cardioprotection against adverse cardiac remodeling in mice. *Am J Pathol* **182**, 2005-2014, doi:10.1016/j.ajpath.2013.02.012 (2013).
- 103 Moon, J. S., Hisata, S., Park, M. A., DeNicola, G. M., Ryter, S. W., Nakahira, K. & Choi, A. M. K. mTORC1-Induced HK1-Dependent Glycolysis Regulates NLRP3 Inflammasome Activation. *Cell Rep* **12**, 102-115, doi:10.1016/j.celrep.2015.05.046 (2015).
- 104 Choi, J. S., Park, C. & Jeong, J. W. AMP-activated protein kinase is activated in Parkinson's disease models mediated by 1-methyl-4-phenyl-1,2,3,6-tetrahydropyridine. *Biochem Biophys Res Commun* **391**, 147-151, doi:10.1016/j.bbrc.2009.11.022 (2010).
- 105 Wang, J., Yang, L., Rezaie, A. R. & Li, J. Activated protein C protects against myocardial ischemic/reperfusion injury through AMP-activated protein kinase signaling. *Journal of thrombosis and haemostasis : JTH* **9**, 1308-1317, doi:10.1111/j.1538-7836.2011.04331.x (2011).

- 106 Bock, F., Shahzad, K., Wang, H., Stoyanov, S., Wolter, J., Dong, W., Pelicci, P. G., Kashif, M., Ranjan, S., Schmidt, S., Ritzel, R., Schwenger, V., Reymann, K. G., Esmon, C. T., Madhusudhan, T., Nawroth, P. P. & Isermann, B. Activated protein C ameliorates diabetic nephropathy by epigenetically inhibiting the redox enzyme p66Shc. *Proc Natl Acad Sci U S A* **110**, 648-653, doi:10.1073/pnas.1218667110 (2013).
- 107 Dong, W., Wang, H., Shahzad, K., Bock, F., Al-Dabet, M. M., Ranjan, S., Wolter, J., Kohli, S., Hoffmann, J., Dhople, V. M., Zhu, C., Lindquist, J. A., Esmon, C. T., Grone, E., Grone, H. J., Madhusudhan, T., Mertens, P. R., Schluter, D. & Isermann, B. Activated Protein C Ameliorates Renal Ischemia-Reperfusion Injury by Restricting Y-Box Binding Protein-1 Ubiquitination. *J Am Soc Nephrol* **26**, 2789-2799, doi:10.1681/ASN.2014080846 (2015).
- 108 Mosnier, L. O., Gale, A. J., Yegneswaran, S. & Griffin, J. H. Activated protein C variants with normal cytoprotective but reduced anticoagulant activity. *Blood* **104**, 1740-1744, doi:10.1182/blood-2004-01-0110 (2004).
- 109 Kaneider, N. C., Leger, A. J., Agarwal, A., Nguyen, N., Perides, G., Derian, C., Covic, L. & Kuliopulos, A. 'Role reversal' for the receptor PAR1 in sepsis-induced vascular damage. *Nature immunology* **8**, 1303-1312, doi:10.1038/ni1525 (2007).
- 110 Madhusudhan, T., Wang, H., Straub, B. K., Grone, E., Zhou, Q., Shahzad, K., Muller-Krebs, S., Schwenger, V., Gerlitz, B., Grinnell, B. W., Griffin, J. H., Reiser, J., Grone, H. J., Esmon, C. T., Nawroth, P. P. & Isermann, B. Cytoprotective signaling by activated protein C requires protease-activated receptor-3 in podocytes. *Blood* **119**, 874-883, doi:10.1182/blood-2011-07-365973 (2012).
- 111 Seehaus, S., Shahzad, K., Kashif, M., Vinnikov, I. A., Schiller, M., Wang, H., Madhusudhan, T., Eckstein, V., Bierhaus, A., Bea, F., Blessing, E., Weiler, H., Frommhold, D., Nawroth, P. P. & Isermann, B. Hypercoagulability inhibits monocyte transendothelial migration through protease-activated receptor-1-, phospholipase-Cbeta-, phosphoinositide 3-kinase-, and nitric oxide-dependent signaling in monocytes and promotes plaque stability. *Circulation* **120**, 774-784, doi:10.1161/CIRCULATIONAHA.109.849539 (2009).

- 112 Shahzad, K., Bock, F., Dong, W., Wang, H., Kopf, S., Kohli, S., Al-Dabet, M. M., Ranjan, S., Wolter, J., Wacker, C., Biemann, R., Stoyanov, S., Reymann, K., Soderkvist, P., Gross, O., Schwenger, V., Pahernik, S., Nawroth, P. P., Grone, H. J., Madhusudhan, T. & Isermann, B. Nlrp3-inflammasome activation in non-myeloid-derived cells aggravates diabetic nephropathy. *Kidney Int* **87**, 74-84, doi:10.1038/ki.2014.271 (2015).
- 113 Shahzad, K., Bock, F., Al-Dabet, M. M., Gadi, I., Kohli, S., Nazir, S., Ghosh, S., Ranjan, S., Wang, H., Madhusudhan, T., Nawroth, P. P. & Isermann, B. Caspase-1, but Not Caspase-3, Promotes Diabetic Nephropathy. *J Am Soc Nephrol* **27**, 2270-2275, doi:10.1681/ASN.2015060676 (2016).
- 114 Shahzad, K., Bock, F., Al-Dabet, M. M., Gadi, I., Nazir, S., Wang, H., Kohli, S., Ranjan, S., Mertens, P. R., Nawroth, P. P. & Isermann, B. Stabilization of endogenous Nrf2 by minocycline protects against Nlrp3-inflammasome induced diabetic nephropathy. *Sci Rep* **6**, 34228, doi:10.1038/srep34228 (2016).
- 115 Tanaka, S., Matsumoto, T., Matsubara, Y., Harada, Y., Kyuragi, R., Koga, J. I., Egashira, K., Nakashima, Y., Yonemitsu, Y. & Maehara, Y. BubR1 Insufficiency Results in Decreased Macrophage Proliferation and Attenuated Atherogenesis in Apolipoprotein E-Deficient Mice. *J Am Heart Assoc* **5**, doi:10.1161/JAHA.116.004081 (2016).
- 116 Weischenfeldt, J. & Porse, B. Bone Marrow-Derived Macrophages (BMM): Isolation and Applications. *CSH Protoc* **2008**, pdb prot5080, doi:10.1101/pdb.prot5080 (2008).
- 117 Zhong, Z., Liang, S., Sanchez-Lopez, E., He, F., Shalapour, S., Lin, X. J., Wong, J., Ding, S., Seki, E., Schnabl, B., Hevener, A. L., Greenberg, H. B., Kisseleva, T. & Karin, M. New mitochondrial DNA synthesis enables NLRP3 inflammasome activation. *Nature* **560**, 198-203, doi:10.1038/s41586-018-0372-z (2018).
- 118 Finsen, A. V., Lunde, I. G., Sjaastad, I., Ostli, E. K., Lyngra, M., Jarstadmarken, H. O., Hasic, A., Nygard, S., Wilcox-Adelman, S. A., Goetinck, P. F., Lyberg, T., Skrbic, B., Florholmen, G., Tonnessen, T., Louch, W. E., Djurovic, S., Carlson, C. R. & Christensen, G. Syndecan-4 is essential for development of concentric

- myocardial hypertrophy via stretch-induced activation of the calcineurin-NFAT pathway. *PLoS One* **6**, e28302, doi:10.1371/journal.pone.0028302 (2011).
- 119 Kashif, M., Hellwig, A., Kolleker, A., Shahzad, K., Wang, H., Lang, S., Wolter, J., Thati, M., Vinnikov, I., Bierhaus, A., Nawroth, P. P. & Isermann, B. p45NF-E2 represses Gcm1 in trophoblast cells to regulate syncytium formation, placental vascularization and embryonic growth. *Development* **138**, 2235-2247, doi:10.1242/dev.059105 (2011).
- 120 Shahzad, K., Thati, M., Wang, H., Kashif, M., Wolter, J., Ranjan, S., He, T., Zhou, Q., Blessing, E., Bierhaus, A., Nawroth, P. P. & Isermann, B. Minocycline reduces plaque size in diet induced atherosclerosis via p27(Kip1). *Atherosclerosis* **219**, 74-83, doi:10.1016/j.atherosclerosis.2011.05.041 (2011).
- 121 Cates, C., Rousselle, T., Wang, J., Quan, N., Wang, L., Chen, X., Yang, L., Rezaie, A. R. & Li, J. Activated protein C protects against pressure overload-induced hypertrophy through AMPK signaling. *Biochem Biophys Res Commun* **495**, 2584-2594, doi:10.1016/j.bbrc.2017.12.125 (2018).
- 122 Kain, V., Prabhu, S. D. & Halade, G. V. Inflammation revisited: inflammation versus resolution of inflammation following myocardial infarction. *Basic Res Cardiol* **109**, 444, doi:10.1007/s00395-014-0444-7 (2014).
- 123 Sandanger, O., Ranheim, T., Vinge, L. E., Bliksoen, M., Alfsnes, K., Finsen, A. V., Dahl, C. P., Askevold, E. T., Florholmen, G., Christensen, G., Fitzgerald, K. A., Lien, E., Valen, G., Espevik, T., Aukrust, P. & Yndestad, A. The NLRP3 inflammasome is up-regulated in cardiac fibroblasts and mediates myocardial ischaemia-reperfusion injury. *Cardiovasc Res* **99**, 164-174, doi:10.1093/cvr/cvt091 (2013).
- 124 Xie, M., Yu, Y., Kang, R., Zhu, S., Yang, L., Zeng, L., Sun, X., Yang, M., Billiar, T. R., Wang, H., Cao, L., Jiang, J. & Tang, D. PKM2-dependent glycolysis promotes NLRP3 and AIM2 inflammasome activation. *Nat Commun* **7**, 13280, doi:10.1038/ncomms13280 (2016).
- 125 Howell, J. J., Hellberg, K., Turner, M., Talbott, G., Kolar, M. J., Ross, D. S., Hoxhaj, G., Saghatelian, A., Shaw, R. J. & Manning, B. D. Metformin Inhibits Hepatic mTORC1 Signaling via Dose-Dependent Mechanisms Involving AMPK

- and the TSC Complex. *Cell Metab* **25**, 463-471, doi:10.1016/j.cmet.2016.12.009 (2017).
- 126 Marti-Carvajal, A. J., Sola, I., Gluud, C., Lathyris, D. & Cardona, A. F. Human recombinant protein C for severe sepsis and septic shock in adult and paediatric patients. *Cochrane Database Syst Rev* **12**, CD004388, doi:10.1002/14651858.CD004388.pub6 (2012).
- 127 Kim, H. J., Lee, D. W., Ravichandran, K., D, O. K., Akcay, A., Nguyen, Q., He, Z., Jani, A., Ljubanovic, D. & Edelstein, C. L. NLRP3 inflammasome knockout mice are protected against ischemic but not cisplatin-induced acute kidney injury. *The Journal of pharmacology and experimental therapeutics* **346**, 465-472, doi:10.1124/jpet.113.205732 (2013).
- 128 Szeto, H. H., Liu, S., Soong, Y., Seshan, S. V., Cohen-Gould, L., Manichev, V., Feldman, L. C. & Gustafsson, T. Mitochondria Protection after Acute Ischemia Prevents Prolonged Upregulation of IL-1beta and IL-18 and Arrests CKD. *J Am Soc Nephrol*, doi:10.1681/ASN.2016070761 (2016).
- 129 Minutoli, L., Puzzolo, D., Rinaldi, M., Irrera, N., Marini, H., Arcoraci, V., Bitto, A., Crea, G., Pisani, A., Squadrito, F., Trichilo, V., Bruschetta, D., Micali, A. & Altavilla, D. ROS-Mediated NLRP3 Inflammasome Activation in Brain, Heart, Kidney, and Testis Ischemia/Reperfusion Injury. *Oxid Med Cell Longev* **2016**, 2183026, doi:10.1155/2016/2183026 (2016).
- 130 Lyden, P., Levy, H., Weymer, S., Pryor, K., Kramer, W., Griffin, J. H., Davis, T. P. & Zlokovic, B. Phase 1 safety, tolerability and pharmacokinetics of 3K3A-APC in healthy adult volunteers. *Curr Pharm Des* **19**, 7479-7485 (2013).
- 131 Joyce, D. E., Gelbert, L., Ciaccia, A., DeHoff, B. & Grinnell, B. W. Gene expression profile of antithrombotic protein c defines new mechanisms modulating inflammation and apoptosis. *J Biol Chem* **276**, 11199-11203, doi:10.1074/jbc.C100017200 (2001).
- 132 Latz, E., Xiao, T. S. & Stutz, A. Activation and regulation of the inflammasomes. *Nat Rev Immunol* **13**, 397-411, doi:10.1038/nri3452 (2013).
- 133 van Hout, G. P., Bosch, L., Ellenbroek, G. H., de Haan, J. J., van Solinge, W. W., Cooper, M. A., Arslan, F., de Jager, S. C., Robertson, A. A., Pasterkamp, G. &

- Hoefler, I. E. The selective NLRP3-inflammasome inhibitor MCC950 reduces infarct size and preserves cardiac function in a pig model of myocardial infarction. *Eur Heart J*, doi:10.1093/eurheartj/ehw247 (2016).
- 134 Kovacs, P., Bak, I., Szendrei, L., Vecsernyes, M., Varga, E., Blasig, I. E. & Tosaki, A. Non-specific caspase inhibition reduces infarct size and improves post-ischaemic recovery in isolated ischaemic/reperfused rat hearts. *Naunyn Schmiedebergs Arch Pharmacol* **364**, 501-507 (2001).
- 135 Mocanu, M. M., Baxter, G. F. & Yellon, D. M. Caspase inhibition and limitation of myocardial infarct size: protection against lethal reperfusion injury. *Br J Pharmacol* **130**, 197-200, doi:10.1038/sj.bjp.0703336 (2000).
- 136 Salloum, F. N., Chau, V., Varma, A., Hoke, N. N., Toldo, S., Biondi-Zoccai, G. G., Crea, F., Vetrovec, G. W. & Abbate, A. Anakinra in experimental acute myocardial infarction--does dosage or duration of treatment matter? *Cardiovascular drugs and therapy / sponsored by the International Society of Cardiovascular Pharmacotherapy* **23**, 129-135, doi:10.1007/s10557-008-6154-3 (2009).
- 137 Bracey, N. A., Gershkovich, B., Chun, J., Vilaysane, A., Meijndert, H. C., Wright, J. R., Jr., Fedak, P. W., Beck, P. L., Muruve, D. A. & Duff, H. J. Mitochondrial NLRP3 protein induces reactive oxygen species to promote Smad protein signaling and fibrosis independent from the inflammasome. *J Biol Chem* **289**, 19571-19584, doi:10.1074/jbc.M114.550624 (2014).
- 138 Shigeoka, A. A., Mueller, J. L., Kambo, A., Mathison, J. C., King, A. J., Hall, W. F., Correia Jda, S., Ulevitch, R. J., Hoffman, H. M. & McKay, D. B. An inflammasome-independent role for epithelial-expressed Nlrp3 in renal ischemia-reperfusion injury. *Journal of immunology* **185**, 6277-6285, doi:10.4049/jimmunol.1002330 (2010).
- 139 Grundmann, S., Bode, C. & Moser, M. Inflammasome activation in reperfusion injury: friendly fire on myocardial infarction? *Circulation* **123**, 574-576, doi:10.1161/CIRCULATIONAHA.111.018176 (2011).

- 140 Ikeda, U., Ikeda, M., Kano, S. & Shimada, K. Neutrophil adherence to rat cardiac myocyte by proinflammatory cytokines. *J Cardiovasc Pharmacol* **23**, 647-652 (1994).
- 141 Moon, J. S., Nakahira, K., Chung, K. P., DeNicola, G. M., Koo, M. J., Pabon, M. A., Rooney, K. T., Yoon, J. H., Ryter, S. W., Stout-Delgado, H. & Choi, A. M. NOX4-dependent fatty acid oxidation promotes NLRP3 inflammasome activation in macrophages. *Nat Med* **22**, 1002-1012, doi:10.1038/nm.4153 (2016).
- 142 Huang, L., Dai, K., Chen, M., Zhou, W., Wang, X., Chen, J. & Zhou, W. The AMPK Agonist PT1 and mTOR Inhibitor 3HOI-BA-01 Protect Cardiomyocytes After Ischemia Through Induction of Autophagy. *J Cardiovasc Pharmacol Ther* **21**, 70-81, doi:10.1177/1074248415581177 (2016).
- 143 Kezic, A., Becker, J. U. & Thaiss, F. The effect of mTOR-inhibition on NF-kappaB activity in kidney ischemia-reperfusion injury in mice. *Transplant Proc* **45**, 1708-1714, doi:10.1016/j.transproceed.2013.02.110 (2013).
- 144 Dalle Pezze, P., Sonntag, A. G., Thien, A., Prentzell, M. T., Godel, M., Fischer, S., Neumann-Haefelin, E., Huber, T. B., Baumeister, R., Shanley, D. P. & Thedieck, K. A dynamic network model of mTOR signaling reveals TSC-independent mTORC2 regulation. *Sci Signal* **5**, ra25, doi:10.1126/scisignal.2002469 (2012).
- 145 Saxton, R. A. & Sabatini, D. M. mTOR Signaling in Growth, Metabolism, and Disease. *Cell* **168**, 960-976, doi:10.1016/j.cell.2017.02.004 (2017).
- 146 Saxton, R. A. & Sabatini, D. M. mTOR Signaling in Growth, Metabolism, and Disease. *Cell* **169**, 361-371, doi:10.1016/j.cell.2017.03.035 (2017).
- 147 Yamaji, K., Wang, Y., Liu, Y., Abeyama, K., Hashiguchi, T., Uchimura, T., Krishna Biswas, K., Iwamoto, H. & Maruyama, I. Activated protein C, a natural anticoagulant protein, has antioxidant properties and inhibits lipid peroxidation and advanced glycation end products formation. *Thrombosis research* **115**, 319-325, doi:10.1016/j.thromres.2004.09.011 (2005).
- 148 Baltzer, C., Tiefenbock, S. K. & Frei, C. Mitochondria in response to nutrients and nutrient-sensitive pathways. *Mitochondrion* **10**, 589-597, doi:10.1016/j.mito.2010.07.009 (2010).

- 149 Darzynkiewicz, Z., Zhao, H., Halicka, H. D., Li, J., Lee, Y. S., Hsieh, T. C. & Wu, J. M. In search of antiaging modalities: evaluation of mTOR- and ROS/DNA damage-signaling by cytometry. *Cytometry A* **85**, 386-399, doi:10.1002/cyto.a.22452 (2014).
- 150 Burnier, L. & Mosnier, L. O. Novel mechanisms for activated protein C cytoprotective activities involving noncanonical activation of protease-activated receptor 3. *Blood* **122**, 807-816, doi:10.1182/blood-2013-03-488957 (2013).
- 151 Butts, B., Gary, R. A., Dunbar, S. B. & Butler, J. The Importance of NLRP3 Inflammasome in Heart Failure. *J Card Fail* **21**, 586-593, doi:10.1016/j.cardfail.2015.04.014 (2015).

9 Acknowledgement

I thank Almighty ALLAH whose mercy and blessings made it possible for me to accomplish this thesis.

First of all I would like to express my deep gratitude for respected Prof. Berend Isermann for his supervision, advice and guidance from the very early stage of this research as well as giving me extraordinary experiences throughout the work. Above all and the most needed, he provided me constant encouragement and support in various ways. His truly scientist intuition has exceptionally inspired and enriches my growth as a student, a researcher and a scientist want to be. I thank him for his systematic guidance and great effort he put into training me in the scientific field.

I would like to pay my special thanks to Dr. Khurram Shahzad for his support, guidance and helpful suggestions during the course of my research work. This piece of work would not have been possible without your help. I have learned a lot from you, thanks for being there for me every time.

I especially thank from core of my heart to my brother Dr. Al- Dabet and sister Ala for being there every time for me whenever I asked for any help professionally or personally. I am truly inspired by you. I am privileged to have another brother Ahmed and sister Shireen for providing me great company, care and love thought-out these years.

I would like to thanks sincerely to my sister, colleague and a true friend Sanchita Ghosh for her support, love, care and guidance during my research work. For providing me great company and best Bengali Fish. I am grateful to Dr. Shrey Kohli for his valuable advices during this project, for entertaining me in lab and for typical Indian food. Thanks for correcting my English and German as well, I really had a great time with you.

Additionally, I would like to thanks my all lab colleagues, Ihsan Gadi, Zafar Ali Abro, Jaya Kumar Manoharan, Satish Ranjan, Rajiv Rana, Dheerendra Gupta, Shruthi

Krishnan, Kruthika, Akash Mathew, Silke Zimmerman, Mortiz, Franziska Lochmann, Paulina Markmeyer, Lukas 'Breitenstein, Sophie Mathieu and Ronald Biemann for their help, support and care. Thanks for the friendship and memories.

I am really grateful to Ms. Deneser, Ms. Judin, Ms. Makarova, Mr. Rudat and Ms. Friedrich for their technical support. I am also benefited by outstanding work from Johannes Lauf help with his particular skills in myocardial ischemia reperfusion injury in animal house.

In addition I would like to thank my Uncle Javed Iqbal and auntie Asia and my little sister Rabita who supported me as my family and made me feel at home.

I am forever indebted to my loving Parents whose great efforts with unceasing prayers and encouragement has enabled me to reach the present position in the life. I would like to express my warm thanks to my loving sisters, brother in laws, my brother and my sister in law for their care, support and affection.

I thank all those who have helped me directly or indirectly in the successful completion of my thesis.

10 Declaration

Ich erkläre, dass ich die der Medizinischen Fakultät der Otto-von-Guericke-Universität zur Promotion eingereichte Dissertation mit dem Titel

Cytoprotective activated protein C averts Nlrp3 inflammasome induced ischemia reperfusion injury via mTORC1 inhibition

im Institut für Klinische Chemie und Pathobiochemie der Medizinischen Fakultät der Otto-von-Guericke-Universität Magdeburg

mit Unterstützung durch Prof. Dr. med. Berend Isermann

selbständig verfasst ohne sonstige Hilfe durchgeführt und bei der Abfassung der Dissertation keine anderen, als die dort aufgeführten Hilfsmittel benutzt habe.

Bei der Abfassung der Dissertation sind Rechte Dritter nicht verletzt worden.

Ich habe diese Dissertation bisher an keiner in- und ausländischen Hochschule zur Promotion eingereicht. Ich übertrage der Medizinischen Fakultät das Recht, weitere Kopien meiner Dissertation herzustellen und zu vertreiben.

Magdeburg, den 18.09.2018

Sumra Nazir

11 Curriculum Vitae and list of publications

11.1 Curriculum Vitae

Sumra Nazir

Email: sumra.nazir@med.ovg.de

Address: Otto-von-Guericke-University (OvGU) Magdeburg

Medical faculty / Institute of Clinical Chemistry and Pathobiochemsitry

Leipzigerstraße 44, 39120 Magdeburg

Tel: +49 176 34136402

Date of birth: 25/01/1990

Nationality: Pakistan

Education

- 2014-till PhD student, Institute for Clinical Chemistry und Pathobiochemistry, medical university of Magdeburg, Germany.
- 2012-2014 M.Phil. in Zoology from Lahore College for Women University, Lahore, Pakistan.
- 2009-2011 M.Sc in zoology from University of the Punjab, Lahore, Pakistan
- 2007-2009 B.sc (Botany,Zoology,Chemistry) from University of the Punjab, Lahore; Pakistan
- 2005-2007 Intermediate, Pre-medical from Lahore Garrison Education system, Lahore, Pakistan.
- 2003-2005 Matriculation, Science Group, Army Public School for Girls Lahore, Pakistan.

Talks and poster presentations

Talks

S. Nazir; Shahzad K; F. Bock; Ina Thielmann; B. Nieswandt ; M. Thati; B. Isermann. Differential effects of direct fXa versus fIIa inhibition on coagulation and inflammation: **International Society for Thrombosis and Haemostasis, Berlin, 2017, Germany**

S. Nazir; Shahzad K; F. Bock; Ina Thielmann; B. Nieswandt ; M. Thati; B. Isermann. Defining the differential effects of novel anticoagulants: fXa versus fIIa inhibition on coagulation and inflammation: **German Society for Thrombosis and Haemostasis, Münster, 2016, Germany**

S. Nazir; Shahzad K; F. Bock; Ina Thielmann; B. Nieswandt ; M. Thati; B. Isermann. Differential effects of novel anticoagulants: fXa versus fIIa inhibition on coagulation and inflammation: **German Society for Clinical Chemistry, Leipzig, 2015, Germany**

Poster Presentations

Shahzad K, F. **S. Nazir**, Bock, M. Thati, H. Wang, R. Satish, J. Wolter,, P. Nawroth, B. Isermann: Activated protein C protects against accelerated atherosclerosis in diabetes by epigenetically restricting p66Shc expression in macrophages. **American Heart Association 2017, Anaheim, USA.**

S. Nazir, K. Shahzad, F. Bock, Ina Thielmann, B. Nieswandt, B. Isermann: A Cytoprotective activated protein C averts Nlrp3 inflammasome induced ischemia reperfusion injury via mTORC1 inhibition. **American Heart Association 2017, Anaheim, USA.**

Shahzad K, Bock F, Al-Dabet MM, **S. Nazir**, Gadi I, Kohli S, Wolter J, Thati M, Isermann B. Stabilization of endogenous Nrf2 protects against Nlrp3 inflammasome induced diabetic nephropathy. - Kidney Week 2016- **American Society of Nephrology; Chicago, USA.**

Shahzad K, Al-Dabet MM, Bock F, **S. Nazir**, Gadi I, Kohli S, Wolter J, Thati M, Isermann Bn Shrey Kohli Madhusudhan Thati Hongjie Wang Juliane Wolter. (2015). Defining the role of pyroptosis and apoptosis in diabetic nephropathy: **European Association for the Study of Diabetes - 51st Meeting; Stockholm, Sweden.**

11.2 List of publications

1. **Nazir S**, Gadi I, Al-Dabet MM, Elwakiel A, Kohli S, Ghosh S, Manoharan J, Ranjan S, Bock F, Braun-Dullaeus RC, Esmon CT, Huber TB, Camerer E, Dockendorff C, Griffin JH, Isermann B and Shahzad K. Cytoprotective activated protein C averts Nlrp3 inflammasome induced ischemia reperfusion injury via mTORC1 inhibition.
Blood 2017. doi: 10.1182/blood-2017-05-782102 **IF: 15.13**
2. Madhusudhan T, Wang H, Ghosh S, Dong W, Kumar V, Al-Dabet MM, Manoharan J, **Nazir S**, Elwakiel A, Bock F, Kohli S, Marquardt A, Sogut I, Shahzad K, Muller AJ, Esmon CT, Nawroth PP, Reiser J, Chavakis T, Ruf W and Isermann B. Signal integration at the PI3K-p85-XBP1 hub endows coagulation protease activated protein C with insulin-like function.
Blood. 2017;130:1445-1455. **IF: 15.13**
3. Marquardt A, Al-Dabet MM, Ghosh S, Kohli S, Manoharan J, ElWakiel A, Gadi I, Bock F, **Nazir S**, Wang H, Lindquist JA, Nawroth PP, Madhusudhan T, Mertens PR, Shahzad K and Isermann B. Farnesoid X Receptor Agonism Protects against Diabetic Tubulopathy: Potential Add-On Therapy for Diabetic Nephropathy.
J Am Soc Nephrol. 2017;28:3182-3189 **IF: 9.46**
4. Shahzad K, Bock F, Al-Dabet MM, Gadi I, Kohli S, **Nazir S**, Ghosh S, Ranjan S, Wang H, Madhusudhan T, Nawroth PP and Isermann B. Caspase-1, but Not Caspase-3, Promotes Diabetic Nephropathy.
J Am Soc Nephrol. 2016;27:2270-5. **IF: 9.46**
5. Shahzad K, Bock F, Al-Dabet MM, Gadi I, **Nazir S**, Wang H, Kohli S, Ranjan S, Mertens PR, Nawroth PP and Isermann B. Stabilization of endogenous Nrf2 by minocycline protects against Nlrp3-inflammasome induced diabetic nephropathy.
Sci Rep. 2016;6:34228. **IF: 5.46**

6. Kohli S, Ranjan S, Hoffmann J, Kashif M, Daniel EA, Al-Dabet MM, Bock F, **Nazir S**, Huebner H, Mertens PR, Fischer KD, Zenclussen AC, Offermanns S, Aharon A, Brenner B, Shahzad K, Ruebner M and Isermann B. Maternal extracellular vesicles and platelets promote preeclampsia via inflammasome activation in trophoblasts.

Blood. 2016;128:2153-2164.

IF: 15.13